UAB
Universitat Autònoma de Barcelona

Doctoral thesis

Liquid biopsy in hepatocellular carcinoma: Utility of circulating cell-free DNA profiling and cytokine levels in hepatocellular carcinoma management

Author:

Elena Vargas Accarino

Doctoral thesis directors:

Dr Beatriz Mínguez Rosique

Dr Francisco Rodríguez-Frías

Dr María del Mar Riveiro Barciela

Doctoral thesis tutor:

Dr María Asunción Buti Ferret

Doctoral program in Medicine

Department of Medicine

Universitat Autònoma de Barcelona

Barcelona, 2023

Acknowledgements

Acknowledgements

¡Por fin ha llegado el día! Desde que llegué al VHIR he tenido la suerte de estar rodeada de personas que me han hecho disfrutar de estos años y aprender cada día. Me gustaría daros las gracias a todos, porque sin vosotros no lo habría conseguido.

En primer lugar, quería dar las gracias a mis directores de tesis. A la Dra Beatriz Mínguez, al Dr Francisco Rodríguez-Frías y a la Dra Mar Riveiro por todo lo que he podido aprender de ellos durante estos años, las críticas constructivas y, sobre todo, por la pasión que tienen por su trabajo y que consiguen contagiar a los que los rodean.

Mi más sincero agradecimiento a Beatriz. Por tu interés y dedicación a esta tesis y por encontrar siempre un hueco para responder todas mis dudas. Por no conformarte y perseguir siempre el trabajo bien hecho. Muchas gracias por esta oportunidad ¡me ha encantado poder formar parte del "HCC lab"!

A Paco, porque ¡contigo empezó todo! Desde las prácticas de la carrera conseguiste contagiarme tu ilusión por la ciencia y ha sido una de las razones por las que estoy hoy aquí.

Quería agradecer también a mi tutora, la Dra María Buti. María muchas gracias por confiar y contar siempre conmigo, y por tu insistencia que consigue sacar adelante cualquier proyecto.

Si a alguien quiero agradecer también es a la Dra Mónica Higuera. Moni muchas gracias por hacer de esta tesis la tuya, por enseñarme todo día a día y técnica tras técnica, por responder a cada una de mis preguntas siempre y por aconsejarme en todo momento. Consejos no solo de laboratorio sino también de la vida que me han hecho aprender tanto. ¡Ha sido una gran suerte tenerte a mi lado!

portada de tesis más bonita que podía tener. Y a Cris, Marina y Sandra, porque aún y estando lejos habéis sido un gran apoyo.

A Pablo, por haberme acompañado durante toda la tesis y por conseguir sacarme una carcajada hasta en los peores momentos. Gracias por cuidarme, animarme y apoyarme siempre.

Y por supuesto a toda mi familia y en especial a mis padres, por cuidarme, ayudarme y quererme tanto, y por haberme transmitido el valor del trabajo duro y la pasión por la ciencia. Ha sido un honor empezar mi carrera en el mismo sitio que vosotros.

¡Muchas gracias a todos!

Abbreviations

Abbreviations

A
_____

AFP   Alpha-fetoprotein

ALBI   Albumin-bilirubin

APC   Antigen presenting cells

ARID   AT-Rich interacting domain

ALT   Alanine aminotrasferase

AST   Aspartate aminotransferase

ATM   Ataxia-telangiectasia mutated

B
_____

BAF   BRG-1 associated factor

BCLC   Barcelona clinic liver cancer

Breg   Regulatory B cell

BSC   Best supportive care

BST   Banc de sang i teixits

BTLA   B and T Lymphocyte Attenuator

bTMB   Blood tumor mutational burden

C
_____

cccDNA   Convalently closed circular DNA

CCNE1   Cyclin E1

CDKN2A   Cyclin dependent kinase inhibitor 2

cfDNA	Cell free DNA
CNV	Copy number variation
CR	Complete response
CSPH	Clinically significant portal hypertension
CT	Computed tomography
CTC	Circulating Tumor Cells
CTCFL	CCCTC-binding factor
ctDNA	Circulating tumor DNA
CTLA-4	Cytotoxic T lymphocyte associated antigen 4

D

DAA	Direct acting antivirals
DC	Dendritic cells
DCP	Des-carboxy-prothrombin
ddPCR	Droplet digital PCR
DMSO	Dimethyl sulfoxide
DNA	Deoxyribonucleic acid

E

EB	Elution buffer
ECOG	Eastern cooperative oncology group
EGFR	Epidermal growth factor receptor
EpCAM	Epithelial cell adhesion molecule

EV	Extracellular vesicles
F	

FDA	Food and drug administration
FGF	Fibroblast growth factor
FGFR	Fibroblast growth factor receptor
G	

GM-CSF	Granulocyte-macrophage colony-stimulating factor
GPC3	Glypican-3
GSK	Glycogen-synthetase kinase
GTP	Guanosine phosphatase
H	

HBV	Hepatitis B virus
HCC	Hepatocellular carcinoma
HCV	Hepatitis C virus
HDV	Hepatitis delta virus
HGDN	High-grade dysplastic nodules
HGF	Hepatocyte growth factor
HR	Hazard ratio
I	

ICI	Immune checkpoint inhibitors
IDO	Indoleamine 2,3-dioxygenase-1

IFN	Interferon
IGN	Insulin-like growth factor
IGFBP7	Insulin like growth factor binding protein 7
IL	Interleukin
IQR	Interquartile range
IRE	Irreversible electroporation
iRECIST	Immune RECIST
ITH	Intra-tumoral heterogeneity

L

LAG-3	Lymphocyte activation gene 3
LD	Liver disease
LGDN	Low grade displasic nodules
LINE	Long interspersed nuclear elements
LITT	Laser interstitial thermotherapy
LT	Liver transplantation

M

MAFLD	Metabolic disfunction associated fatty liver disease
MCP-1	Monocyte chemoattractant protein 1
MDM2	Murine doble minute 2
MDSCs	Myeloid-derived suppressor cells
MELD	Model of end-stage liver disease

MHC	Major histocompatibility complex
miRNA	micro RNA
mRECIST	modified RECIST
MRI	Magnetic resonance imaging
mRNA	Messenger RNA
mVI	Microvascular invasion
MWA	Microwave ablation

N

NE	Non evaluable
NGS	Next generation sequencing
NR	No response
NSCLC	Non-small-cell lung cancer
NTRK2	Neutrophic receptor tyrosine kinase 2
NY-ESO1	New York oesophageal squamous cell carcinoma 1

O

OR	Objective response
OS	Overall survival

P

PCR	Polymerase chain reaction
PD-1	Programed cell death protein-1
PDGF	Platelet-derived growth factor

Abbreviations

PDGFR	Platelet-derived growth factor receptor
PD-L1	Programed cell death-ligand 1
PEI	Percutaneous ethanol injection
PFS	Progression free survival
PBMC	Peripheral blood mononuclear cells
PPARG	Peroxisome proliferation-activated receptor gamma
PR	Progressive disease
PS	Performance status

R

RAF	Rapidly accelerated fibrosarcoma
Rb	Retinoblastoma
RECIST	Response evaluation criteria in solid tumors
RFA	Radiofrequency ablation
RNA	Ribonucleic acid
ROS	Reactive oxygen species

S

SD	Stable disease
SNV	Single nucleotide variant
SVR	Sustained virological response

T

TACE	Transarterial chemoembolization

TARE	Transarterial radioembolization
TCF/LEF	T cell factor/lymphoid enhancer factor family
TCR	T cell receptor
TERT	Telomerase reverse transcriptase
TGF	Transforming growth factor
TH	T helper
TIE2	Tyrosine-protein kinase receptor
TIM-3	T cell Immunoglobulin and mucin-domain containing-3
TKI	Tyrosine kinase inhibitor
TMB	Tumor mutational burden
TME	Tumor microenvironment
TNF	Tumor necrosis factor
TP53	Tumoral protein 53
Treg	Regulatory T cells

U

UEB	Unitat d´Estadística i Bioinformàtica

V

VAF	Variant allele frequency
VEGA	Vascular endothelial growth factor angiogenesis
VEGF	Vascular endothelial growth factor
VEGFR	Vascular endothelial growth factor receptor

Abbreviations

VHIR	Vall d'Hebron research institute
VI	Vascular invasion
W	
WES	Whole-genome sequencing

Table of Contents

Table of Contents

Summary

Summary

Hepatocellular carcinoma is the second leading cause of cancer-related death, and its incidence is increasing globally. Surgery remains as the first therapeutic option for patients with early HCC, but most patients are diagnosed at late clinical stages due to the lack of early symptoms. Curative treatments are only applicable to patients diagnosed at early stages, which are less than half of the patients diagnosed with HCC. In the case of surgical resection, tumor recurrence is close to 70% at 5 years; its prompt detection or a prognostic estimation would be necessary in clinical practice.

Systemic therapies, that are the treatment of choice for patients with advanced HCC, are rapidly changing. Immunotherapy, and in particular immune checkpoint inhibitors, have revolutionized the therapeutic landscape of advanced HCC, increasing the expected survival of these patients. However, objective radiological response to these therapies has been reported to occur in around 20% of patients. The precise identification of patients that could benefit from those therapies would optimize the rational use of these drugs, avoiding their potential side effects in patients who a priori will not benefit from them, and so allowing to design the therapeutic strategy in a more rational way, refining the current clinical algorithms.

In the first study we prospectively collected tumoral tissue, paired nontumor adjacent tissue and blood samples from 30 HCC patients undergoing curative therapies, to analyze the most prevalent mutations in HCC (TERT promoter, TP53, CTNNB1, AXIN1 and ARID1A) in plasma cfDNA by next-generation sequencing, aiming to elucidate their value as prognostic noninvasive biomarkers. In our study, total amount of cfDNA was related to survival during follow-up. The number of mutated genes and the number of detectable mutations on cfDNA were correlated with recurrence and overall survival. Moreover, dynamic changes in cfDNA mutations were monitored during follow-up, showing appearance or an increase of these mutations before radiological detection of HCC recurrence.

Summary

In the second study plasma samples from 25 patients with non resectable HCC treated with immune checkpoint inhibitors were prospectively collected, at the beginning of the treatment and after 3 months under treatment. Twenty-four inflammatory cytokine levels were analyzed by ELISA as well as the levels of cfDNA, ctDNA and percentage of TERT mutation by ddPCR, at both time points. Basal cfDNA profiling from 21 of these patients was analyzed by Onco-500 TruSight. Results showed that basal differences in total amount of cfDNA, CTLA-4 and CNV were significantly different between patients with and without radiological response to ICIs treatment. Levels of MCP-1 and TNF-α, and total amount cfDNA and ctDNA after three months of ICIs treatment were significantly different in patients presenting radiological response compared to those not presenting stable or progressive disease as best radiological response.

Resumen

El carcinoma hepatocelular es la segunda causa de muerte relacionada con el cáncer y su incidencia está aumentando en todo el mundo. Los tratamientos con intención curativa solo son aplicables a los pacientes diagnosticados en estadios iniciales, que son menos de la mitad de los pacientes diagnosticados de CHC. En el caso de la resección quirúrgica, la recidiva tumoral se acerca al 70% a los 5 años; siendo su detección precoz o su estimación pronóstica una necesidad en práctica clínica.

Las terapias sistémicas, tratamiento de elección en los pacientes con CHC avanzado, están cambiando rápidamente. La inmunoterapia, y en particular, los inhibidores de punto de control inmunitario, han supuesto un avance relevante, con una traducción clara en el incremento de supervivencia de estos pacientes. Sin embargo, la respuesta radiológica objetiva a estas terapias se estima en torno al 20% de pacientes. La identificación precisa de los pacientes que podrían beneficiarse de cada terapia sería deseable para optimizar el uso racional de medicamentos, evitando sus potenciales efectos secundarios a pacientes que a priori no se beneficiarán de ellos, pudiendo diseñar de un modo más racional las estrategias terapéuticas y refinando los actuales algoritmos clínicos.

En el primer estudio se recogieron muestras de tejido tumoral, tejido adyacente no tumoral y de sangre de 30 pacientes con CHC sometidos a terapias curativas, para analizar las mutaciones más prevalentes en el CHC (promotor de TERT, TP53, CTNNB1, AXIN1 y ARID1A) en el cfDNA plasmático mediante secuenciación de nueva generación, con el objetivo de dilucidar su valor como biomarcadores pronósticos no invasivos. En nuestro estudio, la cantidad total de cfDNA se relacionó con supervivencia durante el seguimiento. El número de genes mutados o el número de mutaciones detectadas en el cfDNA se correlacionaron con recurrencia y supervivencia. Además, se detectaron cambios dinámicos en las mutaciones del cfDNA durante el seguimiento, con incremento o aparición de estas antes de la detección radiológica de la recidiva del CHC.

Summary

En el segundo estudio se recogieron muestras de plasma de una cohorte prospectiva de 25 pacientes tratados con inhibidores de punto de control inmunitario al iniciar el tratamiento y después de 3 meses de tratamiento. Se analizaron los niveles de 24 citoquinas inflamatorias mediante ELISA, así como los niveles de cfDNA, ctDNA y el porcentaje de mutación de TERT mediante ddPCR, al inicio y después de 3 meses del tratamiento. El perfil de cfDNA basal de 21 de estos pacientes se analizó mediante Onco-500 TruSight. Los resultados mostraron que las diferencias basales en la cantidad total de cfDNA, CTLA-4 y CNV eran significativamente diferentes entre los pacientes con y sin respuesta radiológica al tratamiento con ICIs. Los niveles de MCP-1 y de TNF-α y la cantidad total de cfDNA y ctDNA después de tres meses de tratamiento con ICIs fueron significativamente diferentes en los pacientes que presentaron respuesta radiológica comparado con los que presentaron enfermedad estable o progresión como mejor respuesta radiológica.

Introduction

1. Introduction

1.1. Liver cancer

Liver cancer is the fourth most common cause of cancer-related deaths after lung, breast and colorectal cancer; and the sixth in terms of incident cases, with 800.000 new cases and more than 900.000 deaths in 2020 (Figure 1) (1)(2). Liver cancer remains a global health challenge and its incidence is growing worldwide (3). It is estimated that between 2020 and 2040 new liver cancer cases will increase by 55% with a possible 1,4 million individuals diagnosed in 2040 (4).

Estimated age-standardized incidence rates (World) in 2020, liver, both sexes, all ages
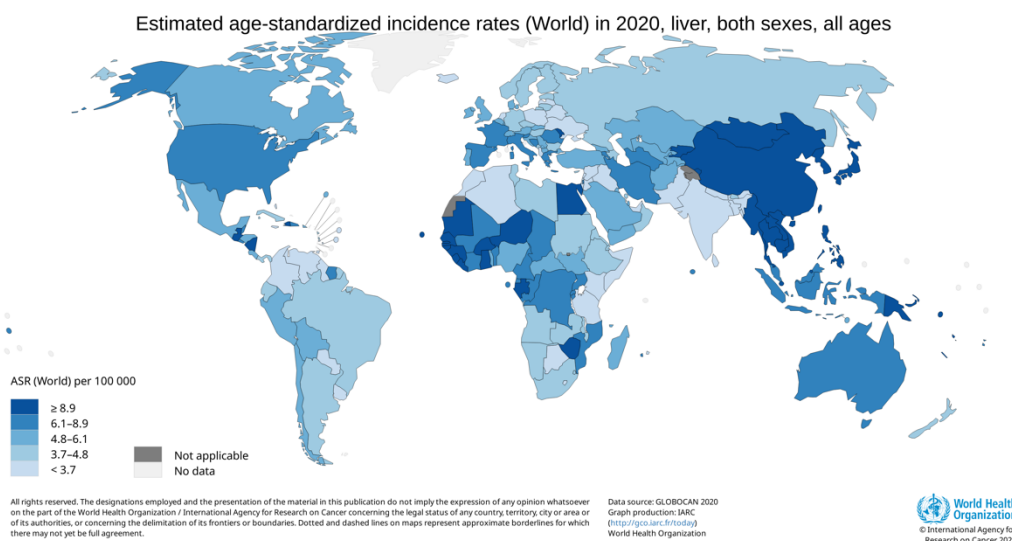
Figure 1. Worldwide incidence of liver cancer in 2020. Data are expressed as the age-standardized rate (ASR) per 100.000 population. From the International Agency for Research on Cancer (accessed on September 27, 2022) (1).

There are several histopathological subtypes of liver cancer with very different prevalence; the most common type of primary liver cancer globally is hepatocellular carcinoma (HCC), being the 90% of all adult's liver tumors, followed by cholangiocarcinoma, being approximately the other 10%. Mixed hepatocellular

cholangiocarcinoma, fibrolamellar HCC, and the pediatric neoplasm hepatoblastoma account for less than 1% of cases (5).

1.2. Hepatocellular carcinoma

The majority of HCC occur in patients with underlying liver disease mostly liver cirrhosis, which developes in the context of well-known risk factors, as viral hepatitis infection (hepatitis B virus (HBV) or hepatitis C virus (HCV)), alcohol abuse and metabolic associated (obesity, diabetes..) fatty liver disease (3). Other less prevalent risk factors for HCC include cirrhosis from primary biliary cholangitis, haemochromatosis and α1-antitrypsin deficiency among others (6).

HCC is infrequent among patients without liver disease and is twice or thrice as common in men as in women. Cirrhosis of any cause increases the risk of HCC, with an annual incidence between 2 and 4%. This risk varies according to cause, geographic area, gender, age, and degree of liver damage (2)(3).

1.3. Risk factors

1.3.1. Viral hepatitis

1.3.1.1. Hepatitis B virus infection

HBV is a major risk factor worldwide for developing HCC and contributes to HCC development through direct and indirect mechanisms (7). On average, 25% of untreated individuals with chronic HBV infection will die of cirrhosis complications and/or HCC (8).

HBV is a DNA virus that infects hepatocytes, the major cell of the liver, and replicate by reverse transcription of a terminally redundant viral RNA, the pregenome. Upon infection, the circular, partially double-stranded virion DNA is converted in the nucleus to a covalently closed circular DNA (cccDNA) that assembles into a minichromosome, the template for viral mRNA synthesis (9).

HBV DNA integration into the host genome occurs at early steps of clonal tumor expansion and induces both genomic instability and direct insertional mutagenesis of diverse cancer-related genes. Prolonged expression of the viral regulatory protein HBx and/or altered versions of the preS/S envelope proteins dysregulates cell transcription and proliferation control and sensitizes liver cells to carcinogenic factors (7).

At the early 90s HBV vaccinations programs were established (7). Long-term follow-up studies provides evidences that universal HBV immunization in infants has successfully prevented liver cancer in both children and young adults (9).

Dietary exposure to aflatoxin B1 amplifies the risk of hepatocellular carcinoma among patients with HBV infection, through a specific TP53 mutation (3).

1.3.1.2. Hepatitis C virus infection

HCV is an RNA virus that does not integrate into the host genome, therefore, HCC in hepatitis C patients occur predominantly in those patients with cirrhosis or chronic liver damage with fibrosis (10)(11). In European and North American studies, the annual incidence of HCC in subjects with hepatitis C-related cirrhosis is 0,5-5% (12).

With the highly effective and well-tolerated direct-acting antiviral agents (DAA) HCV treatment rates and number of patients achieving sustained virological response (SVR) have increased dramatically, resulting in a 50-80% reduction in the risk of HCC (13). However, racial/ethnic minorities, socioeconomically disadvantaged patients, lost to follow-up patients that remain unaware of their infection (14)(15) and patients treated with DAA with cirrhosis continue to have a >2% risk of developing HCC so they should remain under close surveillance (13).

1.3.1.3. Hepatitis D virus infection

Hepatitis delta virus (HDV) is a small RNA defective virus that needs HBV to replicate and propagate. It has been suggested that HDV accelerates the disease course, leading

to cirrhosis and likely enhancing HCC development, compared to HBV monoinfection (16)(17).

1.3.4. Alcohol

Alcohol consumption is an independent risk factor for several malignancies, starting with a dose of 10 g/1 unit/day. It has a relative risk of developing HCC of 2,07 for heavy drinkers compared to non-drinkers, being also slightly increased in occasional drinkers (18). Moreover, alcohol synergizes with other risk factors for HCC, such as diabetes mellitus and viral hepatitis (19).

A number of pathophysiological factors are specific to hepatic alcohol-mediated carcinogenesis including: 1) the formation of acetaldehyde and its direct detrimental effects on proteins and DNA; 2) an elevated production of CYP2E1 and iron-induced reactive oxygen species (ROS); 3) changes in the immune system and the induction of chronic inflammation; 4) interference with methyl group transfer and alterations to gene expression (18)(20).

1.3.5. Metabolic fatty liver disease

One quarter of the global population is estimated to have metabolic associated fatty liver disease (MAFLD). Its incidence is projected to increase by up to 56% in the next 10 years and, consequently, the prevalence of MAFLD-related HCC is likely to increase (21). Nowadays the proportion of HCC attributed to MAFLD represents 15-20% of cases in the West (22).

Many risk factors for MAFLD are also independently associated with HCC, including obesity, diabetes, Hispanic ethnicity, and genetic polymorphisms in PNPLA3, TM6SF2, GCKR, MBOAT7 and HSD17B13. Steatosis-related lipotoxicity and oxidative DNA damage can induce hepatocarcinogenesis (23). These factors may explain the association between MAFLD and HCC, especially in the absence of cirrhosis (24) (25-30% of MAFLD-associated HCC cases occur in the absence of cirrhosis) (6).

1.4. Clinical managements of HCC

1.4.1. Diagnosis

As mentioned before, most HCC occur in an identifiable at-risk population. According to this, **surveillance** strategies have been implemented in order to detect HCC at early stages. For that purpose, it is recommended that patients with cirrhosis undergo abdominal ultrasound evaluation every six months (25). However, >50% of cases are diagnosed at more advanced stages, identifying a liver mass on cross-sectional imaging performed for other reasons or after developing abdominal pain, weight loss or worsening of liver dysfunction (6).

Patients with an abnormal surveillance test, that is, detection of a liver nodule in abdominal ultrasonography or high serum α-fetoprotein levels (>20 ng/ml), belong to at-risk populations and require timely diagnostic evaluation (Figure 2) (3)(6)(26).

When a lesion ≥1 cm is detected in the liver ultrasound, either **multiphasic computed tomography (CT) or magnetic resonance imaging (MRI)** should be performed. The differences in blood flow and extracellular volume between HCC tissues and non-neoplastic cirrhotic liver tissue lead to hallmark imaging characteristics during the multiphasic flow of contrast, including arterial phase hyperenhancement, subsequent washout appearance, and capsule appearance (27)(28)(29).

If there is a clinical suspicion for HCC but the appearance is atypical by imaging, a **biopsy** or second contrast-enhanced study should be performed. The sensitivity of a biopsy is ~70% and is even lower in tumors <2 cm because of the potential for missed lesions as well as the difficulty in distinguishing well-differentiated HCC from dysplastic nodules. Patients with a negative biopsy should continue to be followed with serial contrast-enhanced imaging. If the lesion enlarges but retains its atypical appearance for HCC, a repeat biopsy should be considered (6)(26)(30).
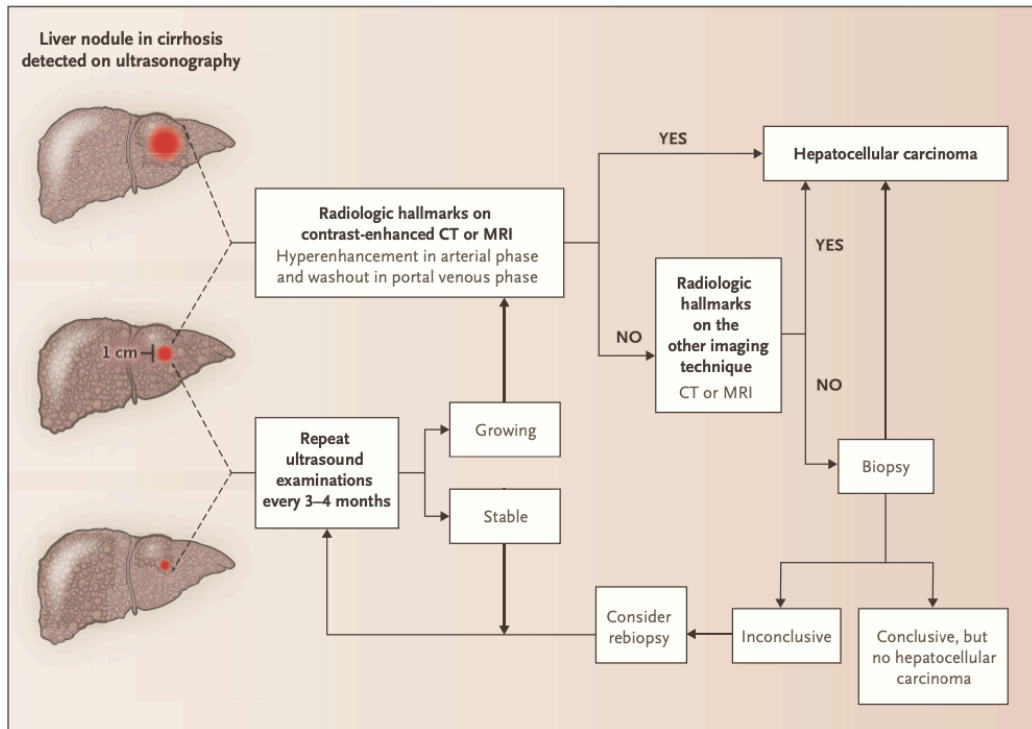
Figure 2. Diagnosis Algorithm for a Liver Nodule in Patients with Cirrhosis. CT: Computed Tomography, MRI: Magnetic Resonance Imaging. From Villanueva A et al. N Engl J Med. 2019 (3).

1.4.2. Staging

Since 80-90% of HCC patients also have concomitant liver disease, the clinical management of this disease is complex and needs to be addressed carefully. The patient's overall health status and the benefits of treating the tumor must be balanced against the potential harms of medical interventions (3)(6).

The **Barcelona Clinic Liver Cancer (BCLC)** classification is a worldwide recognized HCC clinical algorithm for the stratification of patients, that was firstly introduced in 1999 (31). It is endorsed by the European and American Guidelines (26)(32) and it takes into account not only tumor burden, but also liver function and health performance status and classify patients according to these characteristics into 5 stages, linking each one of them with a treatment of choice and a prognostic estimation. It has been externally

validated in different clinical settings (33)(34) and is an evolving system that has been continuously updated according to the growing scientific evidence in the field (35). So far, the only biomarker included in the BCLC algorithm remains alpha-fetoprotein (AFP), despite the amount of research and greater knowledge of molecular pathogenesis of HCC.

Other staging system exist but their implementation is restricted to certain geographic areas, for example, the Hong Kong Liver Cancer staging system (36) or the Cancer of the Liver Italian Program (37).

The BCLC algorithm classifies patients as being in one of five stages (Figure 3) (35):

- **BCLC 0 (or very early HCC)**: Patients in this stage have a solitary HCC ≤2 cm without vascular invasion or extrahepatic spread in a patient with preserved liver function and no cancer-related symptoms (PS 0). The expected median survival of patients with BCLC 0 HCC is more than 5 years.
- **BCLC A (or early HCC)**: These patients present solitary HCC irrespective of size or as a multifocal HCC up to 3 nodules (none of them >3 cm), without macrovascular invasion, extrahepatic spread or cancer-related symptoms (PS 0). Liver function must be preserved. HCC patients in this stage have a median survival of more than 5 years.
- **BCLC B (or intermediate stage)**: Patients with a multifocal HCC (exceeding BCLC-A criteria) with preserved liver function, no cancer-related symptoms (PS 0) and no vascular invasion or extrahepatic spread. BCLC B HCC patients have a median survival of 2,5 years.
- **BCLC C (or advanced stage)**: This stage includes patients presenting with vascular invasion or extrahepatic spread who are still relatively fit, as reflected by a PS ≤2 at staging work-up, and who have preserved liver function. HCC patients at this stage have a median survival of 2 years.

- **BCLC D (or terminal stage)**: Patients with major cancer-related symptoms (PS >2) and/or impaired liver function without the option of liver transplantation due to HCC burden or non-HCC-related factors. BCLC D HCC patients have a median survival of 3 months.
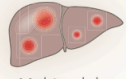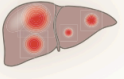
Figure 3. Clinical Algorithm for the Management of Hepatocellular Carcinoma. ECOG: Eastern Cooperative Oncology Group. PS: Performance status. Modified from Villanueva A et al. N Engl J Med. 2019 (3).

1.4.3. Management

The management of HCC has improved over the past decade. The treatment depends on the tumor stages and the expected benefits of major interventions, as based on the BCLC staging system (Figure 4) (35).
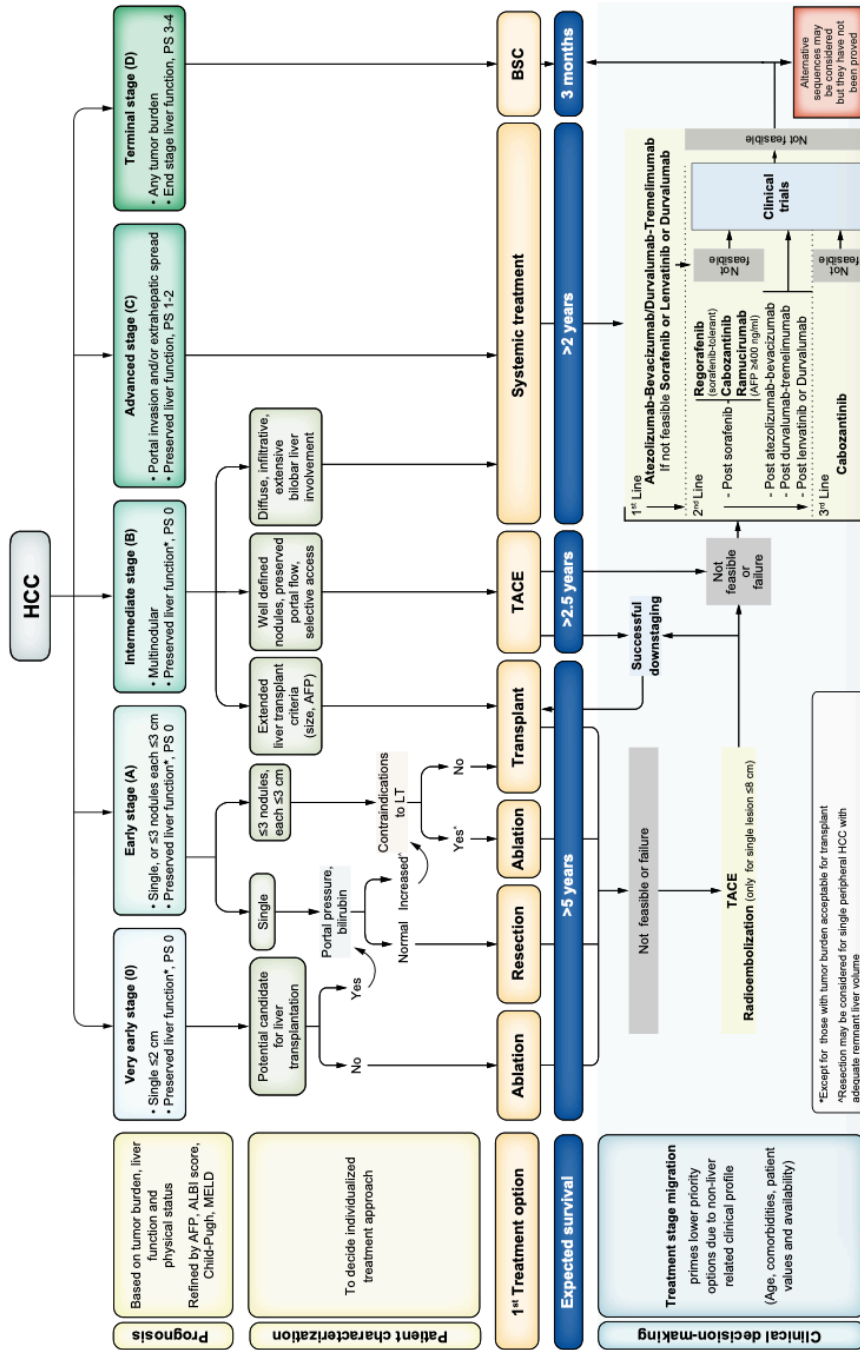
1.4.3.1. Surgical therapies

Surgical treatment, which include hepatic resection and liver transplantation, are curative treatments of HCC with a 5-year survival of 70-80% (6).

The decision between resection and liver transplantation requires consideration of the patient's liver function, the presence and extent of portal hypertension, performance status, and tumor characteristics such as size, number and involvement of the hepatic and portal veins (6)(32)(26).

Resection

Resection is recommended as the primary treatment for HCC in patients with a single tumor, Child class A liver function with total bilirubin <1mg/dL, no evidence of clinically significant portal hypertension, and excellent performance status (32)(26). The criteria also require patients to have no evidence of extrahepatic disease or invasion of portal or hepatic veins on imaging (38).

Resection is associated with survival >60% at 5 years and with a low postoperative mortality of <3% (3).

70% of these patients that undergo HCC resection have tumor recurrence (39). Recurrences can be divided into either early (<2 years), resulting from micrometastases following resection, or late (>2 years), resulting from de novo tumors (40). No adjuvant therapies have been shown to reduce recurrence until now (41), however in January 2023, a press release has notified that the combination of Tecentriq (Atezolizumab) in combination with Avastin (Bevacizumab) tested in a Phase III trial reduce the risk of

cancer returning in certain types of early stage liver cancer (42). Extended data in presentations and publications are currently awaited.

To date, recurrence risk can only be estimated according to anatomopathological findings such as presence of satellitosis, multifocality or microscopic vascular invasion (43). In fact, the presence of any of these poor prognosis anatomopathological findings in the surgical specimen implies to consider the patient as a transplant candidate (indications *ab initio*) before tumor recurrence (25)(44). Due to this high risk of recurrence, it would be of great importance to identify patients who could benefit from a change of therapeutic strategy before recurrence occurs.

Liver transplantation

Patients with cirrhosis, a single tumor $\leq$ 5cm or 2-3 tumor $\leq$ 3cm without vascular invasion are considered for liver transplantation according to the so-called Milan criteria (45); macrovascular tumor invasion or extrahepatic spread are formal contraindications for liver transplantation because of the high risk of tumor recurrence. In addition to removing the tumor, transplantation has the advantage of curing the liver disease (3).

Long-term outcomes of liver transplantation are considered superior than resection, which has a 70% recurrence rate and a 10-year survival of 7-15% (46)(6).

1.4.3.2. Local tumor ablation

Tumor ablation is recommended in patients with BCLC 0 or A not candidates for resection or liver transplantation.

Ablation is used to direct injury the tumor, and can be achieved with chemicals, such as percutaneous ethanol injection (PEI), thermal ablation, which includes radiofrequency ablation (RFA), microwave ablation (MWA), cryoablation and laser interstitial thermotherapy (LITT) or electrical methods as irreversible electroporation (IRE)(47).

The main method is image-guided, percutaneous radiofrequency ablation, and as compared with resection, has fewer complications but provides worse local control for larger tumors (48).

1.4.3.4. Transarterial therapies

Patients with BCLC stage B tumors should be considered for transarterial therapies (26)(32). The main transarterial therapy is transarterial chemoembolization (TACE), which consists in an intraarterial infusion of a cytotoxic agent, followed by embolization of the vessels that feed the tumor.

TACE associated mortality is below 1%, mostly due to liver failure. Estimated overall survival is >30 months (47)(49). TACE should not be considered in patients with decompensated cirrhosis (3).

Another transarterial therapy is transarterial radioembolization (TARE). TARE is a procedure involving the intra-arterial delivery of glass microspheres or resin microspheres embedded with yttrium (6).

Randomized phase 3 studies are currently evaluating the combinations of ICIs with TACE and radioembolization (50). TACE combined with TKIs has been evaluated in several randomized trials, only obtaining negative results (51)(52).

1.4.3.5. Systemic therapies

Systemic therapies are recommended for patients with BCLC C or for BCLC B patients not benefiting from transarterial therapies due to extension or unsuccessful prior TACE (26)(32). It is estimated than 50% of HCC patients are treated with systemic therapies, due to diagnosis at more advanced stages or because progression of the disease over time (6)(53).

HCC systemic treatments had evolved rapidly over the past 5 years with the approval of additional first-and second-line systemic treatments (Figure 5), after a decade with sorafenib as the only standard of care for advanced HCC.
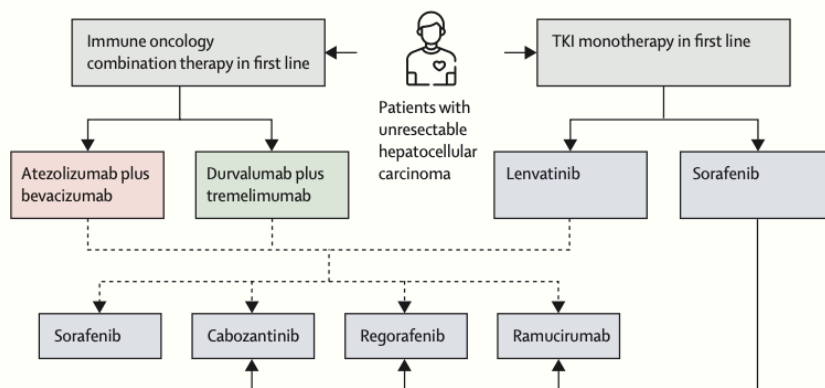
Figure 5. Systemic therapies options for patients with hepatocellular carcinoma. TKI: tirosin kinase inhibitors. From Vogel A et al. Lancet. 2022 (54)*.*

First-line therapies

For a decade, **sorafenib** was the only approved first-line treatment and the standard of care in advanced HCC since its approval in 2007.

Sorafenib is a multitarget tyrosine kinase inhibitor (TKI) that targets VEGF receptor, PDGF receptor, RAF and several other tyrosine kinases, and it was the first targeted therapy to show efficacy in patients with advanced HCC (55).

The SHARP trial demonstrated the superiority of sorafenib to placebo (55). It was a multicenter, phase 3, doble-blind, placebo-controlled trial that included 602 patients with advanced hepatocellular carcinoma who had not received previous systemic treatment. Sorafenib treatment significantly increases the overall survival of patients in comparison with placebo (10,7 vs 7,9 months; hazard ratio (HR) 0.69; 95% confidence interval (CI), 0.55 to 0.87; p<0.001) (55).

On 2018, **lenvatinib** was approved as a first-line treatment for advanced HCC, 10 years after sorafenib approval. Lenvatinib is an oral multikinase inhibitor that targets VEGF receptors 1-3, FGF receptors 1-4, PDGF receptors α, RET and KIT (56).

The REFLECT study demonstrated lenvatinib efficacy (56). It was an open-label, phase 3, multicenter, non-inferiority trial that included 954 patients with advanced HCC who had not received treatment for advanced disease, patients were randomly assigned to lenvatinib or sorafenib. Median survival time for lenvatinib of 13,6 months was non-inferior to sorafenib, that was 12,3 months (HR 0,92, 95% CI, 0,79 to 1,06) (56).

Both treatments are associated with grade 3-4 drug-related adverse events in 50% of treated patients.

Atezolizumab and bevacizumab (anti-PD-L1 antibody and anti-VEGF antibody respectively) combination was the first treatment to improve overall survival compared to sorafenib. The IMbrave150 trial demonstrated the efficacy of this combination in 2020 (57). It was a global, open-label, phase 3 trial, that included 501 patients with unresectable HCC who had not previously received systemic treatment. Median survival was 19,2 months for patients who received atezolizumab plus bevacizumab and 13,4 months for the sorafenib group (HR 0,58, 95% CI, 0,42 to 0,79; p<0.001). Median progression-free survival was 6,8 months and 4,3 months in the atezolizumab-bevacizumab and sorafenib group respectively. As a consequence of these positive results, atezolizumab and bevacizumab combination has become first-line therapy for advanced HCC for patients with no formal contraindication (35).

The combination of **tremelimumab and durvalumab** (anti-CTLA-4 and anti-PD-L1 respectively) has also been reported to be superior to sorafenib according to the HIMALAYA trial results (58), and has been recently approved by FDA (Food and Drug Administration), showing an overall survival HR for durvalumab-tremelimumab versus sorafenib of 0,78 (96% CI, 0,65 to 0,93; p<0.005). The median overall survival was 16,43

months with durvalumab-tremelimumab, 16,56 months with durvalumab, and 13,77 months with sorafenib (58).

For patients with advanced HCC that may not be appropriate candidates for atezolizumab-bevacizumab, or durvalumab-tremelimumab, TKIs (sorafenib or lenvatinib) could still be considered as a first-line treatment (59).

Second-line therapies

As second-line treatments, three TKIs (regorafenib, cabozantinib and ramucirumab) have been approved for the treatment of HCC patients progressing to sorafenib.

Regorafenib is a multi-kinase inhibitor targeting VEGFRI-3 and other kinases, it demonstrated a survival of 10,6 months versus 7,8 months (HR 0,63, 95% CI, 0,50 to 0,79; p<0·0001) in the placebo group in the RESORCE study (60).

Cabozantinib is a multi-kinase inhibitor targeting VEGFR2, AXL and MET. Its efficacy was demonstrated in the CELESTIAL trial, demonstrating an overall survival of 10,2 months compared with the placebo group that was 8 months (HR 0,76; 95% CI, 0,63 to 0,92; p=0.005) (61).

Ramucirumab is the only biomarker-guided therapy for HCC, with is indicated for patients with baseline α-fetoprotein levels of $\geq$400ng/dl. The REACH-2 trial demonstrated an improvement in the median overall survival for ramucirumab (8,5 months) compared with placebo (7,3 months) (HR 0,71, 95% CI, 0,531 to 0,949; p=0,0199) (62).

Other emerging treatments

New immunotherapy combination strategies are being developed and tested. Two treatments (nivolumab plus ipilimumab and pembrolizumab) had received FDA accelerated approval based on phase II studies (53).

Introduction

Nivolumab is an anti-PD-1 antibody. It received the FDA accelerated approval after the results of the phase I/II CheckMate 040 trial (63). However, the phase III trial (CheckMate 459) did not show significantly differences in the overall survival between the nivolumab group (16,4 months) and the sorafenib group (14,7 months) (HR 0,85, 95% CI, 0,72 to 1,02; p=0,075) (64). **Nivolumab plus ipilimumab** (anti-CDLA 4) achieved promising results in the phase I/II CheckMate040 (65). Phase III trial is currently ongoing (66).

Despite the promising results of **pembrolizumab** (anti-PD-1) in the KEYNOTE-224 phase II trial (67), the KEYNOTE-240 phase III trial showed there were no significantly differences between the median overall survival of the pembrolizumab group (13,8 months) and the placebo group (10,6 months) (HR 0,781, 95% CI, 0,611 to 0,998; p=0,0238) (68). By contrast, KEYNOTE-240 phase III in a subgroup of patients from Asia showed an overall survival of 13,8 months for pembrolizumab vs 8,3 months for placebo (HR 0,55; 95% CI, 0.37 to 0.80) (69).

Biomarkers that are predictive of response to anti-PD-1 therapy include PD-L1 expression when assessed by immunohistochemistry, which has been shown to be associated with response to anti-PD-1 therapy in several cancers and is approved as a diagnostic assay for treatment of non-small-cell lung and gastric cancers. By contrast, tumor PD-L1 was not associated with response to nivolumab nor pembrolizumab in patients with hepatocellular carcinoma (63)(67).

So, immunotherapies, and in particular ICIs, have revolutionized the therapeutic landscape of advanced HCC, however, objective radiological responses are limited to around 20% of patients depending on the trial (57)(58)(65)(69), and some of the patients will not benefit at all, presenting progression of the disease, so it is of utmost relevance to identify biomarkers of response to ICIs in this setting.

1.4.3.6. Assessment of response

The gold standard for radiological response assessment in solid tumors is **RECIST 1.1** (Response Evaluation Criteria in Solid Tumors), that measures the sums of the maximum diameters of target lesions at baseline and the changes during the follow-up (70). **mRECIST** (modified RECIST) criteria was developed to capture response under systemic therapies that impact cytostatic or cytotoxic effects (71). **iRECIST** (immune RECIST) defines objective changes in tumor size which can be used in immunotherapy clinical trials (72).

1.5. Molecular characteristics

1.5.1. Molecular pathogenesis of HCC

1.5.1.1. Hepatocarcinogenic process and drivers

HCC develops in 80% of cases in the setting of liver cirrhosis, harboring particular molecular alterations. The natural history of HCC in cirrhosis include a sequence of events starting with precancerous cirrhotic nodules, called low-grade dysplastic nodules (LGDN) and high-grade dysplastic nodules (HGDN), which can finally, under different genomic inputs, transform into HCC (73). Replicative stress in hepatocytes induces genetic lesions promoting HCC occurrence and progression (53)(74).

HCC can also develop in the context of chronic liver disease without cirrhosis or marked inflammation, for example in patients with HBV infection. HBV is able to insert in the genome in cancer genes, inducing the formation of HCC (6). HCC in a liver without cirrhosis can also be a late consequence of an hepatocellular adenoma (75).

Beside the environmental factors involved in HCC development, there are genetic factors that predispose to liver disease. These genetic factors include single-nucleotide polymorphisms as PNPLA3 (rs738409), TM6SF2 (rs585542926) and HSD17B13 (rs72613567) (76).

HCC tumors have on average 60-70 somatic mutations. The majority are mutations that do not participate directly in the carcinogenetic process, the called "passenger mutations", but some mutations can be "driver mutations" that activate signaling pathways that are key for liver carcinogenesis (Table 1) (53)(77)(78).

Table 1. Key oncogenic drivers and pathways de-regulated in HCC. From Llovet JM et al. Nat Rev Dis Primers. 2022 (53).

Altered pathway	Altered gene	Type of alteration	Percentage (range)
Telomere maintenance	TERT	Promoting-activating mutation	55 (44-59)
		High-level focal amplification	6 (1-9)
		Viral insertion	3 (1-5)
Cell cycle regulation	TP53	Loss-of-function mutation	27 (18-31)
		Homozygous deletion	2 (0-2)
	ATM	Loss-of-function mutation	4 (2-5)
	RB1	Loss-of-function mutation	4 (3-5)
		Homozygous deletion	5 (4-6)
	CDKN2A	Loss-of-function mutation	2 (1-3)
		Homozygous deletion	5 (4-6)
	MYC	High-level focal amplification	12 (4-18)
	CCND1	High-level focal amplification	7 (5-7)
WNT-β-catenin signaling	CTNNB1	Activating mutation	29 (23-26)
	AXIN1	Loss-of-function mutation	7 (4-10)
	APC	Loss-of-function mutation	2 (0-3)
Chromatin remodeling	ARID1A	Loss-of-function mutation	8 (4-12)
	ARID2	Loss-of-function mutation	7 (3-10)

	KMT2A	Loss-of-function mutation	3 (0-4)
	KMT2C	Loss-of-function mutation	3 (2-5)
	KMT2B	Loss-of-function mutation	2 (0-4)
	BAP1	Loss-of-function mutation	2 (0-5)
	ARID1B	Loss-of-function mutation	1 (0-3)
	RPS6KA3	Unclassified	4 (3-6)
	PIK3CA	Activating mutation	2 (1-4)
	KRAS	Activating mutation	1 (0-1)
Ras-PI3K-mTOR	NRAS	Activating mutation	0 (0-1)
	PDGFRA	Mutation	1 (0-4)
	EGFR	Activating mutation	1 (0-2)
	PTEN	Loss-of-function mutation	1 (0-2)
FGF signaling	FGF19	High-level focal amplification	6 (5-6)
VEGF pathway	VEGFA	High-level focal amplification	5 (1-8)
Oxidative stress	NFE2L2	Activating mutation	4 (2-6)
	KEAP1	Activating mutation	3 (2-5)
Hepatocyte differentiation	ALB	Mutation	9 (5-13)
	APOB	Mutation	8 (1-10)
JAK-STAT	IL6ST	Mutation	2 (0-3)
	JAK1	Mutation	1 (0-3)
TGF-b signaling	ACVR2A	Loss-of-function mutation	4 (1-10)
IGF signaling	IGF2R	Mutation	1 (0-2)

The major signaling pathways disrupted in HCC development are the following (Figure 6):
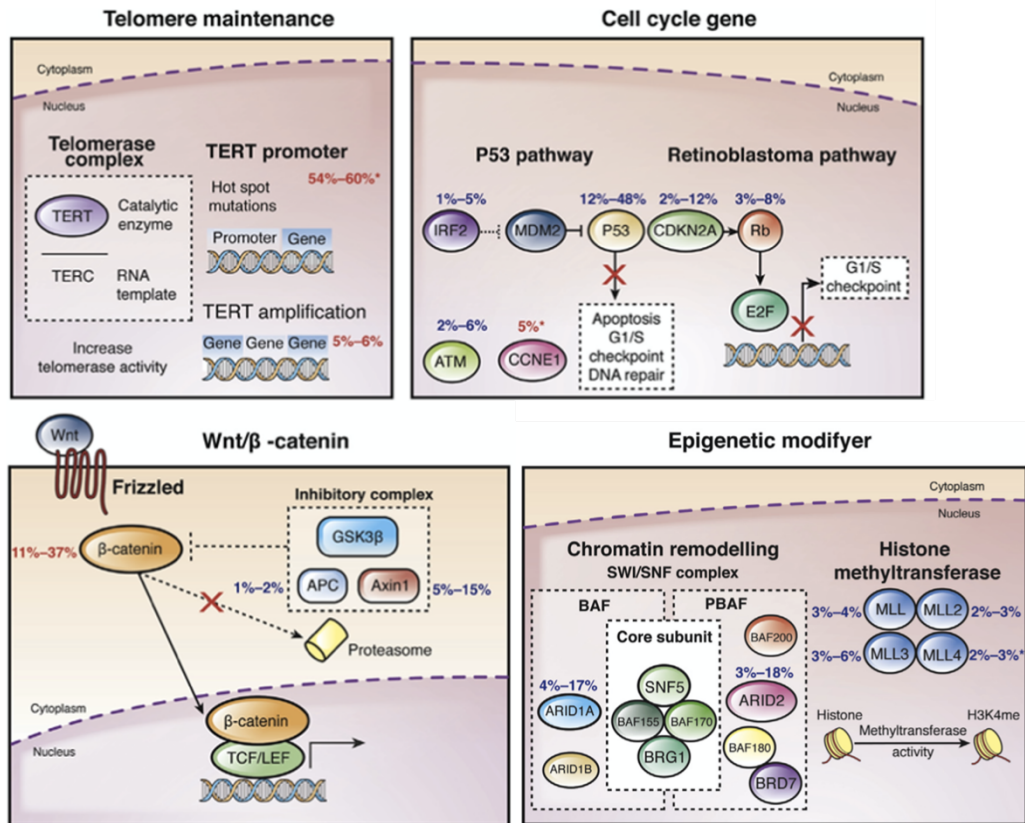
Figure 6. The genetic landscape of HCC. Red: activating mutations of oncogenes, blue: inactivating mutations of tumor suppressors. TERT: telomerase reverse transcriptase, IRF: interferon regulatory factor, MDM2: murine doble minute 2, CDKN2A: cyclin dependent kinase inhibitor 2, Rb: retinoblastoma, ATM: ataxia-telangiectasia mutated, CCNE1: cyclin E1, GSK: glycogen-synthetase kinase, APC: anaphase-promoting complex, TCF/LEF: T cell factor/lymphoid enhancer factor family. Modified from Zucman-Rossi J et al. Gastroenterology. 2015 (73)*.*

Somatic mutations in the **TERT promoter** region are the most prevalent ones, being present in 60% of HCCs (79). TERT codes for telomerase reverse transcriptase, an enzyme essential for telomere elongation and maintenance to prevent chromosome erosion at each cell division (80). Hepatocytes expressing high levels of telomerase exist distributed throughout all liver zones, and this may contribute to hepatocarcinogenesis by preventing cellular senescence (53). Due to the progressive increase of TERT

mutation from LGDN (9%) to HGDN (20%) and to eHCC, TERT is considered as a gatekeeper gene (81). TERT overexpression is mostly related to TERT promoter mutations (55%), but it can also be because of HBV DNA insertion in the promoter (3%), or copy number amplification (6%) (82).

The second most frequent altered gene in HCC is **CTNNB1** (29% of cases). CTNNB1, that codes for β-catenin, is part of the WNT/β catenin pathway that is implicated in physiologic embryogenesis, zonation, and metabolic control in liver. This oncogenic pathway is activated by activating mutations in CTNNB1, but also by inactivating mutations of **AXIN1** (in a 7%) and **APC** (2%). CTNNB1 mutated tumors present a specific gene expression profile characterized by overexpression of classical target genes (for example glutamine synthetase, GLUL, and leucine-rich repeat-containing G protein-coupled receptor 5, LGR5) and a specific histologic pattern with intra-tumor cholestasis (83).

A crosstalk between telomerase reactivation and WNT signaling has been suggested considering that TERT promoter mutation frequently co-occur with CTNNB1 mutations (79)(84).

As seen in other neoplasms, the tumor suppressor gene **TP53** is also mutated in HCC, in 27% of cases. TP53 protein provides essential functions in the cellular response to diverse stresses and safeguards maintenance of genomic integrity. It is the most frequently detected genetic alteration in human cancer (85). On the other hand, also affecting the cell cycle, the retinoblastoma pathway that controls the progression from G1 to S phase of the cell cycle, has been reported to be suppressed in HCC, due to **RB1** and **CDKN2A** mutation or homozygous deletion (86)(87).

Mutations in epigenetic modifiers form chromatin remodeling complex are recurrent in HCC. The most typical ones are inactivating mutations in **ARID1A** and in **ARID2** (8% and 7% respectively), underlining the key role of SWI/SNF chromatin remodeling complexes

(BAF and PBAF) as tumor suppressors. The physiologic role of these complexes is to modify chromatin structure and nucleosome position. Indirectly, they modify transcription fate of the cell (73)(88).

1.4.1.2. Molecular classes of HCC

Genomic, epigenomic, histopathological and immunological studies have divided HCC into two molecular groups that reflect specific alterations, histopathological fingerprints, and clinical outcomes. Nowadays, this classification is not used in clinical practice, further studies are needed to establish its value for patient prognostication and therapy selection (6)(89).

HCC of the **proliferation class** are associated with mutations in TP53, chromosomal instability and enrichment in HBV-associated HCC (73). Tumors of this class have clinical characteristics of aggressive tumors as vascular invasion and present poor prognosis signatures (90)(91). The proliferation class can be divided into two subclasses: 1) The proliferation-progenitor cell group that presents progenitor-like features including expression of EpCAM and α-fetoprotein and activation of classic proliferation pathways as PI3K-AKT-mTOR, RAS or MET; and 2) the proliferation-WNT-TGFβ group that is characterized by non-canonical activation of Wnt (3)(6).

The **non-proliferative class** is more prevalent in alcohol and HCV related HCC and is associated to better outcomes and to lack of strong proliferative signaling and retains molecular features resembling to normal hepatic physiology (6). It can be subdivided into one class characterized by canonical Wnt signaling activation and CTNBB1 mutation and another characterized by IFNα signaling activation (88)(92).

1.4.2. Molecular insight of immunotherapy in HCC

1.4.2.1. Immune microenvironment of HCC

The liver is a central immunomodulator that ensures organ and systemic protection while maintaining immunotolerance (93). In principle, tolerance needs to be induced against antigens from tissues, ingested food or commensal bacteria and against malignant cells (94). Deregulation of this tightly controlled liver immunological network is a hallmark of chronic liver disease and HCC (Figure 7). Immune activation or evasion is dictated by the opposing actions of antitumor effectors and their suppressors in the tumor microenvironment (TME) (95)(96).
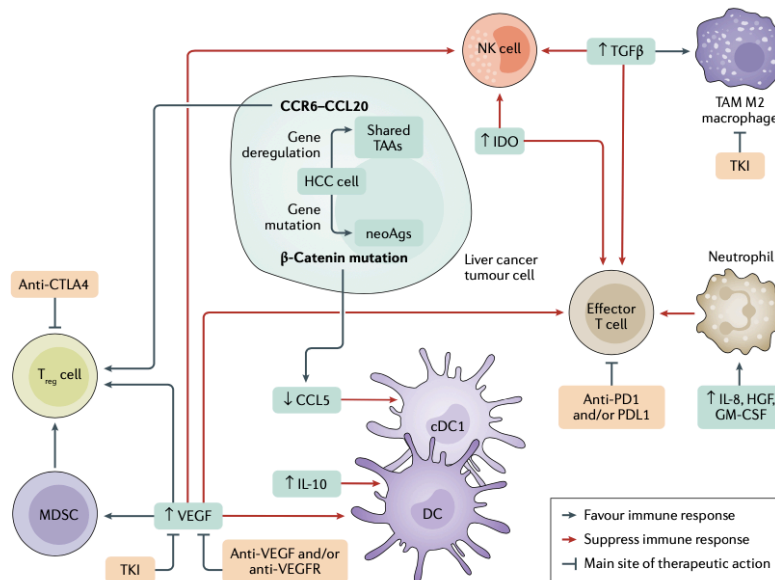
Figure 7. Key players in the hepatocellular carcinoma immune tumor microenvironment. CTLA4: cytotoxic T lymphocyte-associated antigen 4, GM-CSF: granulocyte–macrophage colony-stimulating factor, HGF: hepatocyte growth factor, IDO: indoleamine 2,3-dioxygenase-1, TGFβ: transforming growth factor-β, TKI: tyrosine kinase inhibitor, VEGF: vascular endothelial growth factor, VEGFR: vascular endothelial growth factor receptor. From Sangro B et al. Nat Rev Gastroenterol Hepatol. 2021 (96).

Introduction

In HCC, the first step for the development of a tumor-specific T cell response is the expression of tumor antigens. CD8+ T cells specific for AFP, glypican 3 (GPC3), melanoma-associated gene 1, and New York oesophageal squamous cell carcinoma 1 (NY-ESO1) can be detected in blood and tumor samples from patients with HCC (97)(98). Moreover, genomic mutations occurring during hepatocarcinogenesis might lead to amino acid changes that create cancer neoantigens that enhance the HLA-binding capacity of the peptide, making the novel epitope noticeable to T cells (89).

On the other hand, there are mechanisms that contribute to **immune evasion**. The key cells with major immunosuppressive roles implicated in HCC immune evasion include tissue-resident macrophages (mainly Kupffer cells) as well as monocyte-derived macrophages, regulatory T (Treg) cells and myeloid-derived suppressor cells (MDSCs) (93)(94). These cell types suppress effective innate and adaptive immunity against HCC, in cooperation with dysfunctional dendritic cells (DCs), dysfunctional CD8+PD1+ T cells (in the context of MAFLD), neutrophils and regulatory B (Breg) cells, among others (95)(99).

There are several mechanisms that contribute to hepatocarcinogenesis and immune evasion:

1) **Cytokines** and other soluble mediators. Secretion of TGFβ, IL-10 IDO and arginase in the TME promote immunosuppression (95)(100). The tumor-derived cytokines CXCL5 and CCL15 recruit immunosuppressive neutrophils and monocytes respectively (101), and CXCL13 secreted from hepatic stellate cells recruits B cells. On the other hand, pro-inflammatory cytokines, such as IL-2, IFNγ, CXCL10 and CXCL9, attract cells to mount an antitumor immune response. Therefore, the balance of these stimuli defines the quality of the immune composition and response (93). These observations have implications for patients receiving immunotherapies.

2) Overexpression of **immune-checkpoint** molecules as PD-1, PD-L1, CTLA4, LAG3 and TIM3, that contribute to T cell exhaustion (95).

3) Recruitment of **Treg cells** and IL-17-expressing CD4+ T helper 17 (TH17) cells (93).

4) Promotion of **angiogenesis** by myeloid-derived suppressor cells that produce VEGF, TGFβ and arginase, with suppress T cell activation (92)(93).

5) Downregulation of major histocompatibility complex class II (**MHC II**) and costimulatory molecules (such as CD80 and CD86) (102).

6) Mutations in **tumor-intrinsic signaling cascades** that affect the immune microenvironment. CTNNB1 mutations that activate WNT-β-catenin signaling pathway downregulates the expression of CCL5 and impairs DC recruitment, promoting immune escape and resistance to ICIs (103). MYC overexpression leads to PD-L1 overexpression. TP53 mutations promotes the recruitment of immunosuppressive cells (95). ARID1A mutation that downregulates IFNγ signaling by limiting chromosomal accessibility (104).

1.4.2.2. Mechanism of action of immunotherapies

As previously commented, in the past few years, new systemic therapies have revolutionized the management of HCC, particularly with the arrival of immune checkpoint inhibitors (ICIs) to HCC systemic therapy. Atezolizumab and Durvalumab are anti-PDL1 antibodies, Nivolumab and Pembrolizumab are anti-PD1 antibodies and Ipilumab and Tremelimumab are anti-CTLA-4 antibodies. Bevacizumab is a monoclonal antibody anti-VEGF (Figure 8).
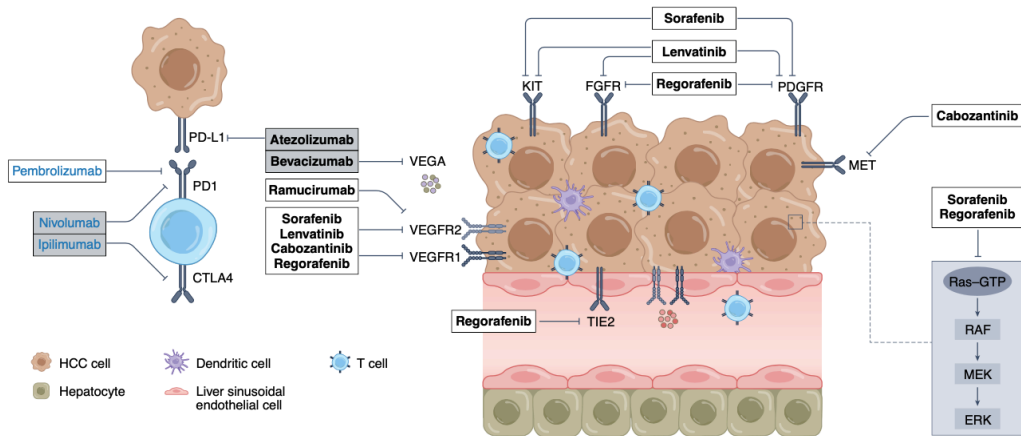
Figure 8. Molecular description of systemic therapies in HCC. PD-1: programmed cell death protein 1, PD-L1: programmed death-ligand 1, CTLA-4: cytotoxic T lymphocyte protein 4, VEGFR: vascular endothelial growth factor receptor, VEGA: vascular endothelial growth factor angiogenesis, KIT: tyrosine-protein kinase, FGFR: fibroblast growth factor receptor, PDGFR: platelet-derived growth factor receptor, TIE2: tyrosin-protein kinase receptor, GTP: guanosine phosphatase. From Llovet JM et al. Nat Cancer. 2022 (53)*.*

Immune checkpoint molecules are a specific subtype of membrane-bound molecules that are key modulators of antitumor T cell responses and can be expressed by T cells, antigen-presented cells (DCs and macrophages) and by tumor cells, among others (105). The immune checkpoints most studied in human cancer are programmed cell death protein 1 (PD-1), cytotoxic T lymphocyte protein 4 (CTLA-4), lymphocyte activation gene 3 protein (LAG-3), B and T lymphocyte attenuator (BTLA), and T cell immunoglobulin and mucin-domain containing-3 (TIM-3) (106)(107).

PD-1 is a key factor on the effector phase in the immune response, **PD-L1** and PD-L2 are their ligands and is up-regulated by various cytokines, in particular IFN-γ. Upon binding to its ligands, PD-1 inhibits CD8 T cell activation by blocking T cell receptor (TCR) signaling and inhibits CD4 activation and proliferation through increasing secretion of IL-10. Cancer cells express PD-1 ligands to escape from immunosurveillance. This process in which PD-1-PD-L1 engagement block TCR signaling and inhibits T cell proliferation and secretion of cytotoxic mediators is called T cell exhaustion (108)(109).

CTLA-4 is essential for the activation of CD4 T cells. Expressed on activated T cells, CTLA-4 has great affinity for CD80 and CD86. The interaction of CD28 with these receptors results in decreased T cell activation upon antigen presentation. Treg also express CTLA-4 constitutively. Treg inhibit the immune response through various mechanisms including depletion of IL-2 and secretion of immunosuppressive factors, such as TGF-b, IL-10 among others (108)(110).

Blockade of other co-inhibitory checkpoints, such as LAG3 or TIM3, as well as other strategies for stimulating the immune system are now being investigated (105).

Clinical trials showed the potential of combining anti PD-1/PD-L1 antibodies with anti-angiogenic TKIs or antibodies, having evidence of synergy of both. Anti-angiogenic TKI or antibodies inhibits VEGF signaling pathway. **VEGF pathway** inhibition could modulate the tumor vasculature and have direct effects in VEGF signaling on immune cells. In the tumor vasculature, VEGF inhibition could affect vessel pruning, resulting in hypoxia, and result in vessel normalization, resulting in improved drug delivery or enhancing immune cell attachment and extravasation. On the other hand, VEGF is an immunomodulatory molecule, so anti-VEGF therapies might reduce the infiltration and activity of MDSCs and T reg cells and decrease M2 macrophage polarization (111)(112).

1.4.2.3. Immune classification of HCC

According to its immune traits, HCC can be divided into two different classes (113). The **inflamed class**, which accounts for 35% of HCCs, is characterized by a high immune cell infiltration, high cytolytic activity and increased levels of PD1 and PD-L1 (95). This class can be divided into three subclasses: 1) The immune active subclass, which is enriched in interferon signaling, overexpression of genes related to adaptative immune response and favorable prognosis; 2) The immune exhausted subclass, that has an activated stroma, high levels of TGFβ signaling, T cell exhaustion and immunosuppressive components and 3) The immune-like subclass characterized by interferon signaling and

immune activation with the presence of CTNNB1 mutations (114). The inflamed class has demonstrated to be enriched in patients who responded to anti-PD1/PD-L1 antibodies. The other 65% of HCCs belongs to the **non-inflamed class**, characterized by T-cell exhaustion and high levels of chromosomal instability. It is divided in two subclasses: 1) Intermediate subclass, enriched in TP53 mutations; and 2) Excluded subclass, with activation of canonical WNT signaling through CTNNB1 mutations (53)(95).

This classification highlights that not all patients respond to these therapies, as seen in clinical practice, and therefore, that it is necessary to find biomarkers of response to ICIs therapies.

1.5. Liquid biopsy

The concept of liquid biopsy refers to the isolation and analysis of tumor components released into the bloodstream or other body fluids that can provide molecular information of the tumor (115). Conversely to standard biopsy, which is invasive and associated with potential risks such as pain, bleeding or seeding the cancer; liquid biopsy has the advantage of being easily repeatable and can provide a dynamic picture of the disease allowing monitoring the tumor progression. In addition, liquid biopsy may reflect different regions of the tumor and represent intra-tumoral heterogeneity (ITH) (116).

Over the past 20 years, few biomarkers have emerged, and despite much promising research, measurement of the tumor marker α-**fetoprotein (AFP)** remains the only biomarker widely used in clinical practice.

AFP is a glycoprotein that is normally produced during gestation by the fetal liver and yolk sac. Normal adult AFP levels are achieved between 8 and 12 months and can be elevated in patients with HCC (117). Although being the most widely used biomarker for HCC evaluation, there are two main reasons for the suboptimal performance of AFP as

serological test: 1) fluctuations in AFP levels are not only because of HCC development, but also might reflect, in patients with cirrhosis, flares of HBV or HCV infection or exacerbation of the underlying liver disease, and 2) only a small proportion of tumors at an early stage (10–20%) present abnormal AFP serum levels (32). An AFP level of 20ng/ml is the commonly used threshold for the evaluation of HCC, nevertheless, AFP at this cutoff, has a sensitivity of approximately 60% and a specificity of 80% for the detection of HCC (118)(119).

There are four main AFP-based scores that predicts the probability of having HCC in patients with chronic liver disease: 1) GALAD score, that combines AFP, des-carboxy-prothrombin (DCP), AFP-L3, gender and age (120); 2) BALAD score that combines bilirubin albumin, AFP-L3%, AFP and DCP (121); 3) Doylestown Algorithm/Doylestown Plus that comprises log(AFP), age, gender, alkaline phosphatase and alanine aminotransferase serum levels (122); and 4) the HES algorithm combining age, AFP, rate of AFP change within 1 year, alanine aminotransferase serum levels and platelet count (123). Results of these scores are being validated in large prospective studies (117).

More recently, the field of liquid biopsy has been deeply studied, mostly nucleic acids, circulating tumor cells, and extracellular vesicles (Figure 9).
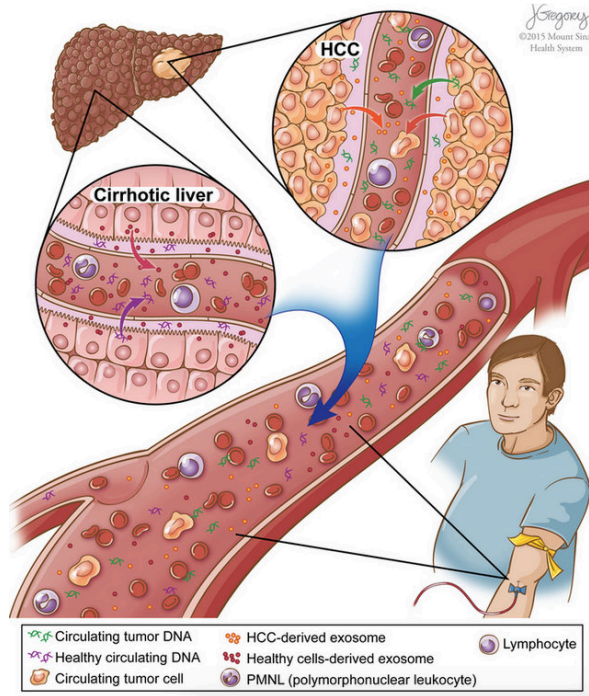
Figure 9. Liquid biopsy in HCC. From Labgaa I et al. Discov Med. 2015 (124)*.*

1.5.1. Circulating tumor DNA

Cell-free DNA (cfDNA) refers to fragmented DNA found in noncellular components of the blood, typically as double-stranded fragments of 150 to 200 base pairs. This DNA fragments are released into the bloodstream by an active or a passive mechanism, being the last one the predominantly mechanism and it is driven by necrosis or apoptosis of the cells (116). cfDNA released by tumor cells is what is called circulating tumor DNA (ctDNA). This occurs at any tumor stage and offers minimally invasive access to key molecular information of the tumor. The fraction of ctDNA in overall cfDNA in patients with cancer can vary from less than 0,1% to more than 90% (125).

ctDNA detection is challenging because of its rapidly degradation and because it requires sensitive and specific techniques. These technologies for ctDNA analysis can be classified into single-target assays and next generation-based (NGS) assay. Single target-

assays only detect aberrations limited to a single nucleotide of interest and is for example Droplet Digital PCR; and next generation-based assay that include whole genome or whole-exome sequencing (WES) or target sequencing of a gene panel of interest. Variant allele frequency (VAF) is the frequency at which a variant can be detected with enough confidence without an inherent sequencing error, it varies depending on the size of the gene panel for example, and this partially explains the differences in accuracy for ctDNA studies (126).

1.5.1.1. cfDNA Mutations

One of the first studies that explore ctDNA in HCC was focused on the Ser-249 mutation of TP53 gene in African population using restriction fragment length polymorphism. This is a "hotspot" mutation in HCC that is known to occur in population that is exposed to aflatoxins. A total of 119 patients were included in this study, and Ser-249 TP53 mutation was detected in a 36% of HCC patients, in a 15% of the cirrhotic patients and in 6% of the control patients (127).

Liquid biopsy may capture **intra-tumoral heterogeneity** (ITH) better than single-lesion tumor biopsy. A study evaluated 42 patients with gastrointestinal cancer with acquired resistances to target therapies showed that cfDNA identified more frequently molecular alterations linked to resistance mechanisms, showing that these alterations were not found in the tumor biopsy in 78% of cases. These data suggest that liquid biopsy may better capture the heterogeneity of acquire resistance than tumor biopsy (128).

Another proof-of-concept study addressed the performance of ctDNA, analyzed by ultra-deep sequencing of all exons with a target panel of 58 genes, to capture tissue HCC mutations. 21 somatic mutations were found in HCC tissue in 6 out of the 8 patients, and 71% of these mutations were also found in ctDNA, demonstrating that ultra-deep sequencing confidently detect somatic mutations found in tissue and that ctDNA is a minimally invasive tool to explore HCC genetics (129).

ctDNA mutations analyzed in **serial samples** allows to capture real-time tumor dynamics, disease progression or response to therapy (116). In a study with 34 long-term follow-up patients with HCC, SNVs and CNVs were analyzed by target sequencing and low-coverage whole genome sequencing, it showed that the levels of CNVs and SNVs decreased after surgery and showed a subsequent increase in those patients developing tumor recurrence, indicating that ctDNA could monitor treatment response or detect minimal residual disease (130). Another example is a study with 81 patients that underwent liver resection, that correlates increased mutant allele frequency with microvascular invasion and recurrence (131).

Although, NGS studies had great results, it could be a long and laborious process. **Droplet Digital PCR** (ddPCR) could be a more rapidly and affordable alternative. In this study, TERT C228T mutation was analyzed by ddPCR in 95 HCC patients and 45 liver cirrhotic patients. Plasma TERT mutation was detected in 44% of HCC patients and in none of non-HCC cirrhotic patients; it was also associated with increased mortality (132).

1.5.1.2. cfDNA methylation changes

DNA methylation changes play a role in cancer development and progression, and it is well known in HCC tissue (133)(134). These methylation changes can also be detected in cfDNA. Several studies showed that methylation changes detected in cfDNA correlate with HCC outcomes: hypomethylation of CTCFL (135) was associated with tumor recurrence and lower survival, and hypomethylation of LINE-1 (136) and methylation of IGFBP7 (137) with lower survival too. Diagnosis, survival and prognostic prediction models have been developed with cfDNA methylation markers with a high specificity and sensitivity (138)(139).

1.5.2. Circulating tumor cells

Circulating tumor cells (CTCs) are malignant cells derived from the primary tumor or metastases that migrate into the systemic circulation. CTCs represent a biomarker different from any of the existing cancer biomarkers as they represent a sampling of the patient's live tumor cells. There are three different categories of techniques used to isolate CTCs: immunoaffinity-based enrichment, biophysical property-based enrichment, and enrichment-free methods (140).

In terms of clinical implementation, CellSearch$^®$ was approved by de FDA and is the most commonly used technique for CTC enumeration. It uses iron-conjugated antibodies against EpCAM (Epithelial Cell Adhesion Molecule) and secondarily, antibodies against cytokeratin 8, 18, 19 (116)(126). Several studies used CellSearch$^®$ in HCC demonstrating EpCAM positive CTCs association with tumor recurrence. For example, in 2013 one study with 123 HCC patients established a cut off of +/=2 CTCs an independent prognostic factor for tumor recurrence (141). Thereafter data reinforced this association between HCC recurrence and EpCAM positive CTCs (142). However, EpCAM based CTC detection have some limitations, less than 30% of HCC have overexpression of EpCAM, being lower the number of CTCs detected in HCC compared with other cancers (143).

Moreover, more sophisticated technologies for CTC isolation have been reported. ImageStream flow cytometry uses imaging flow cytometry, using immunofluorescence of cytokeratin, EpCAM, AFP, glypican-3 and DNA-PK together with analysis of size, morphology and DNA content. A cut off of 1 CTC correlated significantly with overall survival of HCC patients (144).

Other sophisticated technologies, like single-cell RNA sequencing have allowed further characterization of CTC, demonstrating CTCs heterogeneity and detecting known oncogenic drivers in HCC such as IGF2 (145).

1.5.3. Extracellular vesicles

Extracellular vesicles (EVs) include microvesicles and exosomes that are nanoparticles with a lipidic bilayer that protects them from enzymatic degradation. EVs are released by all cells as part of normal physiological function. Exosomes are EVs enriched in cell-type specific, non-coding, regulatory RNA. Several studies analyzed these exosomal miRNA (126)(146). In HCC a specific regulation of exosomal miRNA have been reported. miR-222, miR-18a, miR-221 and miR-224 are upregulated in HCC patients and miR-101, miR-106b, miR-122 and miR-192 are downregulated compared with cirrhotic patients (147).

1.6. Molecular biomarkers of response to immunotherapies

1.6.1. Cytokines

Immune checkpoint inhibitors have revolutionized the therapeutic landscape of HCC, but additional data are required to identify patients who will benefit from immunotherapy. In other cancers such as non-small-cell lung cancer (NSCLC) and melanoma the focus has been on tumor-cell PD-L1 expression (148). Although PD-L1 positivity enriches for populations with clinical benefit, PD-L1 testing alone is insufficient for patient selection (149)(150)(151). More recently, PD-L1 expression has also been investigated in HCC. Pretreatment sPD-L1 levels have been described to be an independent prognostic factor predicting PFS and OS in HCC patients (152)(153), but it was not possible to identify correlations between sPD-L1 changes and tumor response or PFS, due to the limited number of patients in these studies.

Other cytokine levels are being investigated. In melanoma, for example, high baseline levels of IFNγ and IL-10 have been associated with response to nivolumab (154). Another study suggest that MCP1 and TNFα in baseline and early follow-up samples can predict disease progression in metastatic melanoma patients treated with checkpoint inhibitors (155). In HCC, also higher IL-6 and TNFα levels have been related to worse PFS

and OS in patients treated with ICIs (156). IL-6 serum levels are influenced by inflammatory conditions, reducing their specificity; high serum IL-6 levels were more frequently found in females, patients with high AST, AFP, DCP and with reduced liver function (157).

1.6.2. DNA profiling

Next-generation sequencing has provided a comprehensive mutational landscape of early stages HCC. However, data from molecular alterations in advanced HCC is limited. One of the reasons may be the lack of tissue samples in these advanced stages. Analysis of ctDNA mutations could be an alternative to access tumor molecular information (158).

In melanoma, several studies have suggested that Wnt/β-catenin signaling may be involved in the exclusion of CD8+ cells and in anti-PD1 resistance (159). In HCC, is also suggested the role of β-catenin activation in immune escape and resistance to anti-PD1 therapy in a mouse model (103).

Moreover, tumor mutational burden (TMB), defined as the number of non-synonimous mutations per megabase found in DNA of tumor specimen (160), has been associated with checkpoint inhibitors benefit in some cancers. It is possibly because tumors with high TMB present more non-self target neoantigens. Recognition of tumor neoantigens by host T cells is one of the critical factors predicting immunotherapy response. TMB can be measured in ctDNA with a parameter called blood TMB (bTMB) (161).

Regarding anti-PD1 therapy, the only FDA-approved biomarker is high TMB. In 2020, the FDA approved pembrolizumab for the treatment of tumor mutational burden-high (TMB-H) solid tumors (162).

Hypothesis

2. Hypothesis

HCC patients diagnosed at early stages are eligible for curative treatments. However, even after curative resection, there remain a risk of up to 70% of postoperative HCC recurrence. Prediction and early detection of these recurrences would be of utmost interest in clinical practice.

In advanced HCC, immunotherapy and in particular, immune checkpoint inhibitors have revolutionized the therapeutic landscape for advanced HCC. Two combinations of treatments including ICIs have become first line options in the advanced HCC setting after positive results in Phase III trials. However, objective radiological responses occur in around 20% of HCC patients and 30% of HCC treated patients have showed progression as best radiological response. Identify and validate biomarkers of response to these treatments in HCC patients is still an unmet need.

In this doctoral thesis we focused in these two main unmet needs, respectively in early and advanced stages: the prognosis and close follow-up in patients treated with curative therapies; and the identification of potential biomarkers of response to immunotherapies in the advanced setting.

The **main hypothesis** of this doctoral thesis was that liquid biopsy could help to refine current clinical approach and decision-making algorithms. In particular, we hypothesize that:

- Mutations in cfDNA detected by next-generation sequencing could refine the clinical follow-up and monitoring of HCC patients after curative treatments
- And that cytokine levels and cfDNA profiling could be potential markers of response to immune checkpoint inhibitors in advanced HCC patients.

Aims

3. Aims

The **main objective** of this doctoral thesis was to assess the utility of different components of liquid biopsy, cell-free DNA profiling and cytokine levels, as non-invasive plasma biomarkers for HCC management.

The **secondary aims** were:

- To evaluate the concordance degree between mutations detected in cfDNA and in tumor tissue using next-generation sequencing in HCC patients undergoing curative treatments.
- To monitor the evolution of those mutations in HCC patients during follow-up after treatment and assess their prognostic implications in this early-stage HCC cohort.
- To elucidate plasma cytokine levels association with response to immune checkpoint inhibitors in advanced HCC patients.
- To study the potential role of the levels of cfDNA, ctDNA and ctDNA mutational profiling role in identifying patients benefiting more from immune checkpoint inhibitors.

Methodology

4. Methodology

4.1. Study design and participants

4.1.1. Study 1

All patients were recruited at the Liver Unit, Hospital Universitari Vall d'Hebron and prospectively enrolled in the study. Samples from 30 patients with confirmed HCC, either with noninvasive radiological criteria or histological confirmation, were prospectively collected. Matched blood and tissue (HCC and surrounding nontumoral liver) samples were collected simultaneously from these 30 patients receiving curative treatments with surgical resection (n=27) or local ablation (n=3). Historical samples from 2 of these patients, obtained prior HCC diagnosis, were retrieved for this study. Serial blood samples were subsequently collected at multiple follow-up time points. Ten samples from healthy adults were obtained from blood donors from the Blood and Tissue Bank (Banc de sang i teixits, BST, Barcelona, Spain). Additionally, 21 blood samples from HCC patients at intermediate and advanced stages of the disease (BCLC B, n=7; BCLC C, n=8; and BCLC D, n=6) were also prospectively collected.

The detailed study design is shown in Figure 10. In total, 57 tissue (30 HCC tissues and 27 matched surrounding liver tissues) and 113 blood samples (83 plasma samples to extract cfDNA and 30 samples of peripheral blood mononuclear cells (PBMC) to extract germ line) were collected. The study was conducted in accordance with the Declaration of Helsinki. The institutional ethical review board approved the protocol (PR(AG)194/2015), and all patients gave written informed consent before inclusion.
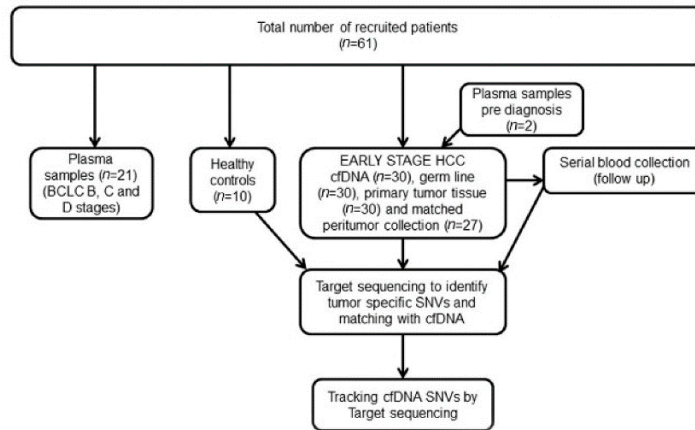
Figure 10. Flow diagram of the study 1 design. cfDNA: cell-free DNA, BCLC: Barcelona Clinic Liver Cancer, SNV: single number variation.

4.1.2. Study 2

Patients were prospectively recruited at the Liver Unit, Hospital Universitari Vall d'Hebron. Plasma samples from 25 non resectable HCC patients candidates to receive immune checkpoint inhibitors were prospectively collected. Treatments applied were respectively Nivolumab monotherapy (n=14), Atezolizumab/Bevacizumab combination (n=8), Durvalumab/Tremelimumab combination (n=2) or Lenvatinib/Pembrolizumab combination (n=1). Plasma samples from all patients were collected before starting immunotherapy and 3 months after the beginning of the treatment. From these 50 samples, cytokine levels by ELISA, cfDNA levels, ctDNA levels and TERT percentage mutation by ddPCR were analyzed. Onco-500 TruSight was performed in basal samples (plasma and PBMC) of 22 of these patients, due to limited ctDNA quantity. One of those 22 patients was excluded for the sequencing analysis because of low cfDNA quality (Figure 11).

The institutional ethical review board approved the protocol (PR(AG)194/2015), and all patients gave written informed consent before inclusion.
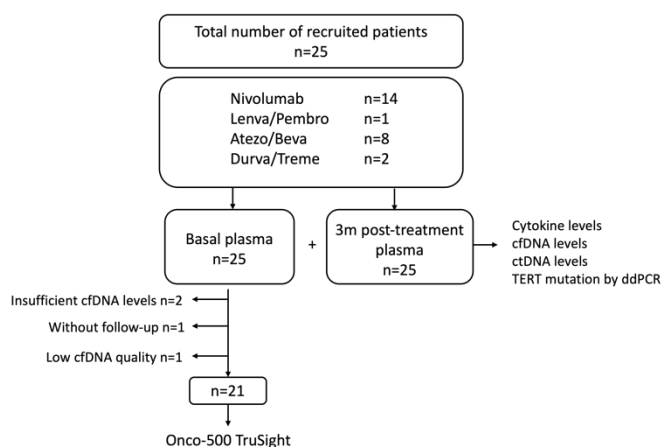
Figure 11. Flow diagram of the study 2 design. cfDNA: cell-free DNA, TERT: telomerase reverse transcriptase, ddPCR: droplet digital PCR.

4.2. Plasma collection

Peripheral venous blood was collected at least within the 24-48 h prior to surgery in a Lithium Heparin Tube (BD Biosciences, Franklin Lakes, NJ, USA) and processed within 4 h of collection. Plasma was collected after a first centrifugation at 1600× g for 15 min at 4 ∘C, and then was further centrifuged at 16,000× g for 10 min at 4 ∘C and was immediately stored at -80 ∘C.

4.3. Tissue collection

Liver specimens were collected ad hoc for this study at the operation room and brought to the Pathology Department to be processed with the help of an expert pathologist for specific tissue sampling and immediately stored at -80 ∘C.

4.4. cfDNA and ctDNA extraction and quantification

Circulating DNA was isolated from 1 mL of plasma using the MagMAXTM Cell-Free DNA Isolation Kit (Thermo Fisher, Waltham, MA, USA). Blood and tissue DNA was isolated using the QIAamp DNA Mini Kit (Qiagen, Hilden, Germany) according to the

manufacturer recommendations. Purified DNA concentration was measured by fluorometric quantitation using Qubit (Thermo Fisher, Waltham, MA, USA).

ctDNA was measured by Agilent D1000 ScreenTape (Agilent Technologies, USA) and analyzed by TapeStation Analysis Software A.02.01 SR1. Considering ctDNA fragments those smaller than 200 bp.

4.5. Droplet Digital PCR (ddPCR)

C228T TERT mutation was analyzed by QuantStudio 3D Digital PCR System (Thermo Fisher, USA), with TaqMan primers and probes also from Thermo Fisher (Hs000000092_rm). A known positive and negative DNA was included as control in each ddPCR run. The PCR reaction was performed using 1X ddPCR Master Mix, 1X TaqMan primer/probe for C228T TERT mutation, and 6,13 µl of DNA to a final reaction volume of 14 µL. The PCR mixture was loaded into the 20K Chip v2 (Table 2) (Table 3).

Table 2. ddPCR Reagent Mix

Reagent	Volume (µl)
Master Mix	7,52
TaqMan prime/probe (40x)	0,35
DNA	6,13

Table 3. ddPCR program

Steps	Temperature (ºC)	Time	Cycles
Initial denaturing	96	10'	1
Denaturing	55	2'	54
Annealing	98	30''	

| Extension | 55 | 2' | 1 |
| Conservation | 10 | ∞ | 1 |

The analysis and quantification of wild type and mutated alleles were performed using the QuantStudio 3D AnalysisSuite Cloud Software from Thermo Fisher.

4.6. Primer design and PCR

Primers were designed to amplify different regions enriched with hotspot containing frequent mutations in ARID1A, AXIN1, CTNNB1, TP53, and TERT promoter. Each primer has the universal sequence M13 incorporated and has different annealing temperatures (Table 4).

Table 4. Primer design for sequencing

Gene name		Primer sequence	5' Genome coordenates	3' Genoms coordenates	Size (pb)	T (◦C)	Size amplicon	Size amplicon +MID (pb)
ARID1A	Fw	TTATGGCACACTCCCTCCAG	26763119	26763100	20	59	157	197
	Rv	CATGGCGACAGCAGTTTCTT	26763256	26763237	20			
AXIN1	Fw	CGGATCTGGACCTGGGGTAT	346835	346816	20	57	151	191
	Rv	AAGTCGGCACAGCCCTCCTG	346685	346704	20			
CTNNB1	Fw	CAGAAAAGCGGCTGTTAGTCA	41224583	41224563	21	54	145	185
	Rv	CTCATACAGGACTTGGGAGGT	41224707	41224687	21			
TP53	Fw	TGGGCCTGTGTTATCTCCTA	7674311	7674292	20	57	148	188
	Rv	GGCAAGTGGCTCCTGACCT	7674182	7674164	19			
TP53	Fw	AAGATGTTTTGCCAACTGGC	7680753	7680734	20	57	166	206
	Rv	CATCGCTATCTGAGCAGCG	7680899	7680881	19			

TERT	Fw	CAGCGCTGCCTGAAACTC	1295036	1295053	18	65	163	203
	Rv	GTCCTGCCCCTTCACCTT	1295198	1295181	18			
M13	Fw	GTTGTAAAACGACGGCCAGT			20	60		
	Rv	CACAGGAAACAGCTATGACC			20			

PCR reactions and conditions were performed with the Start High Fidelity PCR system dNTPack (Roche Applied Science, Penzberg, Germany) following manufacturer recommendations, adding 5 µL of template DNA at 1ng/µl (Table 5)(Table 6).

Table 5. PCR Reaction Mix

Reagent	Volume (µl)
H_2O	14
Buffer 10x	2,5
Primer Fw (20µM)	0,75
Primer Rv (20µM)	0,75
dNTPs	0,5
DMSO	1,25
Polimerase	0,25
DNA	5

Table 6. PCR program

Steps	Temperature (◦C)	Time	Cycles
Initial denaturing	94	4'	1

Denaturing	94	30''	
Annealing	Tm	30''	35
Extension	72	45''	
Final extension	72	7'	1
Conservation	4	∞	1

In order to identify sequencies from different patients, molecular identifiers (MID) were used. PCR products were subjected to 15 cycles of a universal MID PCR using FastStart Taq DNA polymerase (Roche Applied Science, Penzberg, Germany) as previously published (163) (Table 7) (Table 8). The final MID amplification yielded from 185 to 216 bp fragments.

Table 7. MID PCR reaction mix

Reagent	Volume (µl)
H_2O	20,3
Buffer 10x	3,5
Primer Fw (20µM)	0,7
Primer Rv (20µM)	0,7
dNTPs	0,7
DMSO	1,75
Polimerase	0,35
DNA	7

Table 8. MID PCR program

Steps	Temperature (ºC)	Time	Cycles
Initial denaturing	94	4'	1
Denaturing	94	30''	
Annealing	60	30''	15
Extension	72	30''	
Final extension	72	7'	1
Conservation	4	∞	1

The PCR products were analyzed by 2% agarose gel electrophoresis, purified with DNA clean-up (NZY tech, Lisbon, Portugal) and quantified by fluorometric quantitation using Qubit (Thermo Fisher, Waltham, MA, USA). Negative controls (amplifications in the absence of DNA) were included in parallel to ascertain absence of contamination by template nucleic acids. Amplicon quality was analyzed using a BioAnalyzer DNA 1000 LabChip (Agilent, Santa Clara, CA, USA) prior to sequencing using Illumina MiSeq platform (Illumina, San Diego, CA, USA).

4.7. Next-Generation Sequencing

4.7.1. Library preparation

For the sequencing using the MiSeq platform (Illumina, San Diego, CA, USA), amplification products were adjusted to a concentration of 4×10^9 molecules/µl with Elution Buffer (EB) (10mM Tris-HCl, pH 8-8,5) (Qiagen, Valencia, CA, USA) and 10µl of each amplicon were pooled. Then the amplicon pools were purified using Kapa Pure beads (Roche Applied Science, Penzberg, Germany) to remove primers, nucleotides, salts and enzymes. The purified products were quantified by Qubit (ThermoFisher, Waltham, MA, USA). The genomic libraries were processed following the manufacturer

instructions for DNA library preparation kit Kapa Hyper Prep kit (Roche, Applied Science, Penzberg, Germany), during which each pool was indexed using SeqCap Adapter Kit A/B (Roche, Applied Science, Penzberg, Germany).

4.7.2. Library sequencing

Appropriate volumes of each pool were diluted with EB (10mM Tris-HCl, pH 8-8,5) (Qiagen, Valencia, CA, USA) to have a final concentration of 4nM. A final unique pool was made with 2μl of each pool. The final pool was quantified by LightCycler 480 (Roche, Applied Science, Penzberg, Germany) (Table 9).

Table 9. LightCycler 480 program

Steps	Temperature (ºC)	Time	Cycles
Denaturing	95	10′	1
Amplification	95	30″	35
	60	45″	
Melting curve	65	30″	1
	95	7′	1
Conservation	4	∞	1

To obtain a cluster density of 900K/mm^2, the final library pool was adjusted to a concentration of 15pM with HT1 from MiSeq Reagent Kit (Illumina, San Diego, CA, USA). PhiX (sequencing control) was also adjusted to the same concentration, and both were mixed to have a 16% of PhiX proportion. The library+PhiX mix was sequenced using MiSeq sequencing platform with MiSeq Reagent kit v2 (2 × 150 bp mode with the 300 cycle kit) (Illumina, San Diego, CA, USA).

4.8. Multiplex ELISA Technique

Multiplex ELISA was performed on the patients' plasma samples using a commercial kit and according to the manufacturer's guidelines (ProcartaPlex Multiplex Immunoassay, Thermo Fisher, USA). This assay allows testing of 24 chemokines, cytokines and growth factors in plasma samples. The following proteins were tested: BTLA, CD137 (4-1BB), CD152 (CTLA4), CD27, CD28, CD80, GITR, HGF, HVEM, IFN-β, IFN-γ, IL-1 β, IL-10, IL-12/IL-23p40, IL-21, IL-6, IP-10 (CXCL10), LAG-3, MCP-1 (CCL2), PD-1, PD-L1, PD-L2, TIM-3, TNF-α.

All samples, standards and negative controls were tested in duplicate.

The lecture was performed with MagPix Luminex XMAP technology (Thermo Fisher, USA) and analyzed with the ProcartaPlex Analysis App from Thermo Fisher.

4.9. PD-1 and PD-L1 ELISA

The levels of plasma PD-1 and PD-L1 were also measured with an ELISA kit with higher sensitivity (Thermo Fisher, USA). PD-L1 (BMS2212; sensitivity: 0,6 pg/ml, intraassay CV: 2,1%, interassay CV: 3,4%) and PD-1 (BMS2214; sensitivity 1,14 pg/ml, intraassay CV: 3,2%, interassay CV: 6,4%). The lecture was performed with Varioskan Lux Reader (Thermo Fisher, USA) and analyzed by Skanlt Software for Microplate Readers from Thermo Scientific version 6.0.

4.10. TruSight

4.10.1. Quality control of ctDNA

The quantity and quality of the DNAs were evaluated with Qubit dsDNA HS DNA Kit (Thermo Fisher Scientific) and Agarose gels, respectively. Sequencing libraries were prepared following TruSight Oncology 500 ctDNA Reference Guide (Document # 1000000092559 v00) with the corresponding kit (Illumina Inc. TruSight Oncology 500 ctDNA Kit (48 samples)).

4.10.2. Library preparation and enrichment

Using End Repair A-Tailing Master Mix, input DNA (30ng for ctDNAs and 40ng for sonicated-gDNAs) was blunt-ended and the 3' ends were A-tailed. Then, UMI1 adapters that contain unique molecular indexes (UMIs) were ligated to DNA fragments. After ligation product clean-up, library fragments were amplified using primers that add index sequences for sample multiplexing. Following this step, a pool of oligos specific to the 523 genes targeted by TruSight Oncology 500 ctDNA panel were hybridized to DNA libraries. In the next step, targeted regions of the enriched DNA libraries were bound with capture probes a second time. The second hybridization ensures high specificity of the captured regions. Then, Streptavidin Magnetic Beads were used to capture the probes hybridized to the targeted regions of interest. Resuspension buffer was used to rinse the captured libraries and remove nonspecific binding from the beads. Finally, enriched libraries were amplified, and a final clean-up step was performed.

4.10.3. Quality control of amplified libraries

Amplified libraries concentration was determined with Qubit fluorometer using the Qubit®dsDNA HS assay kit (Thermo Fisher Scientific) and their size distribution was assessed running an aliquot on an Agilent Technologies 2100 Bioanalyzer, using an Agilent High Sensitivity DNA Chip (Agilent Technologies). Libraries were then sequenced using TruSight Oncology 500 ctDNA Kit (48 samples) (Illumina, San Diego, CA, USA).

4.11. Data analysis

The raw fastq files acquired from MiSeq were first submitted to FLASH (164) to over-lap the paired-end reads and reconstruct full amplicons. Sequencing data analysis was conducted as previously published (163). An overlapping of paired ends (2 × 300) with a minimum of 20 overlapping bases, and a maximum of 10% differences were established. Full reads carrying 5% or more bases below a Q30 Phred score were discarded. The third step was a demultiplexing by specific amplicon primers with a

maximum of three differences. Reads were then collapsed into haplotypes with corresponding frequencies. All haplotypes with abundances below 0,1%, and not common to both strands were discarded and, finally, we filtered all variants below an abundance of 1% (163)(165).

Raw sequencing data from samples included in this article will be openly available upon publication via Sequence Read Archive of the NCBI (accession number PRJNA791805).

4.12. Statistical analysis

Quantitative clinical variables were described using mean ± standard deviation or median (interquartile range (IQR)) as appropriate to distribution. For qualitative variables, frequency and percentage were calculated. Boxplots by main outcomes have been constructed. Associations between cfDNA levels and clinical outcomes were assessed by nonparametric Mann-Whitney U-test. An ROC analysis was performed to identify cfDNA concentration capacity to discriminate patients with more than two mutations. Kaplan-Meier survival curves were estimated for survival and recurrence by cfDNA level. Hazard ratios and their 95% confidence intervals were calculated from univariate Cox regression for clinical and mutation-related variables. Data analysis was performed in R version 4.1.0 and Stata 15.1. Statistical analysis has been carried out by Statistics and Bioinformatics Unit (UEB), Vall d'Hebron Research Institute (VHIR).

Results

5. Results

5.1. Study 1

5.1.1. Study design and patient characteristics

We prospectively profiled blood and tissue samples from 30 patients with early HCC receiving curative therapy and 10 healthy controls. Matched blood and fresh frozen tissue samples were available for the 30 HCC patients. The median follow-up was 22,5 (1-50) months. At least one follow-up sample was analyzed for every patient (Figure 10). The clinical and demographic parameters of these patients are summarized in Table 10. The median age of HCC patients was 61,5 years, 76,6% were male, and liver cirrhosis was present in 26,6% of patients; viral etiology was observed in 43,2% and 16,6% presented MAFLD. The median diameter of the largest tumor was 3,75cm (range, 1-12 cm), while microvascular invasion (mVI) was present in 20% of the tissue samples. During study follow-up, tumor recurrence was observed in 12 patients (40%) and 7 patients died (23,3%).

Table 10. Clinicopathological characteristics in HCC patients (n=30) and Controls (n=10).

Demographic		Cases
Clinicopathological characteristics		
Gender, n (%)	Male	23 (76,6%)
Age, median (range)		61,5 (86-20)
Race/Ethnicity, n (%)	Caucasian	25 (83,3%)
Etiology, n (%)	HCV	11 (36,6%9
	MAFLD	5 (16,6%)
	Alcohol	4 (13,3%)
	HBV	2 (6,6%)

	Others	8 (26,6%)
Fibrosis, n (%)	F4	8 (26,6%)
	F3	9 (30%)
	F2/F1	13 (43,3%)
BCLC	BCLC 0	5 (16,7%)
	BCLC A	25 (83,3%)
Tumor size (cm), median (range)		3,75 (1-12)
Single tumor (%)	Yes	27 (90%)
	No	3 (10%)
Microvascular invasion (%)	Absent	24 (86,7%)
	Present	6 (20%)
Satellites (%)	Absent	26 (86,7%)
	Present	4 (13,3%)
Tumor Differentiation	Well	5 (16,7%)
	Moderate	22 (73,3%)
	Poor	3 (10%)
Events (%)	Recurrence	12 (40%)
	Death	7 (23,3%)
Follow-up, median months (range)		22,5 (1-50)
Laboratory values		
AFP (mg/dL), median (range)		17 (1,3-3233)
Bilirubin (mg/dL), median (range)		0,77 (0,37-2,25)
Albumin (g/L), median (range)		4,1 (2,5-4,7)

Platelet count (x10^9/L), median (range)		193 (103-266)
Demographics (Control samples)		Cases
Clinicopathological characteristics		
Gender, n (%)	Male	7 (70%)
Age, median (range)		56,6 (50-62)

5.1.2. Quantification of cfDNA in HCC patients

Median level of plasma cfDNA was significantly higher in HCC patients compared to control subjects (1,73 ng/µL, IQR 0,87-3,08 and 0,38 ng/µL, IQR 0,18-0,79; p=0,004) (Figure 12). Median cfDNA levels at diagnosis were significantly higher in patients who died during follow-up (n=7) than in patients remaining alive by the end of follow-up (2,90 ng/µL, IQR 2,23-3,26 and 0,98 ng/µL, IQR 0,70-2,44; p=0.0174) (Figure 12). To investigate the correlation between the concentration of preoperative cfDNA and survival, a cut-off value of 2 ng/µL of cfDNA was established by an ROC curve analysis with AUC=0,782 (Figure 12). Patients presenting with greater than 2 ng/µL of cfDNA had a higher mortality compared to patients with less than 2 ng/µL (mean survival time 24,6 months vs. 31,87 months, p=0,01) based on Kaplan-Meier's survival analysis (Figure 12). No correlation was observed between cfDNA concentration and tumor size, AFP levels or presence of vascular invasion.
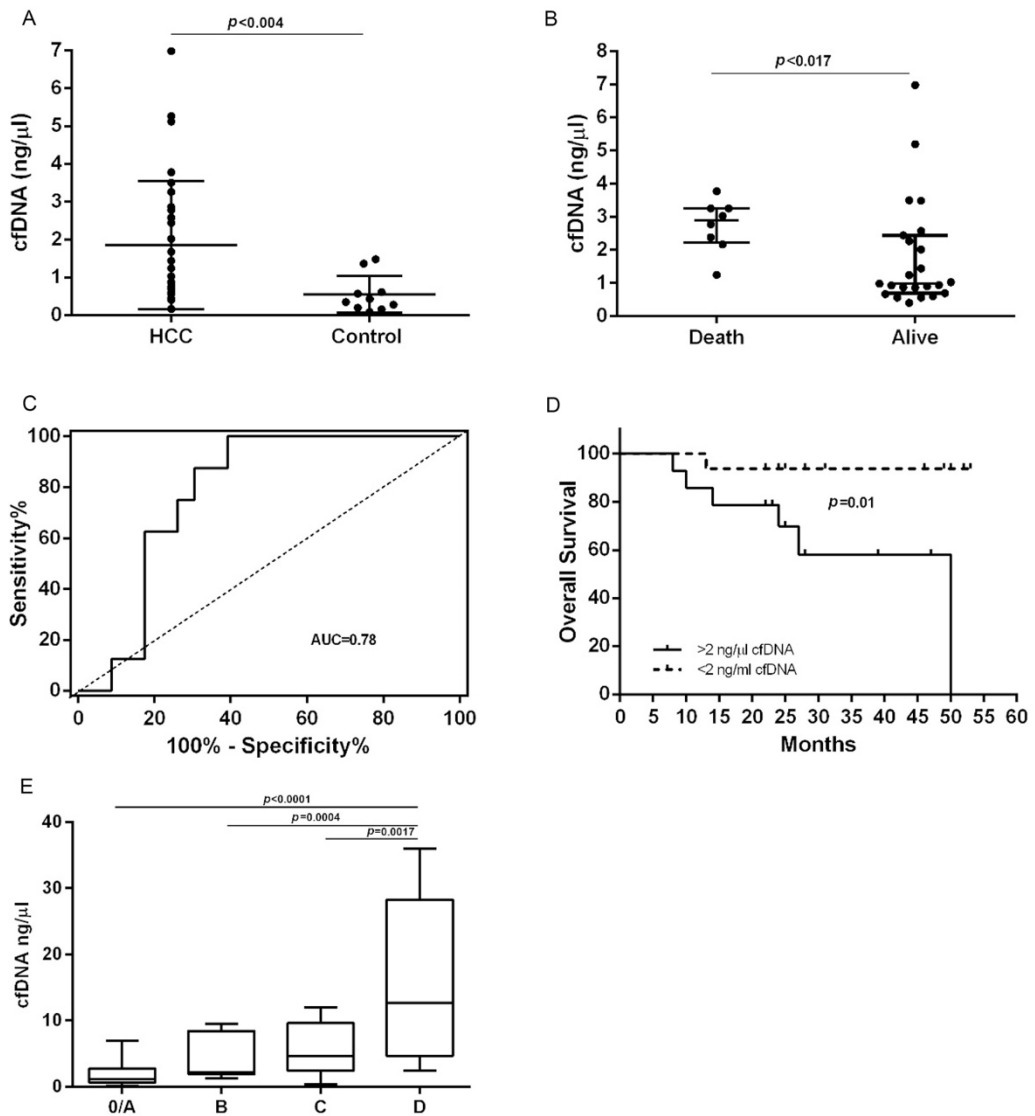
Figure 12. (A) cfDNA concentrations in patients with early-stage HCC and healthy controls. (B) cfDNA con-centrations in patients with early-stage HCC who were dead or alive at the end of follow-up. (C) ROC curve distinguishing patients with more than 2 mutations. (D) Kaplan–Meier curve of overall survival for HCC patients stratified by baseline cfDNA level; p-value from the log-rank test. (E) cfDNA levels stratified by BCLC stage (0: Very early, A: Early, B: Intermediate, C: Advanced and D: End-stage), cfDNA: cell-free DNA.

Additionally, cfDNA was quantified in patients with intermediate and advanced HCC (n=7 BCLC B, n=8 BCLC C and n=6 BCLC D) to compare cfDNA levels along BCLC stages. The clinical and demographic parameters of these patients are summarized in Table 11. As expected, those patients at more advanced stages (BCLC C and D) had a higher median cfDNA level (5,58 ng/μL, IQR 2,42-9.63 and 15,80 ng/μL, IQR 4,65-28,25, respectively) compared to patients at earlier stages (BCLC 0/A) (1,85 ng/μL, IQR 0,65-2) (Figure 12).

Table 11. Clinicopathological characteristics in HCC patients with different BCLC stages (n=51)

Demographics					
Clinicopathological characteristics					
		BCLC 0/A	BCLC B	BCLC C	BCLC D
Gender, n (%)	Male	23 (76,6%)	5 (71,4%)	7 (87,5%)	4 (66,6%)
Age, median (range)	Years	61,5 (20-86)	73,2 (55-83)	71 (51-82)	75 (60-85)
Race/Ethnicity, n(%)	Caucasian	25 (83,3%)	7 (100%)	8 (100%)	6 (100%)
Etiology, n(%)	HCV	11 (36,6%)	4 (57,1%)	2 (25%)	4 (66,7%)
	MAFLD	5 (16,6%)	1 (14,3%)	0 (0%)	0 (0%)
	Alcohol	4 (13,3%)	1 (14,3%)	3 (37,5%)	1 (16,7%)
	HBV	2 (6,6%)	1 (14,3%)	2 (25%)	0 (0%)
Tumor size (cm), median (range)	Rx	3,75 (1-12)	4,3 (1,6-6,5)	NM, 75% Diff/MF	NM, 83% Diff/MF
Single tumor, n (%)	Rx	27 (90%)	3 (42,9%)	2 (25%)	1 (16,7%)
Follow-up, median (range)	Months	22,5 (1-50)	18 (0-51)	3,6 (0-9)	0,63 (0-26)
Laboratory values					

AFP, median (range)	(mg/dL)	17 (1,3-2,25)	8,1 (2,7-2733)	117,9 (3,1-19283)	701,25 (2,5-1400)
Bilirubin, median (range)	(mg/dL)	0,77 (0,35-2,25)	1 (1,76-2,15)	1,46 (0,39-3,92)	0,91 (0,49-3,89)
Albumin, median (range)	(g/L)	4,1 (2,5-4,7)	4,2 (2,2-4,7)	3 (2,7-4,1)	2,55 (2-4,1)
Platelet count, median (range)	(10^9/L)	193 (103-266)	143 (76-173)	162 (97-310)	194 (89-385)

5.1.3. Mutations identified in plasma cfDNA and matched HCC tissue DNA

After observing detectable plasma levels of cfDNA in patients with HCC, NGS analysis was initially performed in early HCC tumor samples, matched surrounding tissue, cfDNA and PBMCs (as a germ line) from the 30 HCC patients who underwent curative treatments (resection n=27 or local ablation n=3); samples were analyzed by NGS with a median read depth of 46,281×. In total, 202 nonsynonymous somatic single-nucleotide variants (SNVs) with at least 1% of frequency were identified in the four types of samples analyzed from each HCC patient (n=30). Among all identified SNVs, 87% of them (174/202) were reported in COSMIC database (166), meaning that their occurrence had been previously observed, and 13% (28/223) were novel mutations.

The majority of patients had at least one mutation in HCC tissue DNA and cfDNA (70,6%-24/30; 86,7%-26/30, respectively). An average of 1,9 (range 0-9) mutations per patient were detected in HCC tissue, 4 (0-30) in cfDNA, 1,1 (0-10) in paired-adjacent tissue and 0,4 (0-3) in PBMCs (Figure 13).
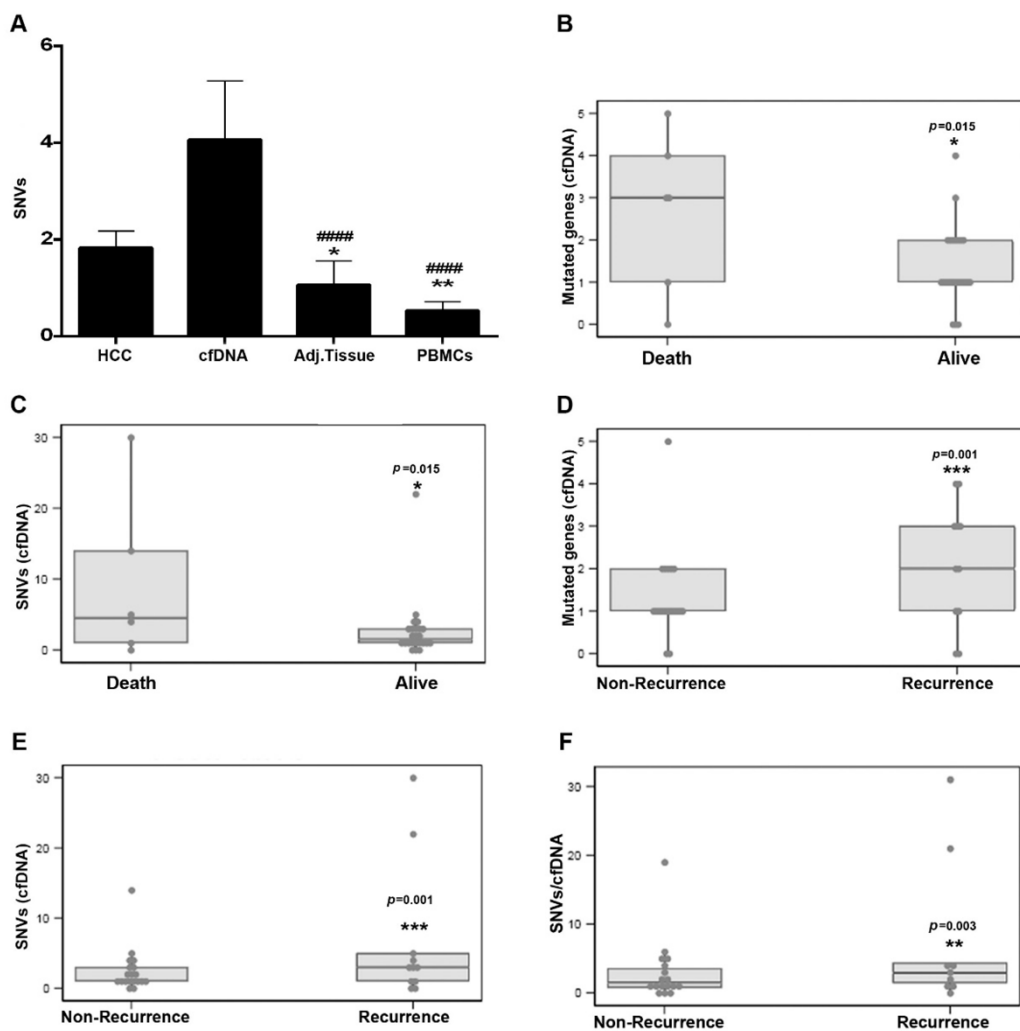
Figure 13. (A) Number of somatic mutations detected in HCC tissue, cfDNA, surrounding liver tissue and PBMCs of early-stage HCC patients, * p < 0.05, ** p < 0.01, *** p<0.001 vs. HCC tissue , #### p < 0.0001 vs. cfDNA. (B) Number of mutated genes detected in the cfDNA and (C) number of SNVs detected in the cfDNA of patients with early-stage HCC according to survival status (i.e., death vs. alive). Number of mutated genes (D), SNVs detected in the cfDNA (E) and ratio SNVs/cfDNA (F) in early-stage HCC patients according to presence/absence of recurrence. cfDNA: cell-free DNA, SNV: single-nucleotide variant, PBMCs: peripheral blood mononuclear cell.

Concordance between genetic variants, both in HCC tissue DNA and cfDNA samples, was analyzed. A total of 55 mutations were found in HCC tissue DNA. Among them, 29 (52,7%) also had evidence of identical carcinogenic mutations in matched cfDNA. Importantly, additional mutations not present in HCC tissue DNA were found in cfDNA. From a total of 104 mutations detected in cfDNA, 75 were additional mutations over those described in HCC tissue DNA. Therefore, mutations identified in cfDNA could provide additional molecular information about the tumor.

We further evaluated whether the number of mutated genes or the number of mutations in cfDNA of patients with early HCC could be useful in predicting prognosis. Subjects who died during follow-up had a significantly higher median number of mutated genes on their cfDNA at baseline than those subjects who remained alive by the end of follow-up (3, 1-4 vs 1, 1-2; p=0,015) (Figure 13 and Table 12). Patients who died were also more likely to have detectable mutations in their cfDNA (4,5; 1-14 vs. 1,5; 1-3; p=0.015) (Figure 13 and Table 12). The number of mutated genes (Figure 13) (p=0,001) and detected mutations (Figure 13) (p=0,001) in cfDNA were also significantly associated with recurrence, as well as the ratio between number of mutations and total amount of cfDNA (number mutations/cfDNA), which was also significantly associated with recurrence of patients with early HCC (1,5; 0,8-3,6 vs. 2,9; 1,4-4,4; p=0,003) (Figure 13 and Table 12).

Table 12. Univariate Cox analysis for mutation-related variables

Variable			Death			Recurrence		
			HR	(95% CI)	p-Value	HR	(95% CI)	p-Value
Presence of mutation in HCC tissue	No		1		0,939	1		0,802
	Yes		0,92	(0,11; 7,91)		0,82	(0,18;3,82)	
Number of mutations in HCC tissue			0,99	(0,82;1,19)	0,886	1,03	(0,93; 1,14)	0,592

Number of mutated genes in HCC tissue		0,76	(0,36;1,59)	0,465	1,11	(0,71;1,73)	0,643
Presence of mutation in cfDNA	No	1		0,589	1		0,484
	Yes	0,55	(0,06; 4,91)		0,57	(0,12; 2,72)	
Number of mutations in cfDNA		1,11	(1,02; 1,20)	0,015*	1,16	(1,06; 1,27)	0,001*
Number of mutated genes in cfDNA		2,37	(1,18; 4,74)	0,015*	2,88	(1,52; 5,47)	0,001*
Number of mutations/cfDNA		1,07	(0,99; 1,16)	0,089	1,2	(1,06; 1,35)	0,003*
Presence of mutations in adj tissue	No	1		0,158	1		0,9280
	Yes	0,21	(0,02; 1,85)		0,95	(0,30; 3,04)	
Number of mutations in adj tissue		0,97	(0,80; 1,17)	0,754	1,06	(0,98; 1,15)	0,1359
Number of mutated genes in HCC tissue		0,25	(0,03; 2,02)	0,193	1,17	(0,79; 1,72)	0,4285

The multivariate analysis showed that detection of more than four mutations in cfDNA correlated with a higher risk of death (long-rank p=0,042) (Figure 14 and Table 13). Those patients with a ratio (number of mutations/cfDNA) higher than six presented a higher risk of recurrence than those with a ratio under six mutations/cfDNA (long-rank p=0,0003) (Figure 14 and Table 13). Patients who presented mutations in more than two genes showed a higher risk of death and recurrence (long-rank p=0,028 and p=0,009, respectively) (Figure 14 and Table 13).

Figure 14. (A) Kaplan–Meier curve of overall survival for HCC patients stratified by number of mutations in the cfDNA. p-value from the log-rank test. (B) Kaplan–Meier curve of recurrence for HCC patients stratified by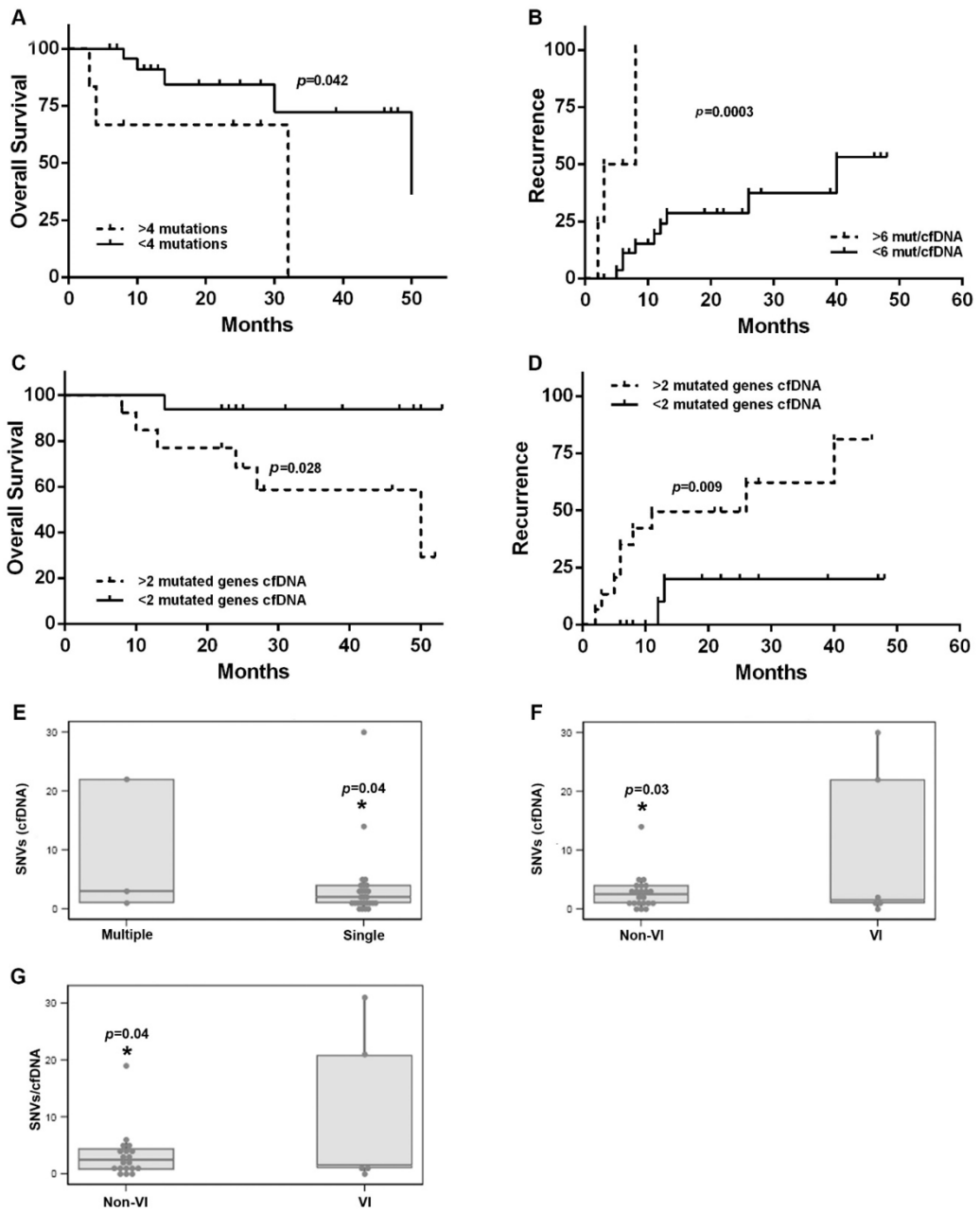 the ratio of number of mutations/cfDNA. p-value from the log-rank test. (C) Kaplan–Meier curve of overall survival for HCC patients stratified by number of mutated genes in cfDNA. p-value from the log-rank test.

*(D) Kaplan–Meier curve of recurrence for HCC patients stratified by number of mutated genes in cfDNA. p-value from the log-rank test. (E–G) Correlation between SNVs with poor prognosis status: number of SNVs detected in the cfDNA of early HCC patients with single or multiple foci of HCC (E), number of SNVs detected in the cfDNA of HCC patients with or without vascular invasion (F) and ratio of SNVs/cfDNA (G) detected in early HCC pa-tients with or without vascular invasion. SNV: single-nucleotide variant, cfDNA: cell-free DNA, VI: vascular invasion. * p < 0.05.*

Table 13. Multivariate Cox regression analysis for mutation-related variables

Cutt-Off Values		Death			Recurrence		
		HR	(95% CI)	p-Value	HR	(95% CI)	p-Value
Number of mutations in HCC tissue	No (<6)	1		0,4796	1		0,346
	Yes (>6)	2,23	(0,24; 20,4)		2,09	(0,45; 9,74)	
Number of mutations in cfDNA	No (<4)	1		0,0078*	1		0,06
	Yes (>4)	11,66	(1,91; 71,2)		3,54	(0,94; 13,35)	
Number of mutated genes in cfDNA	No (<2)	1		0,0287*	1		0,009*
	Yes (>2)	5,31	(1,19; 23,77)		9,61	(1,75; 52,7)	
N mutations/cfDNA	No (<6)	1		0,051	1		0,007*
	Yes (>6)	7,07	(0,99; 50,5)		7,44	(1,71; 32,3)	

Next, we sought to assess the relation between mutational status of cfDNA with well-known poor prognosis factors in clinical practice, observing that those patients with more than one HCC nodule had a higher ratio (number of mutations/cfDNA) (6; 1-31,3 vs 1,7; 0,8-4,0; p=0,04) (Figure 14). Moreover, both the number of mutations detected in the cfDNA and the ratio (number of mutations/cfDNA) were observed to be

significantly associated with the presence of microvascular invasion (p=0,03 and p=0,04, respectively) (Figure 14). Among clinical and analytical parameters included in Table 14, only size of the main nodule was found to be an independent risk factor of tumor recurrence.

Table 14. Univariate Cox analysis of independent risk factors of survival and recurrence

	Survival			Recurrence		
Variable	HR	(95% CI)	p-Value	HR	(95% CI)	p-Value
Age	0,97	(0,93; 1,01)	0,184	0,998	(0,96; 1,03)	0,8993
Gender	0,99	(0,11; 8,47)	0,990	2,04	(0,55; 7,59)	0,2879
cfDNA (ng/ml)	1,16	(0,76; 1,77)	0,501	0,91	(0,63; 1,31)	0,6147
Size main tumor	1,000	(0,77; 1,29)	0,999	1,23	(1,05; 1,45)	0,0109*
N of nodules (single vs multiple)	1,75	(0,19; 15,72)	0,883	2,74	(0,56; 13,46)	0,2189
Glypican	0,54	(0,06; 4,96)	0,589	0,27	(0,05; 1,43)	0,1248
Vascular invasion	1,15	(0,13; 10,35)	0,903	1,09	(0,23; 5,06)	0,9160
Bilirrubin	6,50	(0,84; 50,13)	0,072	2,21	(0,41; 11,89)	0,3570
Albumin (g/L)	0,58	(0,19; 1,77)	0,335	0,88	(0,34; 2,27)	0,7865
Creatinin	0,13	(0,00; 9,74)	0,354	0,10	(0,00; 2,53)	0,1627
AFP (ng/mL)	1,000	(0,97; 1,02)	0,971	1,005	(0,99; 1,01)	0,2679
Platelets (10^9/L)	1,000	(0,98; 1,01)	0,935	1,004	(0,99; 1,01)	0,2667

5.1.4. Variant characteristics in plasma and HCC tissue

Further analysis of mutations showed that the most commonly mutated gene in the total HCC patient cohort was TERT. At least one mutation of TERT promoter was found

in the 76,7% (23/30 patients) in both cfDNA and HCC tissue. At least one mutation in TP53 gene was detected in 50% (15/30) of cfDNA samples versus 33,3% (10/30) of HCC tissue, and CTNNB1 was mutated in 10% of cfDNA (3/30) and 33,3% (10/30) of HCC tissue of patients. Finally, 16,7% (5/30) and 10% (3/10) of patients presented mutations in AXIN1 on their cfDNA or HCC tissue, respectively, and mutations in ARID1A were found in 10% (3/30) and 6,7% (2/30) of patients in cfDNA and HCC tissue (Figure 15).
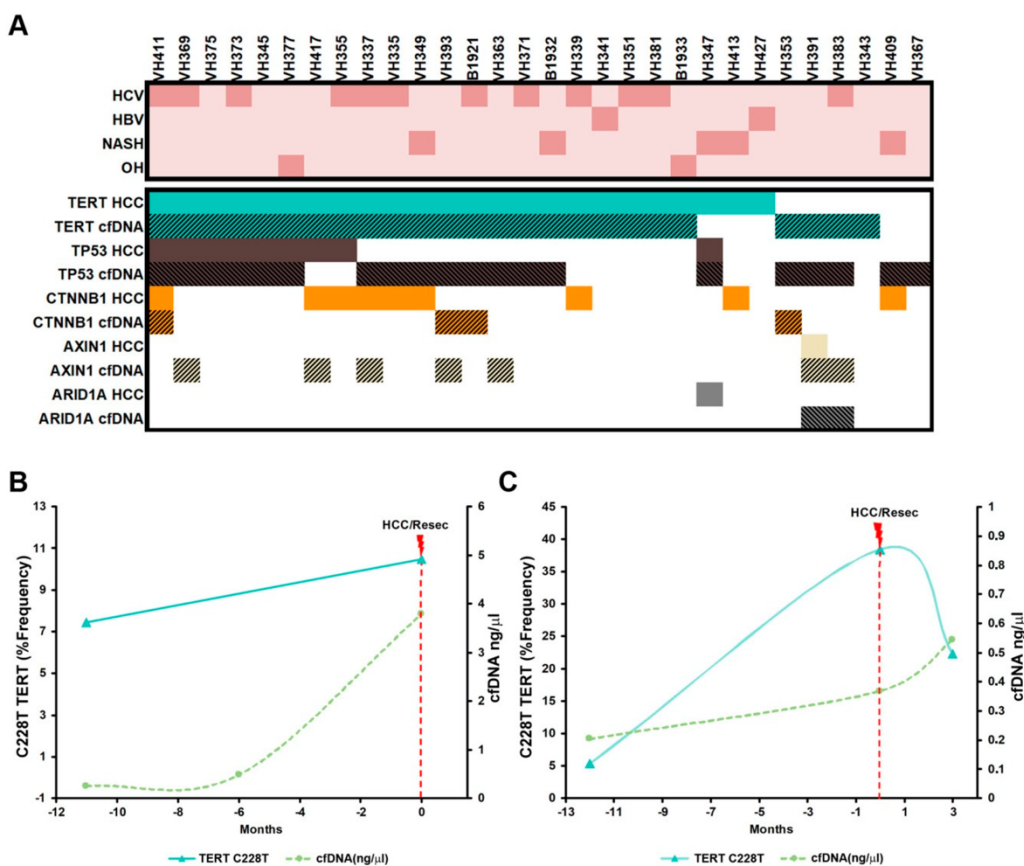
Figure 15. (A) Mutational landscape of patients with early-stage HCC using mutations found in cfDNA and HCC tissue in 30 patients. The heatmap illustrates the nonsynonymous mutations detected in plasma cfDNA and HCC tissue and the etiology information of the 30 HCC patients at the time of the curative intervention. (B,C) Early detection of C228T TERT mutation (−124) before HCC di-agnosis in two patients. The activating TERT promoter mutation C228T was detected in the cfDNA 11 and 12 months before diagnosis in VH341

and VH381 patients, respectively. HCV: hepatitis C virus, HCB: hepatitis B virus, NASH: nonalcoholic steatohepatitis OH: alcohol, cfDNA: cell-free DNA.

5.1.5. Early Detection of mutations in driver genes prior to HCC diagnosis

Very few studies have focused on the evaluation of cfDNA detection in early-stage cancers (BCLC 0/A) with even less data available on the detection of ctDNA in pre- HCC-diagnosis stored blood samples from HCC patients. We had the opportunity to analyze cfDNA from previously stored samples from two HCC patients. Samples were collected months before radiological diagnosis of HCC. Samples were analyzed in order to identify potential driver mutations detectable before the radiological diagnosis of HCC. One TERT mutation was found in the cfDNA of patients VH341 (HBV-related HCC) and VH381 (HCV-related HCC) 11 and 12 months before HCC diagnosis, respectively (Figure 15).

Two mutations were detected in the cfDNA from plasma obtained 11 months before the radiological diagnosis of HCC in patient VH341. The activating TERT promoter mutation C228T was detected at a frequency of 8% 12 months before diagnosis and 10% at the time of diagnosis (Figure 15). Tumor tissue frequency of C228T mutation was 1,95%. R249S mutation in TP53 was also detected at a frequency of 1,65% and 1,4% in cfDNA 11 months before diagnosis and at the time of diagnosis, respectively. The R249S variant was detected at a frequency of 0,4% in tumor tissue.

The activating TERT promoter mutation C228T was also detected 12 months before diagnosis in patient VH381 at a frequency of 5,34%, being 38,4% by the time of HCC diagnosis. Tumor tissue frequency of C228T mutation was 37,72% (Figure 15).

5.1.6. Dynamics of cfDNA and mutations during HCC progression

Next, to further explore whether cfDNA and SNVs dynamically change along with clinical evolution of patients, we analyzed sequential plasma samples collected from our cohort during their clinical course.

As shown in Figure 16, as an example, patient VH335 showed dynamical changes in SNV number and cfDNA levels correlating with HCC progression. Before receiving surgical treatment, low levels of cfDNA (1,03 ng/µL) were quantified and only the C228T in TERT promoter was detected in both cfDNA and HCC tissue (Figure 16). After 31 months of follow-up with no visible tumor lesions by MRI, cfDNA levels increased to 1,99 ng/µL, and a total of 37 mutations were detected in the cfDNA distributed along the five genes tested: TERT (16), TP53 (9), AXIN1 (6), ARID1A (4) and CTNNB1 (2) (Figure 16). Radiological progression was diagnosed 37 months after diagnosis and the patient was then treated with radiofrequency ablation. Both cfDNA levels (from 1,81 to 1,27 ng/µL) and observed tumor SNVs decreased after that therapeutic intervention, when four SNVs were detected in TERT promoter. Finally, after 45 months of follow-up, the patient progressed to an advanced HCC, increasing cfDNA levels to 4,25 ng/µL (Figure 16).
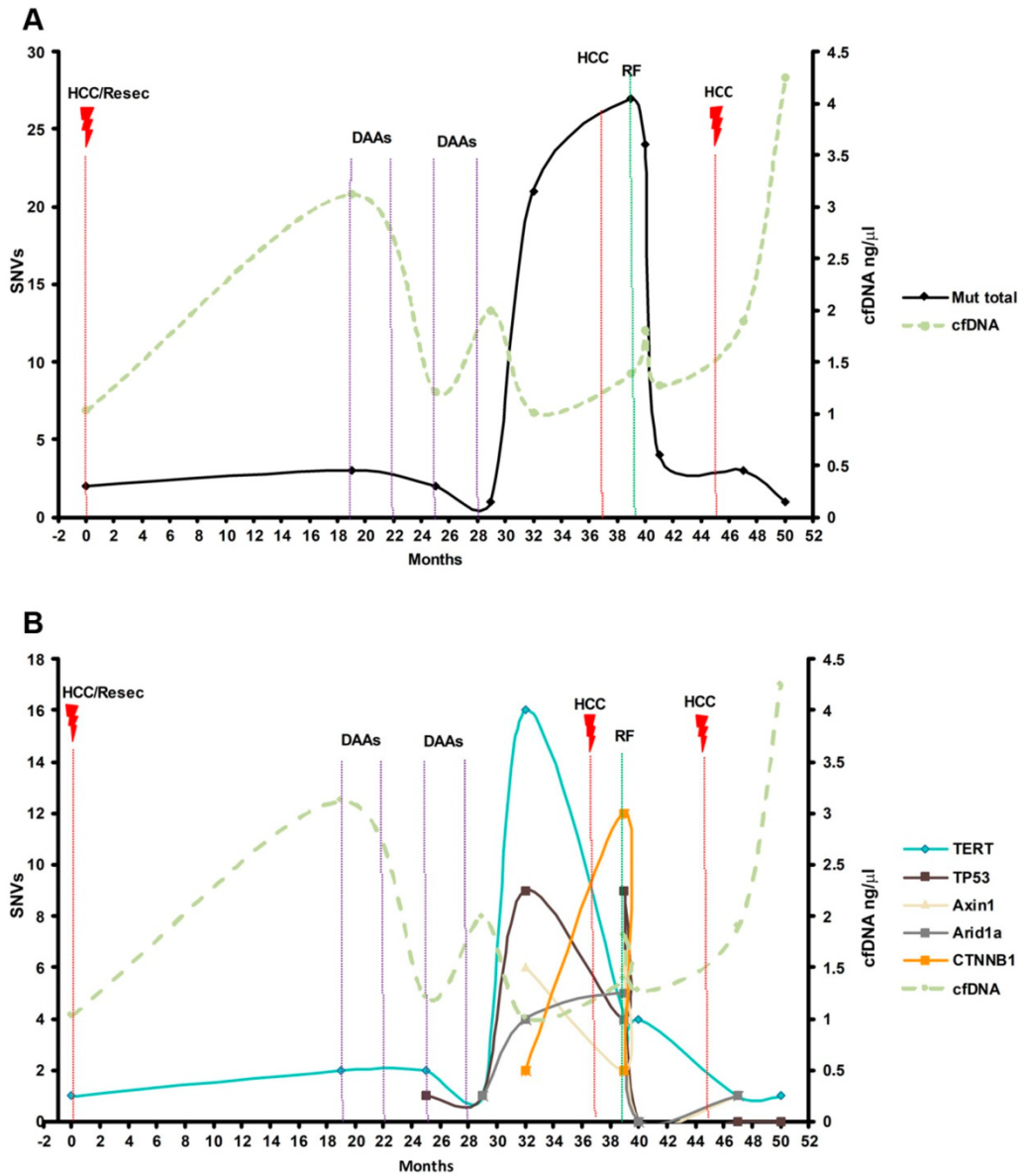
Figure 16. (A) Dynamical changes in cfDNA levels and absolute mutational load correlating with HCC progression (Patient VH335). (B) Dynamical fluctuations in cfDNA levels and number of muta-tions in the five driver genes tested along the 52 months of follow-up. HCC/Resec: detection and surgical resection of HCC, DAAs: HCV treatment with direct-acting antivirals, RF: radiofre-quency ablation, cfDNA: cell-free DNA, SNVs: single-nucleotide variant.

Two other examples of dynamic changes in cfDNA and SNV frequency of another three HCC patients are shown. Patient VH343 presented fluctuation in cfDNA levels and TERT mutation C228T (-124) correlating with HCC progression and tyrosine kinase treatment (Figure 17).

Figure 17. Dynamical changes in cfDNA levels and C228T (-124) TERT mutations frequency correlating with HCC progression in Patient VH343 along 33 months of follow-up

Moreover, patient VH369 showed dynamical changes in cfDNA levels, which were increased before second HCC relapse (16 months) (Figure 18).
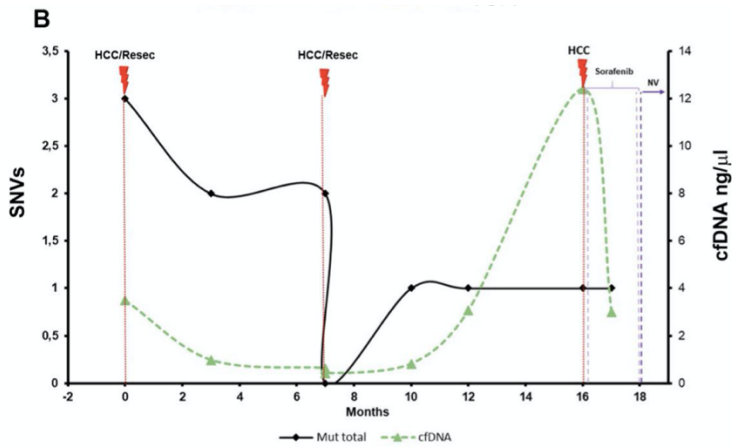
Figure 18. Dynamical fluctuations in cfDNA levels and absolute mutational load correlating with HCC progression along the 18 months of follow-up in Patient VH369. HCC/Resec: Detection and resection of HCC, NV: Systemic treatment with Nivolumab, cfDNA: cell -free DNA, SNVs: Single nucleotide variant.

Patient VH371 presented an increase in cfDNA levels and in the number and frequency of mutations months before radiological detection of relapse, 11 months after surgery (Figure 19).
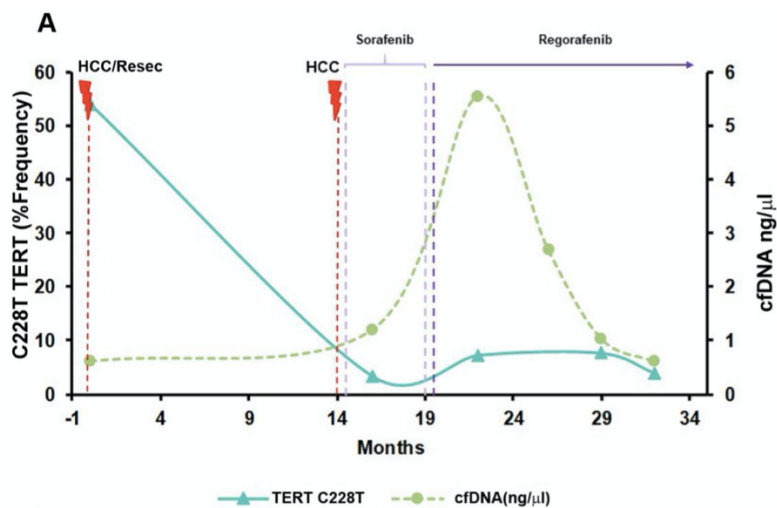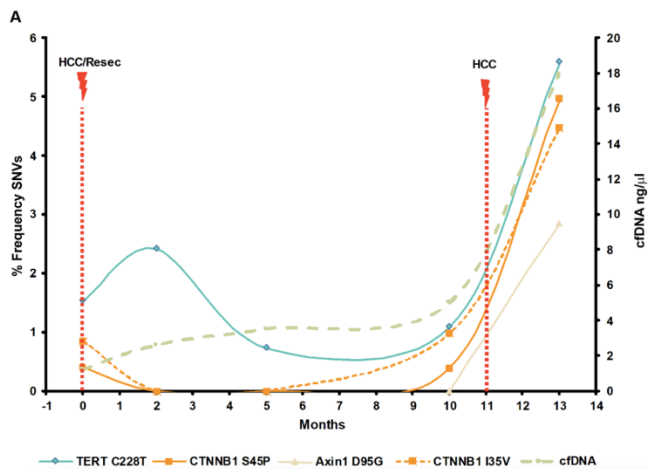

Figure 19. Dynamical changes in cfDNA levels and TERT, CTNNB1 and AXIN1 mutations frequency correlating with HCC progression in Patient VH371 along 13 months of follow-up. HCC/Resec: Detection and resection of HCC, cfDNA: Cell-free DNA, SNVs: Single nucleotide variant.

5.1.7. Validation by ddPCR of C228T TERT mutation

The most common mutation detected in TERT promoter (C228T) was also validated by ddPCR. C228T TERT promoter mutation was detected by ddPCR in 100% of the samples in which this mutation was detected by sequencing and in similar mutation rates in HCC tissue, in adjacent tissue and in cfDNA (Annex Table 19).

5.2. Study 2

5.2.1. Study design and patients characteristics

We prospectively recruited 25 patients candidates to receive systemic treatment with immune checkpoint inhibitors and analyzed their blood samples at the beginning and after 3 months under treatment. Median follow-up of these patients was 17 (3-50) months. Clinical and demographic parameters of these patients are summarized in *Table 15*. 84% of patients were male with a median age of 71 years. Viral etiology was observed in 64% of patients, being HCV infection the most prevalent underlying liver disease, present in 52% of cases. 76% of patients were BCLC-C at the moment of initiating ICIs. 64% of them had received another systemic therapy (TKIs) before starting ICIs. 60% of patients had been treated with locoregional therapies on earlier stages of the disease. For 20% of patients, ICIs was the first received therapy. During study follow-up, tumor progression was observed in 15 patients (60%) and 11 patients (44%) died (Table 15).

Table 15. Clinicopathological characteristics of HCC patients

Demographic		Cases (n=25)
Clinicopathological characteristics		
Gender, n (%)	Male	21 (84%)
Age, median (range)		71 (56-82)
Etiology, n (%)	HCV	13 (52%)
	MAFLD	2 (8%)
	HBV	1 (4%)
	OH	1 (4%)
	OH+HCV	2 (8%)
	OH+MAFLD	1 (4%)
	Others	1 (4%)
	No liver disease	4 (16%)
BCLC, n (%)	BCLC B	6 (24%)
	BCLC C	19 (76%)
Previous treatment, n (%)	Locoregional treatment	4 (16%)

	TKI	5 (20%)
	Locoregional + TKI	11 (44%)
	No previous treatment	5 (20%)
ICI therapy, n(%)	Nivolumab	14 (56%)
	Atezolizumab/Bevacizumab	8 (32%)
	Durvalumab/Tremelimumab	2 (8%)
	Pembrolizumab	1 (4%)
Radiological response RECIST 1.1, n (%)	Complete response (CR)	2 (8%)
	Partial response (PR)	5 (20%)
	Stable disease (SD)	11 (44%)
	Progressive disease (PD)	7 (28%)
Radiological response mRECIST, n (%)	Complete response (CR)	5 (21%)
	Partial response (PR)	2 (8%)
	Stable disease (SD)	11 (46%)
	Progressive disease (PD)	6 (25%)
Follow-up, median months (range)		17 (3-50)
Events, n (%)	Deceased	11 (44%)
Survival, median months (range)		17 (3-50)
Radiological progression, median months (range)		16 (3-50)
Laboratory values		
AFP (mg/dL), median (range)		17,9 (1,3-107614,7)
Bilirubin (mg/dL), median (range)		0,83 (0,47-2,28)
Albumin (g/L), median (range)		3,9 (3-4,7)
Platelet count (10^9/L), median (range)		186 (51-623)

The overall response rate (ORR) and disease control rate (DCR) were evaluated based on RECIST 1.1 being 28% and 72% respectively. From the 25 patients enrolled, 2 (8%) patients presented complete response (CR), 5 (20%) partial response (PR), 11 (44%) stable disease (SD) and 7 (28%) presented progression disease (PD) as best radiological response evaluated by RECIST 1.1. According to mRECIST, 5 (20%) patients presented CR, 2 (8%) PR, 11 (44%) SD and 6 (24%) PD as best radiological response and 1 patient

(4%) was non evaluable (NE). The median PFS was 20 months and the median OS was 38 months (Figure 20).
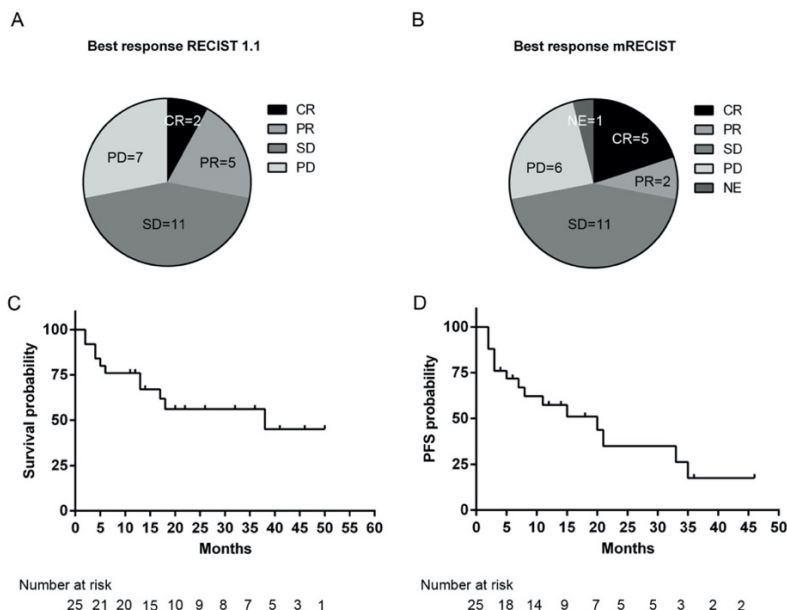
Figure 20. Clinical outcomes. (A) Best radiological response assessed by RECIST 1.1. (B) Best radiological response assessed by mRECIST. (C) Kaplan-Meier curve of overall survival and (D) progression free-survival assessed by RECIST 1.1. CR: complete response, PR: partial response, SD: stable disease, PD: progressive disease, NE: non evaluable, PFS: progression free survival.

12 patients (48%) presented adverse events during ICIs treatment. 7 patients (28%) experienced only one type of treatment-related adverse event, 2 patients (8%) two and 3 patients (12%) three types of adverse events. The most common AEs was thyroiditis and colitis in 7 patients (28%) respectively, followed by dermatological events in 4 patients (16%) and hypophysitis in 2 patients (8%) (Table 16).

Table 16. Adverse events of ICIs treatment

Adverse events (AEs)		
AEs, n (%)		12 (48)
Number, n (%)	0	13 (52)
	1	7 (28)

2	2 (8)
3	3 (12)
Thyroiditis, n(%)	7 (28)
Colitis, n (%)	7 (28)
Dermatological, n (%)	4 (16)
Hypophysitis, n(%)	2 (8)

5.2.2. Cytokine levels

We evaluated the levels of 24 cytokines on plasma samples harvest before starting and after 3 months of ICIs treatment. The 24 cytokines analyzed were: BTLA, CD137 (4-1BB), CD152 (CTLA4), CD27, CD28, CD80, GITR, HGF, HVEM, IFN-β, IFN-γ, IL-1 β, IL-10, IL-12/IL-23p40, IL-21, IL-6, IP-10 (CXCL10), LAG-3, MCP-1 (CCL2), PD-1, PD-L1, PD-L2, TIM-3, TNF-α. We evaluated if plasma cytokine levels had any correlation with radiological response by RECIST 1.1 and overall survival.

5.2.2.1. Basal CTLA-4 levels

CTLA-4 (cytotoxic T lymphocyte antigen 4) levels measured at the time of starting the treatment, were significantly lower in patients presenting CR, PR or SD [mean (SD)] [0,15 (0,67) pg/ml] than in patients presenting PD [76,55 (150,84) pg/ml] as best radiological response ($p < 0.05$) (Figure 21).
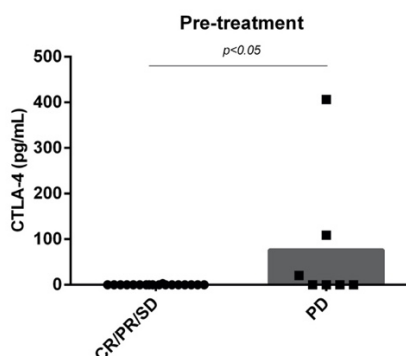

Figure 21. Basal CTLA-4 levels in patients presenting CR/PR/SD vs PD. CTLA-4: cytotoxic T lymphocyte antigen 4, CR: complete response, PR: partial response, SD: stable disease, PD: progressive disease.

5.2.2.2. MCP-1 levels 3 months post-treatment

Of interest, we found that MCP-1 (monocyte chemoattractant protein 1) levels measured after 3 months of ICIs treatment were significantly lower in patients presenting progressive disease (PD) [mean (SD)] [23,03 (34,58) pg/ml] than in patients responding to the treatments (presenting complete or partial response) [73,73 (86,34) pg/ml] ($p<0,05$) (Figure 22A). The same way, when we include patients presenting stable disease, MCP-1 levels are still significantly lower in patients presenting PD than in patients not progressing after the treatment (including patients presenting stable disease and responder patients) [49,25 (25,73) pg/ml] ($p<0,05$).

We then divided patients into two groups based on the median MCP-1 levels (MCP-1 low and MCP-1 high). Patients with lower levels of MCP-1 had a trend to significant to have a poorer overall survival ($p=0,15$) (Figure 22B).
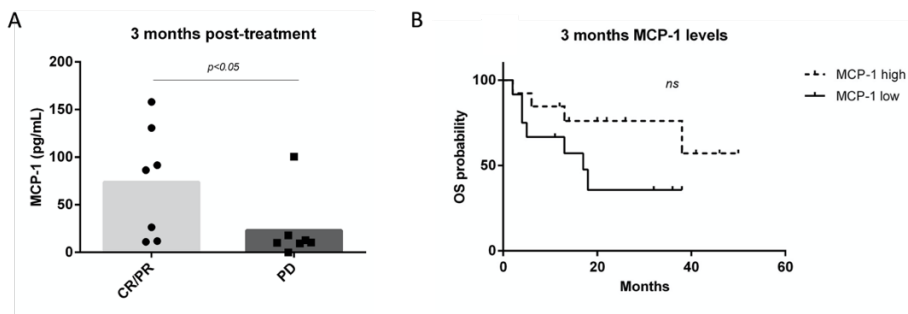
Figure 22. MCP-1 levels after 3 months of treatment. (A) Patients presenting CR/PR vs PD. (B) Kaplan-Meier curve of overall survival according to MCP-1 high or low levels. MCP-1: monocyte chemoattractant protein 1, CR: complete response, PR: partial response, PD: progressive disease. OS: overall survival.

5.2.2.3. TNF-α levels 3 months post-treatment

TNF-α (tumor necrosis factor alpha) measured after 3 months of starting ICIs treatment were also significantly different between patients presenting CR, PR or SD and patients presenting PD as best radiological response. TNF-α levels were significantly lower in

patients presenting CR/PR/SD [mean (SD)] [49, 9 (189,43) pg/ml] than in patients presenting PD [110,4 (239,7) pg/ml] (p<0,05) (Figure 23).
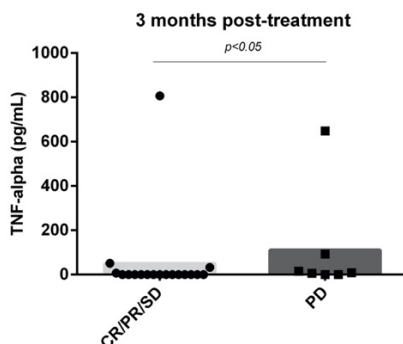
Figure 23. TNF-α levels 3 months after starting the treatment in patients presenting CR/PR/SD vs PD. TNF-α: tumor necrosis factor alpha, CR: complete response, PR: partial response, SD: stable disease, PD: progressive disease.

5.2.2.4. PD-L1 levels 3 months post-treatment

PD-L1 (programmed death-ligand 1) levels do not showed significant differences according to best radiological response to ICIs treatment. However, PD-L1 levels measured 3 months after starting the treatment, were significantly lower in patients presenting PD at any time point of the follow-up [mean (SD)] [4,99 (6,9) pg/ml] than patients not progression during follow-up [12,21 (8,7) pg/ml] criteria (p<0,01) (Figure 24).
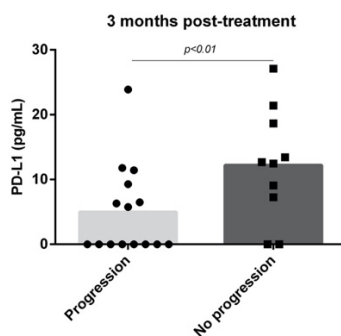
Figure 24. PD-L1 levels measured after 3 months of receiving ICIs treatment according to progression during follow up.

5.2.3. cfDNA levels

5.2.3.1. Basal cfDNA levels

We also evaluated the potential value of cfDNA levels to predict the efficacy of ICIs therapy in HCC patients. Pretreatment cfDNA levels were significantly different between patients presenting CR or PR, patients presenting SD and patients presenting PD [mean (SD)] [2,3 (0,58) ng/μl, 7,67 (5,92) ng/μl and 10,97 (8,28) ng/μl respectively] ($p<0,01$ in CR/PR vs SD and $p<0,05$ in CR/PR vs PD).

cfDNA levels at diagnosis were significantly lower in patients remaining alive by the end of the follow-up [mean (SD)] [4,43 (4,93) ng/μl] than in patients who died during the follow up [10,48 (7,01) ng/μl] ($p<0,005$). To investigate the association between the levels of basal cfDNA and survival, a cut-off value of 3,04 ng/μL of cfDNA was established. Patients presenting higher cfDNA levels than 3,04 ng/μL had a higher mortality and a higher risk of presenting SD or PD compared to patients with less than 3,04 ng/μL based on Kaplan–Meier's survival analysis ($p<0,001$ and $p<0,01$ respectively) (Figure 25).

Figure 25. Basal cfDNA levels. (A) In patients presenting CR/PR vs SD vs PD. (B) In alive vs death patients. (C) Kaplan-Meier curve of overall survival (D) Kaplan-Meier curve of SD/PD risk. cfDNA: cell-free DNA, CR: complete response, PR: partial response, SD: stable disease, PD: progressive disease. OS: overall survival.

5.2.3.2. 3 months post-treatment cfDNA levels

cfDNA levels after 3 months of ICIs treatment were also significantly different between patients presenting radiological response [2,12 (0,92) ng/μl] than those presenting SD [7,59 (3,87) ng/μl] ($p<0,005$) or those presenting PD [13,99 (15,17) ng/μl] ($p<0,01$).

Patients remaining alive during the follow-up also had significantly lower cfDNA levels at 3 months after starting the treatment than patients who died by the end of the follow-up [4,23 (3,81) ng/μl and 12,46 (11,93) ng/μl respectively] ($p<0,005$). A cut-off value of 3,26 ng/μl was assessed to evaluate the association between cfDNA determination 3 months after starting the treatment and survival or risk of presenting SD or PD. Patients with cfDNA levels higher than 3,26 ng/μl presented a higher mortality and a higher risk of presenting SD or PD as best radiological response ($p<0,001$ in both determinations) based on Kaplan-Meier analysis (Figure 26).
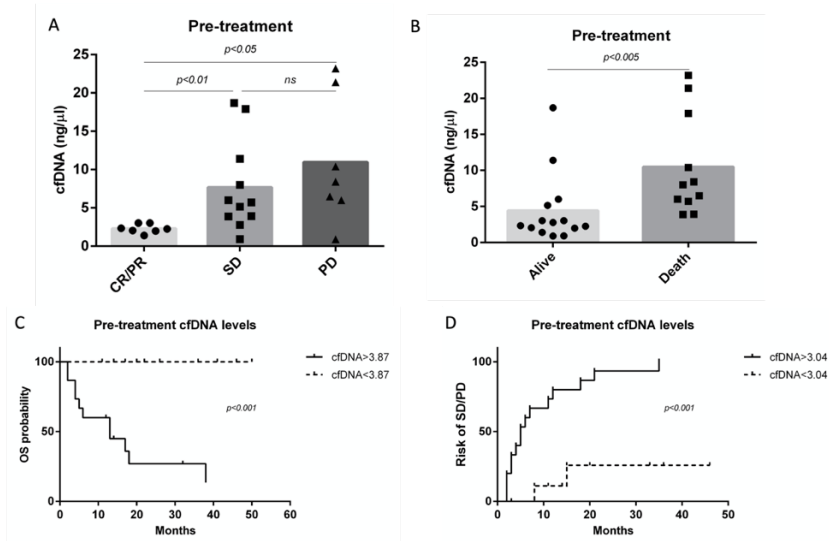
Figure 26. cfDNA levels 3 months post-treatment. (A) In patients presenting CR/PR vs SD vs PD. (B) In alive vs death patients. (C) Kaplan Meier curve of overall survival (D) Kaplan-Meier curve of SD/PD risk. cfDNA: cell-free DNA, CR: complete response, PR: partial response, SD: stable disease, PD: progressive disease, OS: overall survival.

cfDNA levels at starting the treatment and 3 months after starting the treatment are summarized in Table 17.

Table 17. cfDNA levels

cfDNA levels, mean (SD)		
	Pre-treatment	3 months post-treatment
Radiological response		
Complete/Partial Response	2,3 (0,58)	2,12 (0,92)
Stable Disease	7,67 (5,92)	7,59 (3,87)
Progressive Disease	10,97 (8,28)	13,99 (15,17)
Status		
Alive	4,43 (4,93)	4,23 (3,81)
Death	10,48 (7,01)	12,46 (11,93)

Analysis according to mRECIST showed the same significantly association between cfDNA and progression or survival.

5.2.4. ctDNA levels

5.2.4.1. Basal ctDNA levels

Basal ctDNA levels are also associated with a higher risk of death. Patients who stayed alive during the study follow-up had significantly lower levels of basal ctDNA than those who deceased [mean (SD)] [1,1 (0,89) ng/µl and 3,19 (3,38) ng/µl respectively] ($p<0,05$).

With a cut-off value of 1,52 ng/µl of ctDNA, ctDNA levels were associated to survival. Patients with higher levels of ctDNA than 1,52 ng/µl have a significantly higher risk of death than patients with lower levels of ctDNA ($p<0,05$) based on Kaplan-Meier analysis (Figure 27).
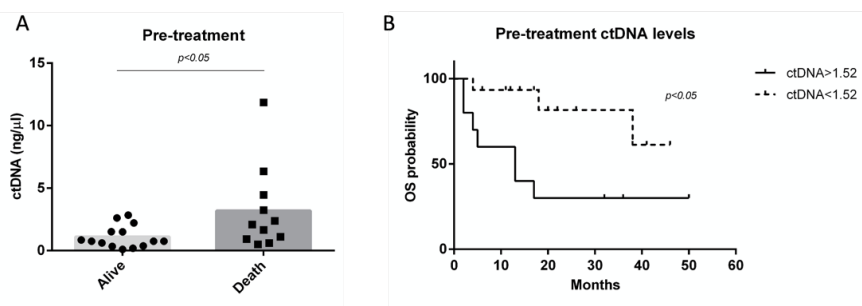
Figure 27. Basal ctDNA levels. (A) In alive vs death patients. (B) Kaplan-Meier curve of overall survival. OS: overall survival.

5.2.4.2. 3 months post-treatment ctDNA levels

ctDNA levels after 3 months of ICIs treatment were significantly different between patients presenting CR or PR [0,55 (0,35) ng/µl] and patients presenting SD or PD [4,34 (5,5) ng/µl] ($p<0,005$).

Patients remaining alive by the end of the follow-up had significantly lower levels of ctDNA after 3 months of treatment than patients who were dead by the end of the follow-up [1,21 ng/µl (1,47) and 5,74 (5,98) ng/µl respectively] ($p<0,001$). Patients showing ctDNA levels higher than 1,1 ng/µl had a higher risk of not responding to ICI

treatment (SD/PD) and consequently a higher risk of death (p<0,01 in both determinations) based on Kaplan-Meier analysis (Figure 28).
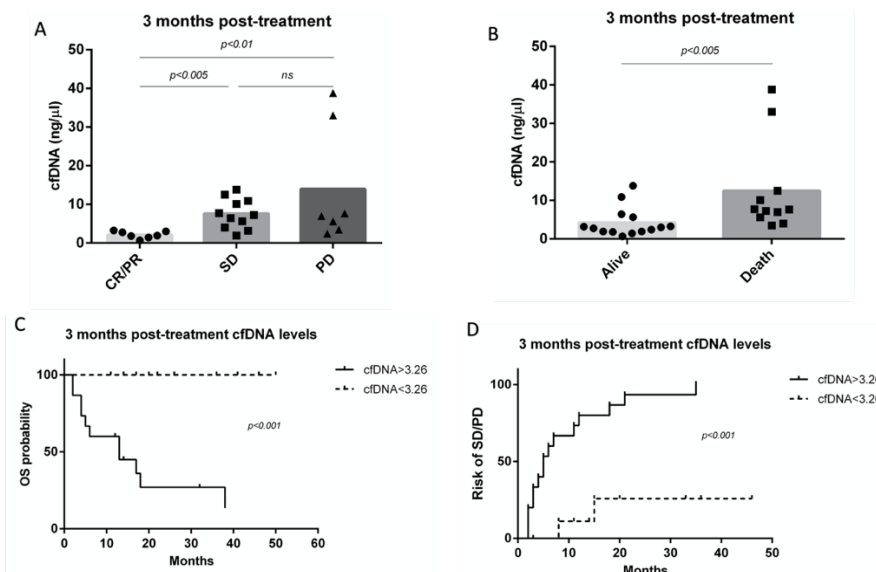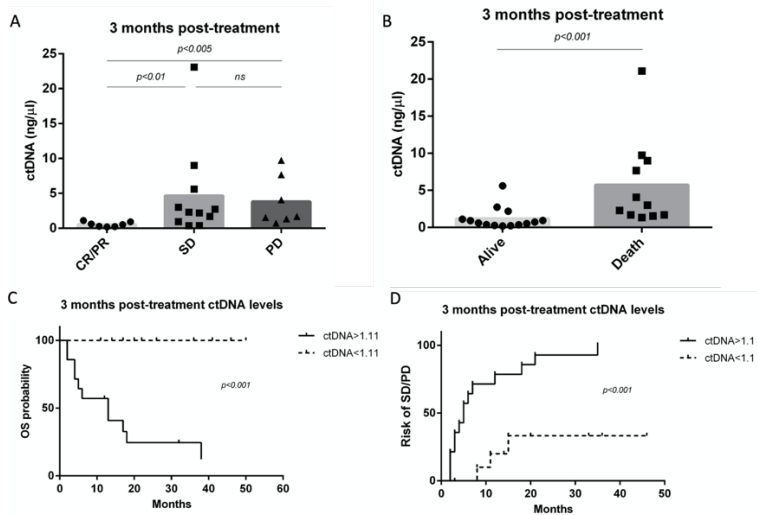

Figure 28. ctDNA levels 3 months post-treatment. (A) In patients presenting CR/PR vs SD vs PD. (B) In alive vs death patients. (C) Kaplan Meier curve of overall survival. (D) Kaplan-Meier curve of SD/PD risk. ctDNA: circulating tumor DNA, CR: complete response, PR: partial response, SD: stable disease, PD: progressive disease, cfDNA: cell-free DNA, OS: overall survival.

ctDNA levels at starting the treatment and 3 months after starting the treatment are summarized in Table 18.

Table 18. ctDNA levels

ctDNA levels, mean (SD) (ng/μl)		
	Pre-treatment	3 months post-treatment
Radiological response		
Complete/Partial Response	1,19 (1,07)	0,56 (0,35)
Stable Disease	2,04 (3,31)	4,67 (6,61)
Progressive Disease	2,7 (2,06)	3,89 (3,54)
Status		
Alive	1,1 (0,89)	1,21 (1,47)
Death	3,19 (3,38)	5,74 (5,98)

Analysis according to mRECIST showed the same significantly association between ctDNA and progression or survival.

5.2.4. C228T TERT promoter mutation

The percentage of C228T TERT promoter mutation in cfDNA was determined at baseline and three months after starting the treatment by ddPCR. 98% of samples had C228T mutation in TERT promoter region between 0,14% and 12,61%. No association was found between the percentage of TERT promoter mutation and PFS or OS, but patients presenting CR, PR or SD showed a trend to significant to have lower percentage of C228T TERT promoter mutation at baseline than patients presenting progressive disease as best radiological response. A cut-off of 1% of C228T TERT promoter mutation was stablished, and patients with more than 1% of mutation showed a trend to significance to have a poorer overall survival than patients with less than 1% of mutation (p=0,15) (Figure 29).
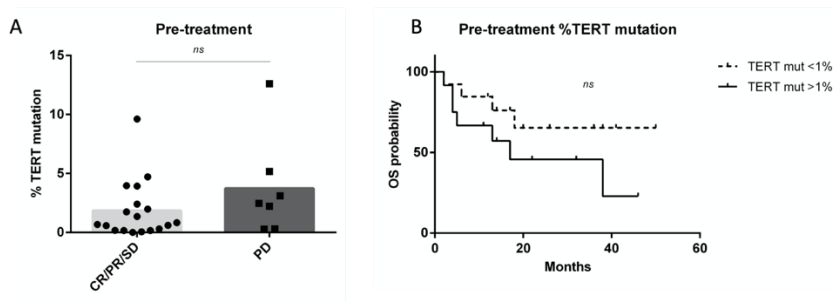
Figure 29. Percentage of C228T TERT promoter mutation at baseline. (A) Percentage of TERT promoter mutation in patients with PD vs patients with SD/PR/CR. (B) Kaplan Meier curve of overall survival in patients with more or less than 1% of TERT promoter mutation. PD: progressive disease, OS: overall survival.

5.2.5. ctDNA profiling

Baseline ctDNA profiling was assessed by Onco-500 TruSight of basal samples from 21 patients.

5.2.5.1. More frequent ctDNA mutations

To evaluate ctDNA in HCC patients treated with ICIs, a panel detecting 500 genes known to be frequently mutated in cancer was performed.
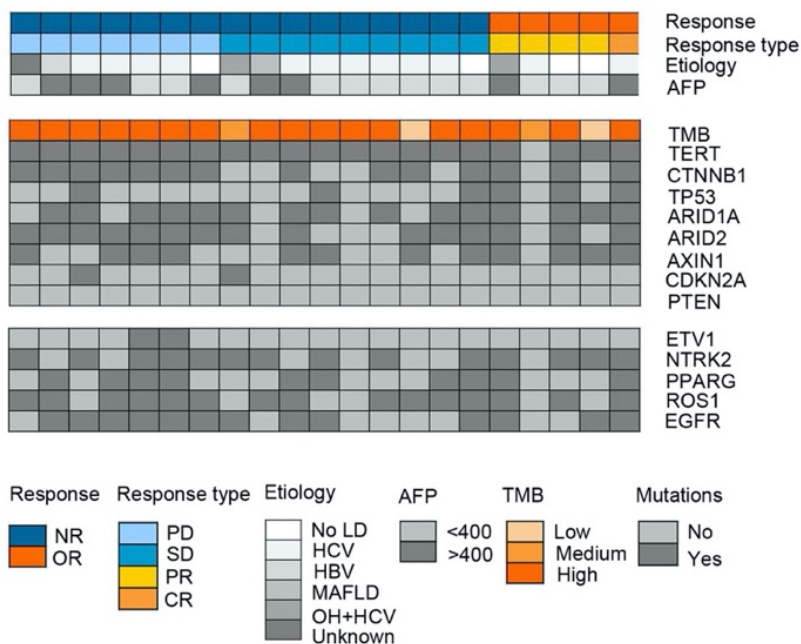
Figure 30. cfDNA profiling of HCC patients treated with ICIs. AFP: alpha-fetoprotein, TMB: tumor mutational burden, NR: no response, OR: objective response, CR: complete response, PR: partial response, SD: stable disease, PD: progressive disease, HCV: hepatitis C virus, HBV: hepatitis B virus, OH: alcohol, MAFLD: metabolic associated fatty liver disease.

The most prevalent mutated genes previously reported in HCC were also analyzed in our cohort. ctDNA C228T TERT promoter mutation was present in 20/21 patients, ctDNA pathological mutations in CTNNB1 were present in 14/21 patients (with 38 total mutations), in TP53 were present in 6/21 patients (with 64 total mutations), in ARID1A in 15/21 patients (with 73 total mutations), in ARID2 in 15/21 (with 85 total mutations), in AXIN1 in 12/21 (with 35 total mutations), in CDKN2A in 2/21 (with 4 total mutations) and no pathological mutations were present in PTEN.

In our cohort, most frequent pathological mutated genes were ETV1 with 700 mutations (in 2/21 patients), NTRK2 with 432 mutations (in 14/21 patients), PPARG with 382 mutations (in 10/21 patients), ROS1 with 327 mutations (in 15/21 patients) and EGFR with 276 mutations (in 13/21 patients) (Figure 30).
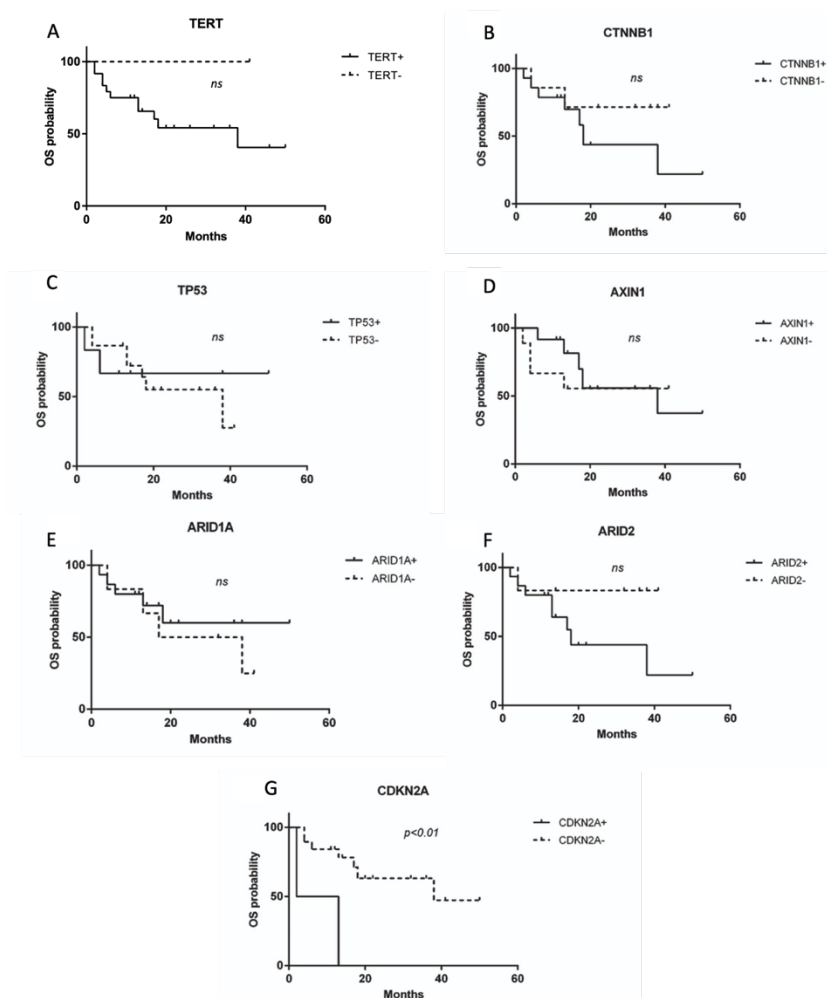
Figure 31. Kaplan-Meier curves of overall survival according to the presence or absence of (A) C228T TERT promoter mutation (B) CTNNB1 pathological mutations, (C) TP53 pathological mutations, (D) AXIN1 pathological mutations, (E) ARID1A pathological mutations, (F) ARID2 pathological mutations, (G) CDKN2A pathological mutations. OS: overall survival.

We then assessed the association of frequently mutated genes in ctDNA with clinical outcomes. The presence or absence of pathological mutations in TERT, CTNNB1, TP53, AXIN1, ARID1A or ARID2 did not affect significatively overall survival. On the other hand, patients with pathological mutations in CDKN2A had a significantly poorer overall survival than patients without pathological mutations in this gene ($p<0,01$) (Figure 31).

5.2.5.2. Mutations in CDKN2A

We then evaluated if the presence of mutations in CDKN2A could predict response to ICIs treatment. We found that patients presenting CR, PR or SD as best radiological response had a significantly lower number of patients presenting mutations in CDKN2A than patients presenting PD. 67% of patients presenting PD had mutations in this gene, but only 7% of patients presenting CR, PR or SD ($p<0,05$). The same way, significant differences were found in the percentage of patients with mutations in CDKN2A depending on if they respond to the treatment (CR/PR) (0% presented mutations in this gene), if they have stable disease (11%) or progressive disease (67%) as best radiological response (Figure 32).
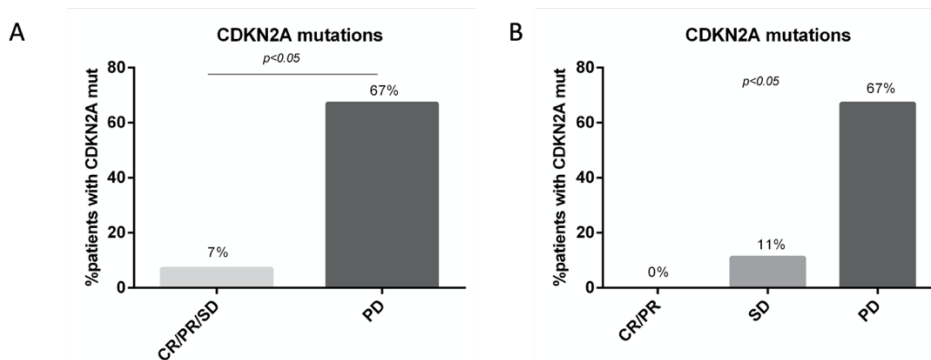
Figure 32. CDKN2A mutations. (A) In patients presenting CR/PR/SD vs PD. (B) In patients presenting CR/PR vs SD vs PD. CR: complete response, PR: partial response, SD: stable disease, PD: progressive disease.

5.2.5.3. Mutations in CTNNB1

We also focused on CTNNB1, as mutations in WNT pathway are described to be associated with a lack of response to ICIs. Pathogenic mutations in CTNNB1 were present in 100% of the patients showing PD as best radiological outcome, but only in 53% of those presenting SD or radiological response. No significant differences were found between the presence of pathological mutations in CTNNB1 and presenting progressive disease as best radiological outcome (Figure 33).
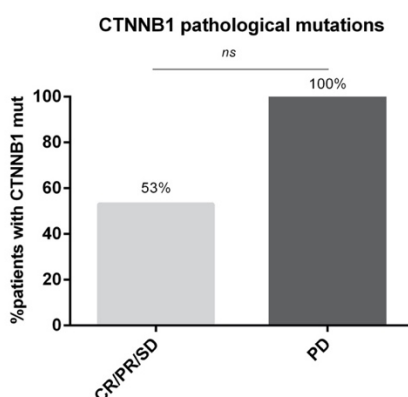
Figure 33. Percentage of patients with mutations in CTNNB1. CR: complete response, PR: partial response, SD: stable disease, PD: progressive disease.

5.2.5.5. Tumor mutational burden

TMB is defined as the total number of mutations present in a tumor specimen over the region of sequenced ctDNA; included non-synonymous mutations in coding regions and excluded germline alterations by subtracting matched normal samples. From the 21 patients, 17 had TMB-high (defined as >30 mutations/Mb), 2 TMB-medium (between 20 and 30 mutations/Mb) and 2 TMB-low (<20 mutations/Mb). No association was found between TMB and PFS or OS (Figure 34).
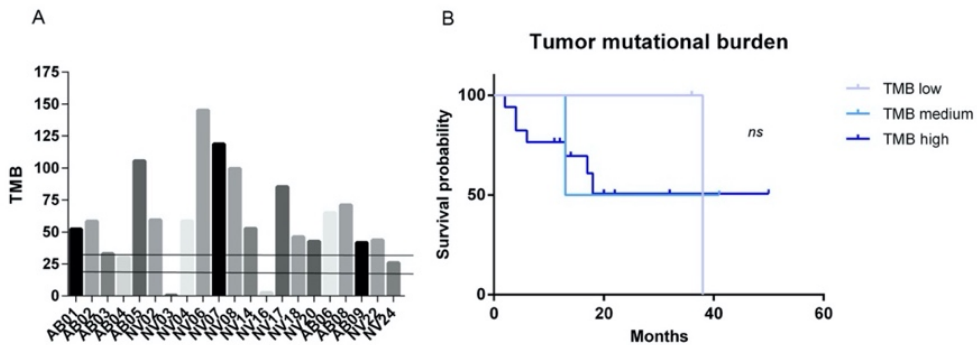
Figure 34. Tumor Mutational Burden (TMB). (A) TMB levels. (B) Kaplan Meier curve of overall survival according to low, medium or high TMB.

5.2.5.6. Copy number variation

Patients with radiological response (either CR or PR) had significantly more copy number variation (CNV) than those without radiological response (SD or PD). Patients with radiological response had a total of 97 CNV and patients without radiological response had only 1 CNV. [Mean (SD)] 16,1 (24,17) in patients with CR or PR and 0,06 (0,26) in patients with SD or PR (p=0,05) (Figure 35).
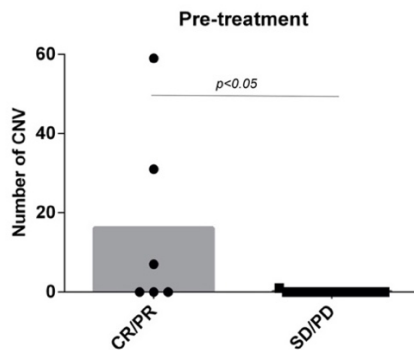
Figure 35. Number of Copy Number Variation (CNV). CR: complete response, PR: partial response, SD: stable disease, PD: progressive disease.

Discussion

6. Discussion

6.1. Overall discussion

Liver cancer incidence is increasing, ranking third in the total number of annual deaths. Most HCC patients are diagnosed at advanced stages, having only 2 years of life expectancy, in contrast with those patients diagnosed at an early stage that are candidates to curative treatments. However, recurrence happens in about 70% of patients after curative treatments. On the other hand, in the advanced HCC setting, despite the latest progresses that have revolutionized the therapeutic approach and life expectancy in the past 5 years, there is a lack of biomarkers to properly classify, allocate optimal treatments and estimate prognosis of HCC patients. The two studies presented in this doctoral thesis aimed to identify **noninvasive serological markers** able to refine the clinical algorithms in predicting early recurrence and prognosis after curative treatments and response to immune checkpoint inhibitors.

The **first study** is an exploratory and prospective study, in which we investigated the usefulness of cfDNA collected at the time of diagnosis and before **curative intervention** (resection or local ablation) for quantification and molecular profiling in early-stage HCC patients. Thirty patients at early stages, mostly candidates to surgical resection were selected, aiming first to evaluate the concordance between cfDNA and tumor tissue mutations and, second, to assess dynamic changes in cfDNA after potentially curative treatment to determine its potential value as a biomarker.

Carcinogenesis of HCC is characterized by accumulation of genetic alterations during the process of long-term chronic hepatitis. cfDNA can reflect these genetic and epigenetic alterations and monitoring levels of these mutations can reflect tumor burden in real time and also overcome intra-tumor genetic heterogeneity during the treatment and the follow-up (167). It has been proposed as a tool to improve early diagnosis and early detection of recurrence after treatment. Recently, the use of cfDNA levels and its

molecular analysis has been reported to provide useful information about tumor burden and diagnosis by genetic and epigenetic analysis (168)(169)(139).

Patients selected for our study had an early-stage HCC. The selection of patients at these stages defines a very homogeneous population to study cfDNA value, but, at the same time, it is less likely to capture events such as HCC recurrence or death during follow-up to estimate the prognostic value of cfDNA. Nevertheless, we considered this design optimal to explore potential biomarkers to be thereafter validated in a larger cohort.

We first evaluated **levels of cfDNA** in healthy controls and in early-stage HCC patients, being cfDNA levels significantly higher in HCC patients than in healthy controls, in concordance with other studies (79). Moreover, plasma of patients with different BCLC HCC stages were analyzed and also as described in previous reports, highest cfDNA levels were detected in patients with more advanced disease, as a consequence of greater tumor cell burden and cfDNA release (79)(170). More interestingly, we found a baseline cut-off value of 2ng/ul (AUC=0,782) that is able to discriminate between patients with high and low mortality during the follow-up. These suggest that only the quantitative amount of detectable cfDNA could have prognostic value.

In this study we also specifically targeted the most significantly mutated genes and regions in HCC: TERT promoter, TP53, CTNNB1, AXIN1 and ARID1A, evidencing that **high-depth sequencing** analysis of plasma-derived cfDNA could be used to detect tumor-related gene mutations in plasma cfDNA.

Paired samples of plasma cfDNA and HCC tissue DNA in this cohort were analyzed. Some studies reported an overall detection rate for tissue mutations in plasma as low as 12% (168); more recent studies increased this rate to around 45% (129)(171), more similar to the 52,7% of concordance we have found. Suggesting that most prevalent mutations in HCC that are identified in cfDNA are representative of those present in the HCC tumor tissue.

Additionally, we observed that a high number of variants in plasma could not be confirmed in tumor samples (104 mutations found in cfDNA vs. 55 mutations found in HCC tissues), suggesting that cfDNA could be more informative at a molecular level than small biopsy/surgical under-representative samples. As previously reported, RNAseq studies from different distant regions within the same tumor have evidenced differences in transcription factor signaling (172). This could explain the fact that finding more mutations in cfDNA than in tumor tissue samples defines the complex molecular **heterogeneity** in HCC (173). Subclones could be localized in a different topographic location in the primary tissue (174)(175)(176), and coexistence of different subclones with distinctive mutational profiles and different spatial location could have considerable practical implications when extracting molecular information from biopsies or partial surgical samples.

The most frequently mutated gene in plasma was **TERT promoter**, with a frequency of 76,7% (23/30 patients), consistent with the known mutational profile of early-stage HCC (80). The second most frequently mutated gene was **TP53** in 50% (15/30) cfDNA samples, consistent with what is being described in previous literature, that describe mutations In TP53 in around 60% of HCC patients (129)(177)(178).

Despite the small number of patients included in our study, we have found that the **mutational load**, defined as the total number of variants detected in cfDNA and the number of mutated genes were associated with overall survival and recurrence in a univariate analysis. In our cohort, patients presenting four or more mutations in cfDNA at baseline had shorter survival. Accordingly, a higher number of mutations detected in cfDNA were also associated with well-described poor prognostic factors in the HCC setting, such as the presence of multiple foci of HCC or the presence of microvascular invasion at pathology exam, as seen in other studies (168).

On the other hand, some prognostic clinic-pathological parameters commonly used in clinical practice, such as number of nodules, presence of microvascular invasion or

alpha-fetoprotein levels, showed no association with recurrence or overall survival in our cohort. This is probably a consequence of the small number of patients evaluated, all of them at early stages of the disease, being less likely to develop events. So, these findings provide the proof of principle to test this approach in a larger multicentric cohort of plasma samples of patients at early stages to validate the potential value of our findings.

In this study, we are also reporting two cases in which analysis of cfDNA was performed in patients with liver disease and with no sign of malignancy during the prior HCC screening by abdominal ultrasound, detecting mutations almost 1 year before imaging detection. With our approach, we found that C228T TERT promoter mutation was detected at a frequency of 8% and 5.34% 12 and 10 months **before diagnosis** in patients VH341 and VH381, respectively. This suggests that cfDNA alterations from our early HCC samples could also be tested in at-risk patients with liver cirrhosis under ultrasound screening programs, given the easy access to blood samples, without needing invasive procedures. Recently, some studies have identified TERT promoter mutations to be key events in HCC progression as they are seen in dysplastic hepatic nodules (80)(179)(180). More multicentric studies analyzing the levels of driver mutations as TERT in cfDNA of cirrhotic patients would be an appealing future approach to further develop the potential usefulness of cfDNA as a diagnostic biomarker. This is exploratory and preliminary evidence, and further support to confirm the potential role of cfDNA in improving early diagnosis of HCC in at-risk patients is required.

Even after curative treatment, relapse remains a significant threat for many cancer patients, and it is difficult to detect minimal residual disease by imaging or tissue biopsy. Previous studies showed that ctDNA could be used for **monitoring disease load**, providing clinically relevant lead times compared to imaging techniques in colorectal cancer (181). It has also been observed that cfDNA-positive patients are more likely to experience a relapse than the cfDNA-negative ones, showing a shorter disease-free

survival (178)(182). Furthermore, it has been reported that cfDNA can be used to monitor **dynamic changes in tumor burden**, analyzing both genetic and epigenetic status, using minimally invasive blood sampling (183)(184). In addition, genetic analysis of cfDNA during clinical follow-up of patients could be useful in identifying the appearance of resistant subclones (185)(186). Another study investigated cfDNA and protein biomarkers in a long-term follow-up of patients with HCC, concluding that both SNVs and CNVs possessed the capability to dynamically reflect HCC tumor burden (130). In this study, we have observed that the somatic mutations on known HCC-related driver genes, such as TERT, TP53 and CTNNB1 in cfDNA, were consistently and dynamically correlated with tumor burden during patient follow-up.

Genetic information from cfDNA could provide a tumor-specific molecular profile of tumors. This information could guide **targeted therapy**, improving the choice of the appropriate treatment for each patient. The half-life of cfDNA in the circulation is between 16 min and 2,5 h (187); for this reason, cfDNA can be considered a real-time snapshot reflecting the molecular evolution of tumors (185). Noninvasive access to molecular information allows real-time monitoring of treatment effectiveness in some type of tumors. Unfortunately, the most prevalent mutations in HCC, explored in the present study, are not therapeutic targets. Our approach, selecting the regions enriched with hotspot containing frequent mutations in TERT promoter, TP53, CTNNB1, AXIN1 and ARID1A, avoids the cost of performing more expensive techniques, such as whole exome or genome sequencing, which is unaffordable for the economic health system.

Analysis of cfDNA requires the evaluation of nontumor variant background noise. To achieve this aim, we included a control group of healthy patients, as well as **PBMCs** from each patient. Nonetheless, there are still many unknown aspects about the origin of variants in plasma and its biological meaning.

Additionally, we have validated with **ddPCR** those C228T TERT promoter mutations in cfDNA and in HCC tissue found by next-generation sequencing, finding a great

percentage of concordance. These would be a great alternative to use for screening in cirrhotic patients as it is a more rapid and affordable technique.

On the other hand, on advanced HCC, significant results have been obtained with immunotherapy, increasing survival of these patients. Despite of that, not all patients receive adequate benefits from this type of treatment. Multiple factors may be associated with this variable effect, depending on the characteristics of the host and the tumor microenvironment. Biomarkers that could identify patients that could benefit from each therapy and avoid potential side effects in patients who will not benefit from them is still an unmet need.

The **second study** focused on plasma biomarkers of response to immune checkpoint inhibitors therapies in advanced HCC. It is a prospective study in which plasma samples of 25 patients treated with **immunotherapy** have been collected at the beginning of the treatment and after three months under ICIs treatment.

Circulating soluble factors, such as **cytokines**, have been evaluated lately as biomarkers over the course of ICI therapy. PD-L1 has been associated with response to PD-1/PD-L1 inhibitors and better survival in several tumor types, therefore, are probably the most commonly used biomarkers in predicting clinical outcomes of cancer patients receiving ICIs (188)(189). Specifically in unresectable HCC treated with ICI, PD-L1 expression detected by immunohistochemistry does not reproducibly correlate with the treatment response to ICIs, as monotherapy or in combination with other agents (63)(67). The predictive value of PD-L1 in HCC is still unclear, with response rates in all patients regardless of PD-L1 expression (190). In our work, we specifically studied plasma **PD-1 and PD-L1** expression at baseline and at three-months follow-up samples. In concordance with latest HCC studies, neither PD-1 or PD-L1 levels were able to discriminate patients according to their best radiological response. However, lower levels of PD-L1 three months after starting the treatment were associated with patients presenting progression at any time point during follow-up, as described previously in

other tumors (188)(189). So, further studies are needed to clarify if PD-L1 may enable prediction of radiological response to ICI in HCC patients.

Similarly, higher levels of CTLA-4 in other types of tumors showed to be favorable biomarkers of response to anti-CTLA-4 therapies (191). Contrary, in our cohort, we have seen that higher basal CTLA-4 levels were associated to patients presenting radiological progression as best radiological response under immunotherapy. These results, however, could be influenced by the fact that in our cohort, only 2 from 25 patients were treated with anti-CTLA-4.

We hypothesize that cytokines levels can be used as predictors of treatment response to checkpoint inhibitors due to their important role during innate and adaptive immune activation. So, apart from PD-1, PD-L1 and CTLA-4 levels, in total 24 cytokines have been evaluated. **MCP-1** levels three months after starting the treatment showed to be significantly lower in patients presenting radiological progression as best radiological response. MCP-1 is a potent chemoattractant factor for monocytes regulating its migration from the blood stream and infiltration to the tissue (192), suggesting that patients with lower levels of MCP-1 could have a lower activated immune system toward the tumor. Lower levels of MCP-1 were also found to be associated with PFS in previous studies in advanced-stage melanoma patients treated with ICI (155).

Therefore, we speculate that lower levels of immune-related cytokines such as MCP-1 could reflect a less activated innate and adaptive immune system within the tumor microenvironment and patients with low cytokine levels may be more likely to progress after checkpoint inhibitors.

However, we found that **TNF-alpha** levels were significantly higher in patients presenting progressive disease as best radiological response. TNF or tumor necrosis factor is also a proinflammatory cytokine, but that depending on the context, can mediate either pro-survival or pro-death signals (193). In melanoma, there are studies

evidencing TNF neutralization may enhance ICI therapy responses (194)(195), in line with what we have seen in our cohort. These studies attributed this effect to TNF activation-induced cell death of tumor-infiltrating lymphocytes and upregulation of secondary immune checkpoint molecules (193). Similarly, **LAG-3** (lymphocyte activation gene-3) suppresses T cells activation and cytokines secretion, and shows a remarkable synergy with PD-1 to inhibit immune responses (196). In our study, patients showing progressive or stable disease as best radiological response had a trend to significance to have higher basal levels of LAG-3 than patients showing radiological response, suggesting LAG-3 is blocking immune activation in those patients not responding to the treatment. **IL-6** showed also a trend to significance to be higher in patients who show progression as best radiological response 3 months post-treatment, and it also has been reported previously to be associated to a poorer response to ICIs (197), as it promotes tumor progression via inhibition of cancer cell apoptosis as well as promotion of angiogenesis (198).

We also investigated the potential of ctDNA/cfDNA profiling as a predictive biomarker. First, we evaluated **cfDNA and ctDNA levels**. We observed that baseline and three months after treatment levels of cfDNA were significantly higher in patients not responding to ICI treatment. cfDNA levels correlated as well to overall survival, being OS significantly poorer in patients with higher levels of cfDNA at baseline and at three months under treatment determination. Similarly, higher ctDNA levels at basal timepoint were associated with a poorer survival and ctDNA levels 3 months after starting the treatment were also significantly higher in those patients not presenting radiological response to ICIs treatment, and were also related to poorer overall survival. This suggest the possibility that simple cfDNA/ctDNA quantification may be useful to predict the clinical outcome of these patients. As we previously described, regarding HCC, several studies have reported that the cfDNA concentration is higher in patients with HCC than in those with chronic hepatitis and healthy controls (199), that is

associated with early recurrence and poor survival after surgical resection (200) and that it may reflect the disease stage (170). There are few data regarding cfDNA quantification as a biomarker for immunotherapy in HCC, but a recent study from Matsumae T et al showed that patients with higher levels of cfDNA had significantly lower OR and shorter PFS and OS than those with lower levels of cfDNA (201). Their results are in concordance with our results.

The percentage of C228T **TERT** promoter mutation in cfDNA was determined by ddPCR in our cohort at baseline and three months after starting the treatment. We have not observed a significant correlation between C228T TERT promoter mutation percentage and response to treatment, but in patients presenting progressive disease as best radiological response, a trend to have higher levels of C228T TERT promoter mutation was observed. As we already mentioned, TERT promoter mutations are associated with poor prognosis after treatment, however, the majority of these studies are with early-stage HCC patients (179). There are also studies with advanced HCC patients that correlate TERT promoter mutations with poor prognosis (201)(202), but its paper is more controversial. Li H et al showed that TERT mutations were associated with higher TMB score, suggesting a greater activity to immunotherapy and that prognosis was better when TERT was mutated in patients treated with CTLA-4 but was similar in patients treated with anti-PD-1/PD-L1 (203).

Regarding **cfDNA profiling**, the order of mutation frequency in ctDNA was mostly consistent with that previously reported in HCC (88). The most frequent mutations were identified in TERT promoter (in 98% of patients), followed by ARID1A (71%), CTNNB1 (67%), AXIN1 (57%), TP53 (29%) and CDKN2A (10%). Interestingly, patients with **CDKN2A** pathological mutations are more likely to progress after the treatment and consequently had a significantly poorer overall survival. This findings in CDKN2A were already observed in other types of cancer, as in NSCLC (204).

In particular we focused on CTNNB1 mutations, due to recent studies suggest that mutations affecting the beta-catenin pathway including **CTNNB1** mutations may predict beneficial effects of immunotherapy (205)(206). CTNNB1 mutations could activate Wnt pathway and lead to T-cell exhaustion and innate resistance to immune checkpoint inhibitors (207). In our cohort, we have observed that 100% of patients with progressive disease as best radiological outcome after ICI treatment have mutations in CTNNB1, and that CTNNB1 mutated was present only in 53% of those presenting stable disease or radiological response. But no significant differences were found between presence of CTNNB1 mutations and progression of the disease, and in overall survival. However, it is recently described that the addition of anti-VEGF agents such as bevacizumab may overcome WNT/β-catenin signaling-mediated resistance to an ICI such as atezolizumab (208)(209). Blockade VEGF is known to increase cytotoxic T cells infiltration and decrease immunosuppressive cells, including regulatory T cells, promoting tumor recognition and cancer cell death (210). So, this could affect our results too, considering that 8/25 of our study patients were treated with anti-VEGF.

Tumor mutational burden (TMB), defined as the overall number of somatic non-synonimous mutations per megabase (211), is another promising biomarker which has been tested in a wide range of tumor types, and several studies have observed an association with TMB and more favorable response to ICI (160)(212). In contrast with these studies, in IMbrave150 trial in HCC patients, where TMB was also assessed, they found that TMB was not associated to survival or response to treatment, only high TMB showed a non-significant trend of longer PFS (208). In our cohort, we have not found any correlation between TMB and patients' outcomes. Moreover, the 90% of our patients TMB are high-TMB (>30 mutations/megabase) and with median TMB of 52,78, in contrast what it is described recently in HCC. Median TMB has been reported to be around 4-5 mutations/megabase and with approximately the 5% of all HCC samples presenting high-TMB (213). Currently, there are no standardized gene platform to

calculate TMB and definitions vary across studies (214), in our study cfDNA mutations are analyzed by Onco-500 TruSight and it is possible that we capture more mutations and consequently a higher TMB than in other studies. It is also described that HCC TMB differs by type and number of risk factors (214), and due to our small cohort, we have not stratify our data so this could have bias our results.

Another indicator of genomic instability could be **copy number variation** (CNV). In NSCLC, a higher number of CNV has been associated to a better response to immunotherapy, as with TMB (215). In our study, patients presenting progressive disease as best radiological response after ICI treatment, have a significantly lower number of CNV, as previously described. Contrary, in a recent study in hepatobiliary cancer including different liver cancer types (216), lower CNV has been associated with a better overall survival in patients treated with ICIs, so further studies are needed to clarify CNV paper in HCC patients.

Immunotherapy, and, in particular, immune checkpoint inhibitors have revolutionized the therapeutic landscape of advance HCC, however, there is no a priori way to identify patients that will present radiological response and significant benefit in terms of survival, or, the other way around, to exclude from this therapeutic approach, patients that will experience no benefit and probably will develop any adverse event. We believe that our results could be helpful for clinicians to improve clinical decision-making in HCC patients and could be the basis of future research in other cancers treated with ICI. The aim is now to translate these findings into large-scale studies of patients and validate the results we have obtained in our study.

6.2. Limitations

The main limitation of our studies is their small sample size, due to the prospective and unicentric nature of both studies. The potential prognostic value of the biomarkers in plasma observed in our series deserves further investigation and validation in larger cohorts of patients. Efforts are being currently made in this direction.

In the second study, in addition to the prospective and unicentric nature of the study, the progressive access to ICIs treatments in clinical practice in our country is the underlying cause of prospective inclusion of patients treated with different types of ICIs and the inclusion of both naïve and previously treated patients. These differences may clearly influence the results. For this reason, as a next step, an external cohort has been identified to validate our results.

Conclusions

7. Conclusions

- Next-generation sequencing can detect cfDNA mutations that are representative of driver mutations found in HCC tissue.

- Total cfDNA levels and detection of the most prevalent HCC mutations have prognostic implications that could refine the standard surveillance after curative treatment of early stage-HCC patients.

- Basal cytokine levels and cytokines measured 3 months after starting the treatment could help to discriminate patients with different responses to immune checkpoint inhibitors.

- cfDNA and ctDNA levels and ctDNA mutational profiling differentiate HCC patients with different radiological response and overall survival under immune checkpoint inhibitors treatment.

Future lines

8. Future lines

The reported data is in line with other contemporary cohorts, but, as the main limitation of these studies is the small sample size of our studies, as a result of the prospective unicentric nature of the work. Although interesting, the results need to be validated in an external and, if possible, larger cohort. Current efforts are aimed at moving in this direction.

In these studies, ddPCR to detect C228T TERT mutation, the most prevalent mutation in HCC development, has been set up. This is a rapid and affordable technique that gives the possibility to detect the early development of HCC. So, plasma samples of cirrhotic patients are currently being analyzed by ddPCR to evaluate the presence of C228T mutation in TERT and its correlation with early HCC detection.

On the same way, ddPCR of other mutations than has been described as predictors of response to systemic treatment in the advanced HCC setting could be set up.

In addition to this work, in which cfDNA and cytokines have been studied, other types of liquid biopsy could be investigated. We are currently working on CTCs isolation in HCC patients undergoing curative treatments and its molecular characterization.

Finally, PBMCs from patients treated with immune checkpoint inhibitors are being collected, so a deeper study of their lymphocytes could be interesting to deepen into their immune responses and correlate them to patients clinical outcomes.

Bibliography

9. Bibliography

1.   International Agency for Research on Cancer. GLOBOCAN 2018. IARC [Internet]. 2020 [cited 2022 Sep 30]. Available from: https://gco.iarc.fr/today/home

2.   Fitzmaurice C, Akinyemiju T, Abera S, Ahmed M, Alam N, Alemayohu MA, et al. The burden of primary liver cancer and underlying etiologies from 1990 to 2015 at the global, regional, and national level results from the global burden of disease study 2015. JAMA Oncol. 2017;3(12):1683–91.

3.   Villanueva A. Hepatocellular carcinoma. N Engl J Med. 2019;380(15):1450–62.

4.   Rumgay H, Arnold M, Ferlay J, Laversanne M, Mcglynn KA. Global burden of primary liver cancer in 2020 and predictions to 2040. J Hepatol. 2022;1–9.

5.   Sia D, Villanueva A, Friedman SL, Llovet JM. Liver Cancer Cell of Origin, Molecular Class, and Effects on Patient Prognosis. Gastroenterology. 2017;152(4):745–61.

6.   Llovet JM, Kelley RK, Villanueva A, Singal AG, Pikarsky E, Roayaie S, et al. Hepatocellular carcinoma. 2021;7(1):6.

7.   Levrero M, Zucman-Rossi J. Mechanisms of HBV-induced hepatocellular carcinoma. J Hepatol. 2016;64(1):S84–101.

8.   Yuen MF, Chen DS, Dusheiko GM, Janssen HLA, Lau DTY, Locarnini SA, et al. Hepatitis B virus infection. Nat Rev Dis Prim. 2018;4:1–21.

9.   Christoph S, Mason WS. Molecular Biology of Hepatitis B Virus Infection. Virology. 2015;0:672–86.

10.   Chen SL, Morgan TR. The natural history of hepatitis C virus (HCV) infection. Int J Med Sci. 2006;3(2):47–52.

11.   Benvegnù L, Gios M, Boccato S, Alberti A. Natural history of compensated viral cirrhosis: A prospective study on the incidence and hierarchy of major

complications. Gut. 2004;53(5):744–9.

12.   Lok AS, Seeff LB, Morgan TR, di Bisceglie AM, Sterling RK, Curto TM, et al. Incidence of Hepatocellular Carcinoma and Associated Risk Factors in Hepatitis C-Related Advanced Liver Disease. Gastroenterology. 2009;136(1):138–48.

13.   Kanwal F, Kramer J, Asch SM, Chayanupatkul M, Cao Y, El-Serag HB. Risk of Hepatocellular Cancer in HCV Patients Treated With Direct-Acting Antiviral Agents. Gastroenterology. 2017;153(4):996-1005.e1.

14.   Jain MK, Rich NE, Ahn C, Turner BJ, Sanders JM, Adamson B, et al. Evaluation of a Multifaceted Intervention to Reduce Health Disparities in Hepatitis C Screening: A Pre-Post Analysis. Hepatology. 2019;70(1):40–50.

15.   Vargas-Accarino E, Martínez-Campreciós J, Domínguez-Hernández R, Rando-Segura A, Riveiro-Barciela M, Rodríguez-Frías F, et al. Cost-effectiveness analysis of an active search to retrieve HCV patients lost to follow-up (RELINK-C strategy) and the impact of COVID-19. J Viral Hepat. 2022;29(7):579–83.

16.   Puigvehí M, Moctezuma-Velázquez C, Villanueva A, Llovet JM. The oncogenic role of hepatitis delta virus in hepatocellular carcinoma. JHEP Reports. 2019;1(2):120–30.

17.   Palom A, Rodríguez-Tajes S, Navascués CA, García-Samaniego J, Riveiro-Barciela M, Lens S, et al. Long-term clinical outcomes in patients with chronic hepatitis delta: the role of persistent viraemia. Aliment Pharmacol Ther. 2020;51(1):158–66.

18.   Ganne-Carrié N, Nahon P. Hepatocellular carcinoma in the setting of alcohol-related liver disease. J Hepatol. 2019;70(2):284–93.

19.   Hassan MM, Hwang LY, Hatten CJ, Swaim M, Li D, Abbruzzese JL, et al. Risk factors for hepatocellular carcinoma: Synergism of alcohol with viral hepatitis

and diabetes mellitus. Hepatology. 2002;36(5):1206–13.

20. Seitz HK, Bataller R, Cortez-Pinto H, Gao B, Gual A, Lackner C, et al. Alcoholic liver disease. Nat Rev Dis Prim. 2018;4(1).

21. Huang DQ, El-Serag HB, Loomba R. Global epidemiology of NAFLD-related HCC: trends, predictions, risk factors and prevention. Nat Rev Gastroenterol Hepatol. 2021;18(4):223–38.

22. Kanwal F, Kramer JR, Mapakshi S, Natarajan Y, Chayanupatkul M, Richardson PA, et al. Risk of Hepatocellular Cancer in Patients with Non-alcoholic Fatty Liver Disease. Gastroenterology. 2018;155(6):1828–37.

23. Mirra S, Gavaldà-Navarro A, Manso Y, Higuera M, Serrat R, Salcedo MT, et al. Armcx3 mediates susceptibility to hepatic tumorigenesis promoted by dietary lipotoxicity. Cancers (Basel). 2021;13(5):1–22.

24. Ioannou GN. Epidemiology and risk-stratification of NAFLD-associated HCC. J Hepatol. 2021;75(6):1476–84.

25. Reig M, Forner A, Ávila MA, Ayuso C, Mínguez B, Varela M, et al. Diagnosis and treatment of hepatocellular carcinoma. Update of the consensus document of the AEEH, AEC, SEOM, SERAM, SERVEI, and SETH. Med Clin (Barc). 2021;156(9):463.e1-463.e30.

26. Marrero JA, Kulik LM, Sirlin CB, Zhu AX, Finn RS, Abecassis MM, et al. Diagnosis, Staging, and Management of Hepatocellular Carcinoma: 2018 Practice Guidance by the American Association for the Study of Liver Diseases. Hepatology. 2018;68(2):723–50.

27. Paisant A, Vilgrain V, Riou J, Oberti F, Sutter O, Laurent V, et al. Comparison of extracellular and hepatobiliary MR contrast agents for the diagnosis of small HCCs. J Hepatol. 2020;72(5):937–45.

28. Roberts LR, Sirlin CB, Zaiem F, Almasri J, Prokop LJ, Heimbach JK, et al. Imaging for the diagnosis of hepatocellular carcinoma: A systematic review and meta-analysis. Hepatology. 2018;67(1):401–21.

29. van der Pol CB, Lim CS, Sirlin CB, McGrath TA, Salameh JP, Bashir MR, et al. Accuracy of the Liver Imaging Reporting and Data System in Computed Tomography and Magnetic Resonance Image Analysis of Hepatocellular Carcinoma or Overall Malignancy—A Systematic Review. Gastroenterology. 2019;156(4):976–86.

30. Forner A, Vilana R, Ayuso C, Bianchi L, Solé M, Ayuso JR, et al. Diagnosis of hepatic nodules 20 mm or smaller in cirrhosis: Prospective validation of the noninvasive diagnostic criteria for hepatocellular carcinoma. Hepatology. 2008;47(1):97–104.

31. Llovet JM, Brú C, Bruix J. Prognosis of hepatocellular carcinoma: The BCLC staging classification. Semin Liver Dis. 1999;19(3):329–37.

32. Galle PR, Forner A, Llovet JM, Mazzaferro V, Piscaglia F, Raoul JL, et al. EASL Clinical Practice Guidelines: Management of hepatocellular carcinoma. J Hepatol. 2018;69(1):182–236.

33. Cabibbo G, Enea M, Attanasio M, Bruix J, Craxí A, Camma C. A meta-analysis of survival rates of untreated patients in randomized clinical trials of hepatocellular carcinoma. Hepatology. 2010;51(4):1274–83.

34. Marrero JA, Fontana RJ, Barrat A, Askari F, Conjeevaram HS, Su GL, et al. Prognosis of hepatocellular carcinoma: Comparison of 7 staging systems in an American cohort. Hepatology. 2005;41(4):707–15.

35. Reig M, Forner A, Rimola J, Ferrer-Fàbrega J, Burrel M, Garcia-Criado Á, et al. BCLC strategy for prognosis prediction and treatment recommendation: The

2022 update. J Hepatol. 2022;76(3):681–93.

36.   Yau T, Tang VYF, Yao TJ, Fan ST, Lo CM, Poon RTP. Development of Hong Kong liver cancer staging system with treatment stratification for patients with hepatocellular carcinoma. Gastroenterology. 2014;146(7):1691-1700.e3.

37.   Manghisi G, Elba S, Mossa A, Giorgio A, Aloisio V, Perrotta A, et al. A new prognostic system for hepatocellular carcinoma: A retrospective study of 435 patients. Hepatology. 1998;28(3):751–5.

38.   Roayaie S, Jibara G, Tabrizian P, Park JW, Yang J, Yan L, et al. The role of hepatic resection in the treatment of hepatocellular cancer. Hepatology. 2015;62(2):440–51.

39.   Roayaie S, Obeidat K, Sposito C, Mariani L, Bhoori S, Pellegrinelli A, et al. Resection of hepatocellular cancer ≤2 cm: Results from two Western centers. Hepatology. 2013;57(4):1426–35.

40.   Imamura H, Matsuyama Y, Tanaka E, Ohkubo T, Hasegawa K, Miyagawa S, et al. Risk factors contributing to early and late phase intrahepatic recurrence of hepatocellular carcinoma after hepatectomy. J Hepatol. 2003;38:200–7.

41.   Samuel M, Chow PKH, Shih-Yen EC, Machin D, Soo KC. Neoadjuvant and adjuvant therapy for surgical resection of hepatocellular carcinoma. Cochrane Database Syst Rev. 2009;1(1):1–26.

42.   F. Hoffmann-La Roche Ltd. Roche's Tecentriq plus Avastin is the first treatment combination to reduce the risk of cancer returning in people with certain types of early-stage liver cancer in a Phase III trial [Internet]. [cited 2023 Jan 22]. Available from: https://www.roche.com/media/releases/inv-update-2023-01-19

43.   Mínguez B, Hoshida Y, Villanueva A, Toffanin S, Cabellos L, Thung S, et al. Gene-

expression signature of vascular invasion in hepatocellular carcinoma. J Hep. 2011;55(6):1325–31.

44.   Ferrer-Fàbrega J, Forner A, Liccioni A, Miquel R, Molina V, Navasa M, et al. Prospective validation of ab initio liver transplantation in hepatocellular carcinoma upon detection of risk factors for recurrence after resection. Hepatology. 2016;63(3):839–49.

45.   Mazzaferro V, Regalia E, Doci R, Andreola S, Pulvirenti A, Bozzetti F, et al. Liver transplantation for the treatment of small hepatocellular carcinomas in patients with cirrhosis. N Engl J Med. 1996;334(11):693–9.

46.   Mazzaferro V, Sposito C, Zhou J, Pinna AD, De Carlis L, Fan J, et al. Metroticket 2.0 Model for Analysis of Competing Risks of Death After Liver Transplantation for Hepatocellular Carcinoma. Gastroenterology. 2018;154(1):128–39.

47.   Llovet JM, De Baere T, Kulik L, Haber PK, Greten TF, Meyer T, et al. Locoregional therapies in the era of molecular and immune treatments for hepatocellular carcinoma. Nat Rev Gastroenterol Hepatol. 2021;18(5):293–313.

48.   Cucchetti A, Piscaglia F, Cescon M, Colecchia A, Ercolani G, Bolondi L, et al. Cost-effectiveness of hepatic resection versus percutaneous radiofrequency ablation for early hepatocellular carcinoma. J Hepatol. 2013;59(2):300–7.

49.   Lencioni R, de Baere T, Soulen MC, Rilling WS, Geschwind JFH. Lipiodol transarterial chemoembolization for hepatocellular carcinoma: A systematic review of efficacy and safety data. Hepatology. 2016;64(1):106–16.

50.   Llovet JM, Vogel A, Madoff DC, Finn RS, Ogasawara S, Ren Z, et al. Randomized Phase 3 LEAP-012 Study: Transarterial Chemoembolization With or Without Lenvatinib Plus Pembrolizumab for Intermediate-Stage Hepatocellular Carcinoma Not Amenable to Curative Treatment. Cardiovasc Intervent Radiol.

2022;45(4):405–12.

51.   Meyer T, Fox R, Ma YT, Ross PJ, James MW, Sturgess R, et al. Sorafenib in combination with transarterial chemoembolisation in patients with unresectable hepatocellular carcinoma (TACE 2): a randomised placebo-controlled, double-blind, phase 3 trial. Lancet Gastroenterol Hepatol. 2017;2(8):565–75.

52.   Kudo M, Han G, Finn RS, Poon RTP, Blanc JF, Yan L, et al. Brivanib as adjuvant therapy to transarterial chemoembolization in patients with hepatocellular carcinoma: A randomized phase III trial. Hepatology. 2014;60(5):1697–707.

53.   Llovet JM, Pinyol R, Kelley RK, El-Khoueiry A, Reeves HL, Wang XW, et al. Molecular pathogenesis and systemic therapies for hepatocellular carcinoma. Nat Cancer. 2022;3(4):386–401.

54.   Vogel A, Meyer T, Sapisochin G, Salem R, Saborowski A. Hepatocellular carcinoma. Lancet. 2022;400(10360):1345–62.

55.   Llovet JM, Ricci S, Mazzaferro V, Hilgard P, Gane E, Blanc J-F, et al. Sorafenib in Advanced Hepatocellular Carcinoma. N Engl J Med. 2008;359(4):378–90.

56.   Kudo M, Finn RS, Qin S, Han KH, Ikeda K, Piscaglia F, et al. Lenvatinib versus sorafenib in first-line treatment of patients with unresectable hepatocellular carcinoma: a randomised phase 3 non-inferiority trial. Lancet. 2018;391(10126):1163–73.

57.   Finn RS, Qin S, Ikeda M, Galle PR, Ducreux M, Kim T-Y, et al. Atezolizumab plus Bevacizumab in Unresectable Hepatocellular Carcinoma. N Engl J Med. 2020;382(20):1894–905.

58.   Abou-Alfa GK, Lau G, Kudo M, Chan SL, Kelley RK, Furuse J, et al. Tremelimumab plus Durvalumab in Unresectable Hepatocellular Carcinoma. NEJM Evid. 2022;1(8):1–12.

59.   Bruix J, Chan SL, Galle PR, Rimassa L, Sangro B. Systemic treatment of hepatocellular carcinoma: An EASL position paper. J Hepatol. 2021;75(4):960–74.

60.   Bruix J, Qin S, Merle P, Granito A, Huang YH, Bodoky G, et al. Regorafenib for patients with hepatocellular carcinoma who progressed on sorafenib treatment (RESORCE): a randomised, double-blind, placebo-controlled, phase 3 trial. Lancet. 2017;389(10064):56–66.

61.   Abou-Alfa GK, Meyer T, Cheng A-L, El-Khoueiry AB, Rimassa L, Ryoo B-Y, et al. Cabozantinib in Patients with Advanced and Progressing Hepatocellular Carcinoma. N Engl J Med. 2018;379(1):54–63.

62.   Zhu AX, Kang YK, Yen CJ, Finn RS, Galle PR, Llovet JM, et al. Ramucirumab after sorafenib in patients with advanced hepatocellular carcinoma and increased α-fetoprotein concentrations (REACH-2): a randomised, double-blind, placebo-controlled, phase 3 trial. Lancet Oncol. 2019;20(2):282–96.

63.   El-Khoueiry AB, Sangro B, Yau T, Crocenzi TS, Kudo M, Hsu C, et al. Nivolumab in patients with advanced hepatocellular carcinoma (CheckMate 040): an open-label, non-comparative, phase 1/2 dose escalation and expansion trial. Lancet. 2017;389(10088):2492–502.

64.   Yau T, Park JW, Finn RS, Cheng AL, Mathurin P, Edeline J, et al. Nivolumab versus sorafenib in advanced hepatocellular carcinoma (CheckMate 459): a randomised, multicentre, open-label, phase 3 trial. Lancet Oncol. 2022;23(1):77–90.

65.   Yau T, Kang YK, Kim TY, El-Khoueiry AB, Santoro A, Sangro B, et al. Efficacy and Safety of Nivolumab plus Ipilimumab in Patients with Advanced Hepatocellular Carcinoma Previously Treated with Sorafenib: The CheckMate 040 Randomized Clinical Trial. JAMA Oncol. 2020;6(11):1–8.

66. US National Library of Medicine [Internet]. Available from: https://clinicaltrials.gov/ct2/show/NCT04039607

67. Zhu AX, Finn RS, Edeline J, Cattan S, Ogasawara S, Palmer D, et al. Pembrolizumab in patients with advanced hepatocellular carcinoma previously treated with sorafenib (KEYNOTE-224): a non-randomised, open-label phase 2 trial. Lancet Oncol. 2018;19(7):940–52.

68. Finn RS, Ryoo BY, Merle P, Kudo M, Bouattour M, Lim HY, et al. Pembrolizumab As Second-Line Therapy in Patients With Advanced Hepatocellular Carcinoma in KEYNOTE-240: A Randomized, Double-Blind, Phase III Trial. J Clin Oncol. 2020;38(3):193–202.

69. Kudo M, Lim HY, Cheng AL, Chao Y, Yau T, Ogasawara S, et al. Pembrolizumab as second-line therapy for advanced hepatocellular carcinoma: A subgroup analysis of asian patients in the phase 3 KEYNOTE-240 trial. Liver Cancer. 2021;10(3):275–84.

70. Schwartz LH, Litière S, Vries E De, Ford R, Mandrekar S, Shankar L, et al. RECIST 1.1 – Update and Clarification: From the RECIST Committee. Eur J Cancer. 2016;62:132–7.

71. Llovet JM, Lencioni R. mRECIST for HCC: Performance and novel refinements. J Hepatol. 2020;72(2):288–306.

72. Seymour L, Cancer C, Group T, Bogaerts J, Perrone A, Medicine T, et al. iRECIST: guidelines for response criteria for use in trials testing immunotherapeutics. Lancet Oncol. 2017;18(3):e143–52.

73. Zucman-Rossi J, Villanueva A, Nault JC, Llovet JM. Genetic Landscape and Biomarkers of Hepatocellular Carcinoma. Gastroenterology. 2015;149(5):1226-1239.e4.

74. Villanueva A, Mínguez B, Forner A, Reig M, Llovet JM. Hepatocellular carcinoma: novel molecular approaches for diagnosis, prognosis and therapy. 2010;61:317–28.

75. Nault JC, Couchy G, Balabaud C, Morcrette G, Caruso S, Blanc JF, et al. Molecular Classification of Hepatocellular Adenoma Associates With Risk Factors, Bleeding, and Malignant Transformation. Gastroenterology. 2017;152(4):880–94.

76. Gellert-Kristensen H, Richardson TG, Davey Smith G, Nordestgaard BG, Tybjærg-Hansen A, Stender S. Combined Effect of PNPLA3, TM6SF2, and HSD17B13 Variants on Risk of Cirrhosis and Hepatocellular Carcinoma in the General Population. Hepatology. 2020;72(3):845–56.

77. Mínguez B, Tovar V, Chiang D, Villanueva A, Llovet JM. Pathogenesis of hepatocellular carcinoma and molecular therapies. Curr Opin Gastroenterol. 2009;25(3):186–94.

78. Mínguez B, Lachenmayer A. Diagnostic and prognostic molecular markers in hepatocellular carcinoma. 2011;31:181–90.

79. Schulze K, Imbeaud S, Letouzé E, Alexandrov LB, Calderaro J, Rebouissou S, et al. Exome sequencing of hepatocellular carcinomas identifies new mutational signatures and potential therapeutic targets. Nat Genet. 2016;47(5):505–11.

80. Nault JC, Calderaro J, Di Tommaso L, Balabaud C, Zafrani ES, Bioulac-Sage P, et al. Telomerase reverse transcriptase promoter mutation is an early somatic genetic alteration in the transformation of premalignant nodules in hepatocellular carcinoma on cirrhosis. Hepatology. 2014;60(6):1983–92.

81. Torrecilla S, Sia D, Harrington AN, Zhang Z, Cabellos L, Cornella H, et al. Trunk mutational events present minimal intra- and inter-tumoral heterogeneity in hepatocellular carcinoma. J Hepatol. 2017;67(6):1222–31.

82.   Sung WK, Zheng H, Li S, Chen R, Liu X, Li Y, et al. Genome-wide survey of recurrent HBV integration in hepatocellular carcinoma. Nat Genet. 2012;44(7):765–9.

83.   Lachenmayer A, Alsinet C, Savic R, Cabellos L, Toffanin S, Hoshida Y, et al. Wnt-pathway activation in two molecular classes of hepatocellular carcinoma and experimental modulation by sorafenib. Mol Cell Biochem. 2012;23(1):1–7.

84.   Totoki Y, Tatsuno K, Covington KR, Ueda H, Creighton CJ, Kato M, et al. Trans-ancestry mutational landscape of hepatocellular carcinoma genomes. Nat Genet. 2014;46(12):1267–73.

85.   Aubrey BJ, Strasser A, Kelly GL. Tumor-Suppressor Functions of the TP53 Pathway. Cold Spring Harb Perspect Med. 2016;6(5):1–16.

86.   Guichard C, Amaddeo G, Imbeaud S, Ladeiro Y, Pelletier L, Maad I Ben, et al. Integrated analysis of somatic mutations and focal copy-number changes identifies key genes and pathways in hepatocellular carcinoma. Nat Genet. 2012;44(6):694–8.

87.   Ahn SM, Jang SJ, Shim JH, Kim D, Hong SM, Sung CO, et al. Genomic portrait of resectable hepatocellular carcinomas: Implications of RB1 and FGF19 aberrations for patient stratification. Hepatology. 2014;60(6):1972–82.

88.   Mungall AJ, Schein JE, Sipahimalani P, Tam A. Comprehensive and integrative genomic characterization of hepatocellular carcinoma. Vol. 176, Cell. 2017. 1327–1341 p.

89.   Rebouissou S, Nault JC. Advances in molecular classification and precision oncology in hepatocellular carcinoma. J Hepatol. 2020;72(2):215–29.

90.   Kaposi-Novak P, Lee JS, Gòmez-Quiroz L, Coulouarn C, Factor VM, Thorgeirsson SS. Met-regulated expression signature defines a subset of human hepatocellular carcinomas with poor prognosis and aggressive phenotype. J Clin

Invest. 2006;116(6):1582–95.

91. Villanueva A, Hoshida Y, Battiston C, Tovar V, Sia D, Alsinet C, et al. Combining Clinical, Pathology, and Gene Expression Data to Predict Recurrence of Hepatocellular Carcinoma. Mol Cell Biochem. 2012;23(1):1–7.

92. Chiang DY, Villanueva A, Hoshida Y, Peix J, Newell P, Minguez B, et al. Focal Gains of Vascular Endothelial Growth Factor A and Molecular Classification of Hepatocellular Carcinoma. Cancer Res. 2008;68(16):6779–88.

93. Ringelhan M, Pfister D, O'Connor T, Pikarsky E, Heikenwalder M. The immunology of hepatocellular carcinoma review-article. Nat Immunol. 2018;19(3):222–32.

94. Heymann F, Peusquens J, Ludwig-Portugall I, Kohlhepp M, Ergen C, Niemietz P, et al. Liver Inflammation Abrogates Immunological Tolerance Induced by Kupffer Cells. Hepatology. 2015;62(1):279–91.

95. Llovet JM, Castet F, Heikenwalder M, Maini MK, Mazzaferro V, Pinato DJ, et al. Immunotherapies for hepatocellular carcinoma. Nat Rev Clin Oncol. 2022;19(3):151–72.

96. Sangro B, Sarobe P, Hervás-Stubbs S, Melero I. Advances in immunotherapy for hepatocellular carcinoma. Nat Rev Gastroenterol Hepatol. 2021;18(8):525–43.

97. Flecken T, Schmidt N, Hild S, Gostick E, Drognitz O, Zeiser R, et al. Immunodominance and functional alterations of tumor-associated antigen-specific CD8+ T-cell responses in hepatocellular carcinoma. Hepatology. 2014;59(4):1415–26.

98. Hou J, Zhang H, Sun B, Karin M. The immunobiology of hepatocellular carcinoma in humans and mice: Basic concepts and therapeutic implications. J Hepatol. 2020;72(1):167–82.

99.   Prieto J, Melero I, Sangro B. Immunological landscape and immunotherapy of hepatocellular carcinoma. Nat Rev Gastroenterol Hepatol. 2015;12(12):681–700.

100.   Han Y, Chen Z, Yang Y, Jiang Z, Gu Y, Liu Y, et al. Human CD14+CTLA-4+ regulatory dendritic cells suppress T-cell response by cytotoxic T-lymphocyte antigen-4-dependent IL-10 and indoleamine-2,3-dioxygenase production in hepatocellular carcinoma. Hepatology. 2014;59(2):567–79.

101.   Zhou SL, Dai Z, Zhou ZJ, Wang XY, Yang GH, Wang Z, et al. Overexpression of CXCL5 mediates neutrophil infiltration and indicates poor prognosis for hepatocellular carcinoma. Hepatology. 2012;56(6):2242–54.

102.   Keenan BP, Fong L, Kelley RK. Immunotherapy in hepatocellular carcinoma: The complex interface between inflammation, fibrosis, and the immune response. J Immunother Cancer. 2019;7(1):1–13.

103.   Galarreta MR De, Bresnahan E, Molina-sánchez P, Lindblad E, Maier B, Sia D, et al. β-catenin activation promotes immune escape and resistance to anti-PD-1 therapy in hepatocellular carcinoma. Cancer Discov. 2019;9(8):1124–41.

104.   Shen J, Ju Z, Zhao W, Wang L, Peng Y, Ge Z, et al. ARID1A deficiency promotes mutability and potentiates therapeutic antitumor immunity unleashed by immune checkpoint blockade. Nat Med. 2018;24(5):556–62.

105.   Greten TF, Sangro B. Targets for immunotherapy of liver cancer. J Hepatol. 2018;68(1):157–66.

106.   Wei SC, Duffy CR, Allison JP. Fundamental mechanisms of immune checkpoint blockade therapy. Cancer Discov. 2018;8(9):1069–86.

107.   Ribas A, Wolchok JD. Cancer immunotherapy using checkpoint blockade. Science (80-). 2018;359(6382):1350–5.

108. Le Mercier I, Lines JL, Noelle RJ. Beyond CTLA-4 and PD-1, the generation Z of negative checkpoint regulators. Front Immunol. 2015;6:1–15.

109. Ahn E, Araki K, Hashimoto M, Li W, Riley JL, Cheung J, et al. Role of PD-1 during effector CD8 T cell differentiation. Proc Natl Acad Sci U S A. 2018;115(18):4749–54.

110. Agdashian D, Eigindi M, Xie C, Sandhu M, Pratt D, David E, et al. The effect of anti-CTLA4 treatment on peripheral and intra- tumoral T cells in patients with hepatocellular carcinoma. Cancer Immunol Immunother. 2019;68(4):599–608.

111. Fukumura D, Kloepper J, Amoozgar Z, Duda1 DG, Jain RK. Enhancing cancer immunotherapy using antiangiogenics. Nat Rev Clin Oncol. 2018;15(5):325–40.

112. Huinen ZR, Huijbers EJM, van Beijnum JR, Nowak-Sliwinska P, Griffioen AW. Anti-angiogenic agents — overcoming tumour endothelial cell anergy and improving immunotherapy outcomes. Nat Rev Clin Oncol. 2021;18(8):527–40.

113. Sia D, Jiao Y, Martinez-Quetglas I, Kuchuk O, Villacorta-Martin C, Castro de Moura M, et al. Identification of an Immune-specific Class of Hepatocellular Carcinoma, Based on Molecular Features. Gastroenterology. 2017;153(3):812–26.

114. Montironi C, Castet F, Haber PK, Pinyol R, Torres-Martin M, Torrens L, et al. Inflamed and non-inflamed classes of HCC: a revised immunogenomic classification. Gut. 2022;1–12.

115. Grinspan LT, Villanueva A. Biomarker Development Using Liquid Biopsy in Hepatocellular Carcinoma. Semin Liver Dis. 2022;42(2):188–201.

116. Labgaa I, Villanueva A, Dormond O, Demartines N, Melloul E. The role of liquid biopsy in hepatocellular carcinoma prognostication. Cancers (Basel). 2021;13(4):1–17.

117.   Johnson P, Zhou Q, Dao DY, Lo YMD. Circulating biomarkers in the diagnosis and management of hepatocellular carcinoma. Nat Rev Gastroenterol Hepatol. 2022;19(10):670–81.

118.   Lok AS, Sterling RK, Everhart JE, Wright EC, John C, Bisceglie AM Di, et al. Des-gamma-carboxy Prothrombin and Alpha fetoprotein as Biomarkers for the Early Detection of Hepatocellular Carcinoma. Gastroenterology. 2010;138(2):493–514.

119.   Marrero JA, Feng Z, Wang Y, Nguyen MH, Befeler AS, Roberts LR, et al. alpha-fetoprotein, des-gamma carboxythrombin, and Lectin-bound alpha-fetoprotein in early hepatocellular carcinoma. Gastroenterology. 2010;137(1):110–8.

120.   Yang JD, Addissie BD, Mara KC, Harmsen WS, Zhang N, Wongjarupong N, et al. GALAD Score for Hepatocellular Carcinoma Detection in Comparison to Liver Ultrasound and Proposal of GALADUS Score. Cancer Epidemiol BIomarkers Prev. 2019;28(3):531–8.

121.   Toyoda H, Kumada T, Osaki Y, Oka H, Urano F, Kudo M, et al. Staging Hepatocellular Carcinoma by a Novel Scoring System (BALAD Score) Based on Serum Markers. Clin Gastroenterol Hepatol. 2006;4(12):1528–36.

122.   Morgan M. Rogers-Carter1 2 JAV 2 KBGAFPMTMMR, Christianson1 JP. The Doylestown algorithm – a test to improve the performance of AFP in the detection of hepatocellular carcinoma. Cancer Prev Res. 2016;9(2):172–9.

123.   Tayob N, Christie I, Richardson P, Feng Z, White DL, Davila J, et al. Validation of the Hepatocellular Carcinoma Early detection Screening (HES) algorithm in a Cohort of Veterans with Cirrhosis. Clin Gastroenterol Hepatol. 2019;17(9):1886–93.

124.   Labgaa I, Villanueva A. Liquid biopsy in liver cancer. Discov Med. 2015;105:263–

73.

125.   Corcoran RB, Chabner BA. Application of Cell-free DNA Analysis to Cancer Treatment. N Engl J Med. 2018;379(18):1754–65.

126.   Von Felden J, Garcia-Lezana T, Schulze K, Losic B, Villanueva A. Liquid biopsy in the clinical management of hepatocellular carcinoma. Gut. 2020;69(11):2025–34.

127.   Kirk GD, Camus-Randon AM, Mendy M, Goedert JJ, Merle P, Trépo C, et al. Ser-249 p53 mutations in plasma DNA of patients with hepatocellular carcinoma from The Gambia. J Natl Cancer Inst. 2000;92(2):148–53.

128.   Parikh AR, Leshchiner I, Elagina L, Goyal L, Siravegna G, Livitz D, et al. Liquid versus tissue biopsy for detecting acquired resistance and tumor heterogeneity in gastrointestinal cancers. 2019;25(9):1415–21.

129.   Labgaa I, Villacorta-Martin C, D'Avola D, Craig A, von Felden J, Martins-Filho SN, et al. A pilot study of ultra-deep targeted sequencing of plasma DNA identifies driver mutations in hepatocellular carcinoma. 2018;37(27):3740–52.

130.   Cai Z, Chen G, Zeng Y, Dong X, Li Z, Huang Y, et al. Comprehensive liquid profiling of circulating tumor DNA and protein biomarkers in long-term follow-up patients with hepatocellular carcinoma. Clin Cancer Res. 2019;25(17):5284–94.

131.   Wang J, Huang A, Wang Y-P, Yin Y, Fu P-Y, Zhang X, et al. Circulating tumor DNA correlates with microvascular invasion and predicts tumor recurrence of hepatocellular carcinoma. Ann Transl Med. 2020;8(5):237–237.

132.   Oversoe SK, Clement MS, Pedersen MH, Weber B, Aagaard NK, Villadsen GE, et al. TERT promoter mutated circulating tumor DNA as a biomarker for prognosis in hepatocellular carcinoma. Scand J Gastroenterol. 2020;55(12):1433–40.

133.   Hernandez-Meza G, Felden J Von, Gonzalez-kozlova EE, Garcia-Lezana T, Peix J,

Portela A, et al. DNA methylation profiling of human hepatocarcinogenesis. 2022;74(1):183–99.

134. Villanueva A, Portela A, Sayols S, Battiston C, Hoshida Y, Méndez-González J, et al. DNA methylation-based prognosis and epidrivers in hepatocellular carcinoma. Hepatology. 2015;61(6):1945–56.

135. Chen M, Zhao R, Chen K, Huang Y, Liu Z, Wei Y, et al. Hypomethylation of CTCFL promoters as a noninvasive biomarker in plasma from patients with hepatocellular carcinoma. Neoplasma. 2013;60(5):607–16.

136. Yeh CC, Goyal A, Shen J, Wu H chen, Strauss JA, Wang Q, et al. Global Level of Plasma DNA Methylation is Associated with Overall Survival in Patients with Hepatocellular Carcinoma. Ann Surg Oncol. 2017;24(12):3788–95.

137. Li F, Qiao CY, Gao S, Fan YC, Chen LY, Wang K. Circulating cell-free DNA of methylated insulin-like growth factor-binding protein 7 predicts a poor prognosis in hepatitis B virus-associated hepatocellular carcinoma after hepatectomy. Free Radic Res. 2018;52(4):455–64.

138. Xu RH, Wei W, Krawczyk M, Wang W, Luo H, Flagg K, et al. Circulating tumour DNA methylation markers for diagnosis and prognosis of hepatocellular carcinoma. Nat Mater. 2017;16(11):1155–62.

139. Lu C-Y, Chen S-Y, Peng H-L, Kan P-Y, Chang W-C, Yen C-J. Cell-free methylation markers with diagnostic and prognostic potential in hepatocellular carcinoma. Oncotarget. 2017;8(4):6406–18.

140. Ahn JC, Teng PC, Chen PJ, Posadas E, Tseng HR, Lu SC, et al. Detection of Circulating Tumor Cells and Their Implications as a Biomarker for Diagnosis, Prognostication, and Therapeutic Monitoring in Hepatocellular Carcinoma. Hepatology. 2021;73(1):422–36.

141. Sun YF, Xu Y, Yang XR, Guo W, Zhang X, Qiu SJ, et al. Circulating stem cell-like epithelial cell adhesion molecule-positive tumor cells indicate poor prognosis of hepatocellular carcinoma after curative resection. Hepatology. 2013;57(4):1458–68.

142. von Felden J, Schulze K, Krech T, Ewald F, Nashan B, Pantel K, et al. Circulating tumor cells as liquid biomarker for high HCC recurrence risk after curative liver resection. Oncotarget. 2017;8(52):89978–87.

143. Yamashita T, Ji J, Budhu A, Forgues M, Yang W, Wang Y, et al. EpCAM-positive hepatocellular carcinoma cells are tumor initiating cells with stem/progenitor cell features. 2009;136(3):1012–24.

144. Ogle LF, Orr JG, Willoughby CE, Hutton C, McPherson S, Plummer R, et al. Imagestream detection and characterisation of circulating tumour cells – A liquid biopsy for hepatocellular carcinoma? J Hepatol. 2016;65(2):305–13.

145. D'Avola D, Villacorta-Martin C, Martins-Filho SN, Craig A, Labgaa I, von Felden J, et al. High-density single cell mRNA sequencing to characterize circulating tumor cells in hepatocellular carcinoma. Sci Rep. 2018;8(1):1–7.

146. Kalluri R, LeBleu VS. The biology, function, and biomedical applications of exosomes. Science (80-). 2020;367(6478):1–47.

147. Mjelle R, Dima SO, Bacalbasa N, Chawla K, Sorop A, Cucu D, et al. Comprehensive transcriptomic analyses of tissue, serum, and serum exosomes from hepatocellular carcinoma patients. BMC Cancer. 2019;19(1):1–13.

148. Gibney GT, Weiner LM, Atkins MB. Predictive biomarkers for checkpoint inhibitor-based immunotherapy. Lancet Oncol. 2016;17(12):542–51.

149. Garon EB, Rizvi NA, Hui R, Leighl N, Balmanoukian AS, Eder JP, et al. Pembrolizumab for the Treatment of Non–Small-Cell Lung Cancer. N Engl J Med.

2015;372(21):2018–28.

150.   Larkin J, Chiarion-Sileni V, Gonzalez R, Jacques Grob J, Lao CD, Schadendorf D, et al. Combined Nivolumab and Ipilimumab or Monotherapy in Previously Untreated Melanoma Corresponding authors. N Engl J Med. 2015;373(1):23–34.

151.   Borghaei H, Paz-Ares L, Horn L, Spigel DR, Steins M, Ready NE, et al. Nivolumab versus Docetaxel in Advanced Non-squamous Non- small Cell Lung Cancer. 2015;373(17):1627–39.

152.   Oh SY, Kim S, Keam B, Kim TM, Kim DW. Soluble PD - L1 is a predictive and prognostic biomarker in advanced cancer patients who receive immune checkpoint blockade treatment. Sci Rep. 2021;11(1):1–11.

153.   Mocan T, Ilies M, Nenu I, Craciun R, Horhat A, Susa R, et al. Serum levels of soluble programmed death-ligand 1 (sPD-L1): A possible biomarker in predicting post-treatment outcomes in patients with early hepatocellular carcinoma. Int Immunopharmacol. 2021;94:1–8.

154.   Yamazaki N, Kiyohara Y, Uhara H, Iizuka H, Uehara J, Otsuka F, et al. Cytokine biomarkers to predict antitumor responses to nivolumab suggested in a phase 2 study for advanced melanoma. Cancer Sci. 2017;108(5):1022–31.

155.   Pedersen JG, Madsen AT, Gammelgaard KR, Aggerholm-Pedersen N, Sørensen BS, Øllegaard TH, et al. Inflammatory cytokines and ctdna are biomarkers for progression in advanced-stage melanoma patients receiving checkpoint inhibitors. Cancers (Basel). 2020;12(6):1–15.

156.   Feun LG, Li Y, Wu C, Wangpaichitr M, Jones PD, Richman SP, et al. Phase 2 Study of Pembrolizumab and Circulating Biomarkers to Predict Anticancer Response in Advanced, Unresectable Hepatocellular Carcinoma. 2020;125(20):3603–14.

157.   Myojin Y, Kodama T, Sakamori R, Maesaka K, Matsumae T, Tawara S, et al.

Interleukin-6 Is a Circulating Prognostic Biomarker for Hepatocellular Carcinoma Patients Treated with. Cancers (Basel). 2022;14(4):1–12.

158. von Felden J, Craig AJ, Garcia-Lezana T, Labgaa I, Haber PK, D'Avola D, et al. Mutations in circulating tumor DNA predict primary resistance to systemic therapies in advanced hepatocellular carcinoma. Oncogene. 2021;40(1):140–51.

159. Spranger S, Bao R, Gajewski TF. Melanoma-intrinsic β-catenin signalling prevents anti-tumour immunity. Nature. 2015;523(7559):231–5.

160. Chan TA, Yarchoan M, Jaffee E, Swanton C, Quezada SA, Stenzinger A, et al. Development of tumor mutation burden as an immunotherapy biomarker: Utility for the oncology clinic. Ann Oncol. 2019;30(1):44–56.

161. Franses JW, Lim M, Burgoyne AM, Mody K, Lennerz J, Chang J, et al. Profile and Predictors of Blood Tumor Mutational Burden in Advanced Hepatocellular Carcinoma. Oncologist. 2022;(August):1–4.

162. Strickler JH, Hanks BA, Khasraw M. Tumor mutational burden as a predictor of immunotherapy response: Is more always better? Clin Cancer Res. 2021;27(5):1236–41.

163. Soria ME, Gregori J, Chen Q, García-Cehic D, Llorens M, de Ávila AI, et al. Pipeline for specific subtype amplification and drug resistance detection in hepatitis C virus. BMC Infect Dis. 2018;18(1):1–15.

164. Magoč T, Salzberg SL. FLASH: Fast length adjustment of short reads to improve genome assemblies. Bioinformatics. 2011;27(21):2957–63.

165. Gregori J, Esteban JI, Cubero M, Garcia-Cehic D, Perales C, Casillas R, et al. Ultra-deep pyrosequencing (UDPS) data treatment to study amplicon HCV minor variants. PLoS One. 2013;8(12):1–13.

166. COSMIC Database [Internet]. Available from:

https://cancer.sanger.ac.uk/cosmic

167. Cai ZX, Chen G, Zeng YY, Dong XQ, Lin MJ, Huang XH, et al. Circulating tumor DNA profiling reveals clonal evolution and real-time disease progression in advanced hepatocellular carcinoma. Int J Cancer. 2017;141(5):977–85.

168. Liao W, Yang H, Xu H, Wang Y, Ge P, Ren J, et al. Noninvasive detection of tumor-associated mutations from circulating cell-free DNA in hepatocellular carcinoma patients by targeted deep sequencing. Oncotarget. 2016;7(26):40481–90.

169. Ikeda S, Tsigelny IF, Skjevik ÅA, Kono Y, Mendler M, Kuo A, et al. Next-Generation Sequencing of Circulating Tumor DNA Reveals Frequent Alterations in Advanced Hepatocellular Carcinoma. Oncologist. 2018;23(5):586–93.

170. Howell J, Atkinson SR, Pinato DJ, Knapp S, Ward C, Minisini R, et al. Identification of mutations in circulating cell-free tumour DNA as a biomarker in hepatocellular carcinoma. Eur J Cancer. 2019;116:56–66.

171. Huang A, Zhao X, Yang X-R, Li F-Q, Zhou X-L, Wu K, et al. Circumventing intratumoral heterogeneity to identify potential therapeutic targets in hepatocellular carcinoma. J Hepatol. 2017;67(2):293–301.

172. Losic B, Craig AJ, Villacorta-Martin C, Martins-Filho SN, Akers N, Chen X, et al. Intratumoral heterogeneity and clonal evolution in liver cancer. Nat Commun. 2020;11(1):291–7.

173. Temraz S, Nasr R, Mukherji D, Kreidieh F, Shamseddine A. Liquid biopsy derived circulating tumor cells and circulating tumor DNA as novel biomarkers in hepatocellular carcinoma. Expert Rev Mol Diagn. 2022;22(5):507–18.

174. Maley CC, Galipeau PC, Finley JC, Wongsurawat VJ, Li X, Sanchez CA, et al. Genetic clonal diversity predicts progression to esophageal adenocarcinoma. Nat Genet. 2006;38(4):468–73.

175.   Clark J, Attard G, Jhavar S, Flohr P, Reid A, De-Bono J, et al. Complex patterns of ETS gene alteration arise during cancer development in the human prostate. Oncogene. 2008;27(14):1993–2003.

176.   Navin N, Krasnitz A, Rodgers L, Cook K, Meth J, Kendall J, et al. Inferring tumor progression from genomic heterogeneity. Genome Res. 2010;20(1):68–80.

177.   Ikeda S, Lim JS, Kurzrock R. Analysis of Tissue and Circulating Tumor DNA by Next-Generation Sequencing of Hepatocellular Carcinoma: Implications for Targeted Therapeutics. Mol Cancer Ther. 2018;17(5):1114–22.

178.   Zhu GQ, Liu WR, Tang Z, Qu WF, Fang Y, Jiang XF, et al. Serial circulating tumor DNA to predict early recurrence in patients with hepatocellular carcinoma: a prospective study. Mol Oncol. 2022;16(2):549–61.

179.   Nault JC, Mallet M, Pilati C, Calderaro J, Bioulac-Sage P, Laurent C, et al. High frequency of telomerase reverse-transcriptase promoter somatic mutations in hepatocellular carcinoma and preneoplastic lesions. Nat Commun. 2013 Jul 26;4(2218):1–6.

180.   Brunner SF, Roberts ND, Wylie LA, Moore L, Aitken SJ, Davies SE, et al. Somatic mutations and clonal dynamics in healthy and cirrhotic human liver. Nature. 2019;574(7779):538–42.

181.   Reinert T, Schøler L V, Thomsen R, Tobiasen H, Vang S, Nordentoft I, et al. Analysis of circulating tumour DNA to monitor disease burden following colorectal cancer surgery. Gut. 2016;65(4):625–34.

182.   Lecomte T, Berger A, Zinzindohoué F, Micard S, Landi B, Blons H, et al. Detection of free-circulating tumor-associated DNA in plasma of colorectal cancer patients and its association with prognosis. Int J cancer. 2002;100(5):542–8.

183.   Tie J, Cohen JD, Wang Y, Li L, Christie M, Simons K, et al. Serial circulating tumour

DNA analysis during multimodality treatment of locally advanced rectal cancer: a prospective biomarker study. Gut. 2019;68(4):663–71.

184.   Tie J, Wang Y, Cohen J, Li L, Hong W, Christie M, et al. Circulating tumor DNA dynamics and recurrence risk in patients undergoing curative intent resection of colorectal cancer liver metastases: A prospective cohort study. PLoS Med. 2021;18(5):1–16.

185.   Wan JCM, Massie C, Garcia-Corbacho J, Mouliere F, Brenton JD, Caldas C, et al. Liquid biopsies come of age: Towards implementation of circulating tumour DNA. Nat Rev Cancer. 2017;17(4):223–38.

186.   Goldberg SB, Narayan A, Kole AJ, Decker RH, Teysir J, Carriero NJ, et al. Early Assessment of Lung Cancer Immunotherapy Response via Circulating Tumor DNA. Clin Cancer Res. 2018;24(8):1872–80.

187.   Diehl F, Schmidt K, Choti MA, Romans K, Goodman S, Li M, et al. Circulating mutant DNA to assess tumor dynamics. Nat Med. 2008 Sep;14(9):985–90.

188.   Reck M. Pembrolizumab as first-line therapy for metastatic non-small-cell lung cancer. Immunotherapy. 2018;10(2):93–105.

189.   Paz-Ares L, Spira A, Raben D, Planchard D, Cho BC, Özgüroğlu M, et al. PACIFIC Extra 1 (muito importante) - Outcomes by PD-L1. Ann Oncol. 2020;31(6):798–806.

190.   Jilkova ZM, Aspord C, Decaens T. Predictive factors for response to PD-1/PD-L1 checkpoint inhibition in the field of hepatocellular carcinoma: Current status and challenges. Cancers (Basel). 2019;11(10):1–14.

191.   Pistillo MP, Fontana V, Morabito A, Dozin B, Laurent S, Carosio R, et al. Soluble CTLA-4 as a favorable predictive biomarker in metastatic melanoma patients treated with ipilimumab: an Italian melanoma intergroup study. Cancer Immunol

Immunother. 2019;68(1):97–107.

192. Deshmane SL, Kremlev S, Amini S, Sawaya BE. Monocyte chemoattractant protein-1 (MCP-1): An overview. J Interf Cytokine Res. 2009;29(6):313–25.

193. Freeman AJ, Kearney CJ, Silke J, Oliaro J. Unleashing TNF cytotoxicity to enhance cancer immunotherapy. Trends Immunol. 2021;42(12):1128–42.

194. Perez-Ruiz E, Minute L, Otano I, Alvarez M, Ochoa MC, Belsue V, et al. Prophylactic TNF blockade uncouples efficacy and toxicity in dual CTLA-4 and PD-1 immunotherapy. Nature. 2019;569(7756):428–32.

195. Bertrand F, Montfort A, Marcheteau E, Imbert C, Gilhodes J, Filleron T, et al. TNFα blockade overcomes resistance to anti-PD-1 in experimental melanoma. Nat Commun. 2017;8(1):2256–69.

196. Long L, Zhang X, Chen F, Pan Q, Phiphatwatchara P, Zeng Y, et al. The promising immune checkpoint LAG-3: From tumor microenvironment to cancer immunotherapy. Genes and Cancer. 2018;9(5–6):176–89.

197. Hoejberg L, Bastholt L, Johansen JS, Christensen IJ, Gehl J, Schmidt H. Serum interleukin-6 as a prognostic biomarker in patients with metastatic melanoma. Transl Res. 2012;22(4):287–93.

198. Nakamura Y. Biomarkers for immune checkpoint inhibitor-mediated tumor response and adverse events. Front Med. 2019;6:1–18.

199. Tran NH, Kisiel J, Roberts LR. Using cell-free DNA for HCC surveillance and prognosis. JHEP Reports. 2021;3(4):1–10.

200. Tokuhisa Y, Iizuka N, Sakaida I, Moribe T, Fujita N, Miura T, et al. Circulating cell-free DNA as a predictive marker for distant metastasis of hepatitis C virus-related hepatocellular carcinoma. Br J Cancer. 2007 Nov 19;97(10):1399–403.

201. Matsumae T, Kodama T, Myojin Y, Maesaka K, Sakamori R, Takuwa A, et al.

Circulating Cell-Free DNA Profiling Predicts the Therapeutic Outcome in Advanced Hepatocellular Carcinoma Patients Treated with Combination Immunotherapy. Cancers (Basel). 2022;14(14):1–14.

202.   Hirai M, Kinugasa H, Nouso K, Yamamoto S, Terasawa H, Onishi Y, et al. Prediction of the prognosis of advanced hepatocellular carcinoma by TERT promoter mutations in circulating tumor DNA. J Gastroenterol Hepatol. 2021;36(4):1118–25.

203.   Li H, Li J, Zhang C, Zhang C, Wang H. TERT mutations correlate with higher TMB value and unique tumor microenvironment and may be a potential biomarker for anti-CTLA4 treatment. Cancer Med. 2020;9(19):7151–60.

204.   Gutiontov SI, Turchan WT, Spurr LF, Rouhani SJ, Chervin CS, Steinhardt G, et al. CDKN2A loss-of-function predicts immunotherapy resistance in non-small cell lung cancer. Sci Rep. 2021;11(1):1–11.

205.   Pinyol R, Sia D, Llovet JM. Immune exclusion-WNT/CTNNB1 class predicts resistance to immunotherapies in HCC. Clin Cancer Res. 2019;25(7):2021–3.

206.   Harking JJ, Nandakumar S, Armenia J, Khalil DN, Albano M, Ly M, et al. Prospective Genotyping of Hepatocellular Carcinoma: Clinical Implications of Next-Generation Sequencing for Matching Patients to Targeted and Immune Therapies. 2020;25(7):2116–26.

207.   Xiao Q, Wu J, Wang W, Chen S, Zheng Y, Yu X, et al. DKK2 imparts tumor immunity evasion through β-catenin- independent suppression of cytotoxic immune cell activation. 2018;24(3):262–70.

208.   Zhu AX, Abbas AR, de Galarreta MR, Guan Y, Lu S, Koeppen H, et al. Molecular correlates of clinical response and resistance to atezolizumab in combination with bevacizumab in advanced hepatocellular carcinoma. Nat Med.

2022;28(8):1599–611.

209. Haber PK, Castet F, Torres-Martin M, Andreu-Oller C, Puigvehí M, Miho M, et al. Molecular Markers of Response to Anti-PD1 Therapy in Advanced Hepatocellular Carcinoma. Gastroenterology. 2022;S0016-5085(2):01039–3.

210. Wallin JJ, Bendell JC, Funke R, Sznol M, Korski K, Jones S, et al. Atezolizumab in combination with bevacizumab enhances antigen-specific T-cell migration in metastatic renal cell carcinoma. Nat Commun. 2016;7:1–8.

211. Rizzo A, Brandi G. Biochemical predictors of response to immune checkpoint inhibitors in unresectable hepatocellular carcinoma. Cancer Treat Res Commun. 2021;27:1–6.

212. Samstein RM, Lee C-H, Shoushtari AN, Hellmann MD, Shen R, Janjigian YY, et al. Tumor mutational load predicts survival after immunotherapy across multiple cancer types. Nat Genet. 2019;51(2):202–6.

213. Pinato DJ, Guerra N, Fessas P, Murphy R, Mineo T, Mauri FA, et al. Immune-based therapies for hepatocellular carcinoma. Oncogene. 2020;39(18):3620–37.

214. Ang C, Klempner SJ, Ali SM, Madison R, Ross JS, Severson EA, et al. Prevalence of established and emerging biomarkers of immune checkpoint inhibitor response in advanced hepatocellular carcinoma. Oncotarget. 2019;10(40):4018–25.

215. Lei Y, Zhang G, Zhang C, Xue L, Yang Z, Lu Z, et al. The average copy number variation (CNVA) of chromosome fragments is a potential surrogate for tumor mutational burden in predicting responses to immunotherapy in non-small-cell lung cancer. Clin Transl Immunol. 2021;10(1):1–16.

216. Yang X, Hu Y, Yang K, Wang D, Lin J, Long J, et al. Cell-free DNA copy number variations predict efficacy of immune checkpoint inhibitor-based therapy in hepatobiliary cancers. J Immunother Cancer. 2021;9(5):1–11.

Annex

10. Annex

10.1. Validation by ddPCR of C228T TERT mutation

Table 19. Comparison of percentage of C228T TERT mutation obtained by ddPCR or by NGS

Sample	Tissue	% Freq ddPCR	% Freq NGS
VH335	HCC	34,63	66,95
VH336	Adj	0,285	9,47
VH1606	cfDNA	8,17	76,84
VH337	HCC	51,68	66,11
VH338	Adj	0,562	1,13
VH1615	cfDNA	5,317	5,83
VH339	HCC	43,628	66,77
VH340	Adj	0,828	1,86
VH1618	cfDNA	2,3	59,46
VH341	HCC	0,348	1,95
VH342	Adj	0	0
VH1607	cfDNA	8,74	10,48
VH343	HCC	0	0
VH344	Adj	0,00664	1,12
VH1632	cfDNA	0,844	54,02
VH345	HCC	9,316	28,4
VH346	Adj	1,207	1,7
VH1635	cfDNA	14,687	23
VH347	HCC	32,256	71,3

VH348	Adj	0,839	2,2
VH1637	cfDNA	0,148	0
VH349	HCC	20,702	52,3
VH350	Adj	0,282	0
VH1641	cfDNA	4,4	12,9
VH351	HCC	34,71	46,5
VH352	Adj	0,144	1
VH1714	cfDNA	1,745	1,2
VH353	HCC	0,00846	0
VH354	Adj	0,00981	0
VH1716	cfDNA	1,67	10,14
VH355	HCC	41,912	74,3
VH356	Adj	0,239	1,8
VH1721	cfDNA	0	0
VH363	HCC	0	0
VH364	Adj	0	0
VH1801	cfDNA	0	0
VH367	HCC	0	0
VH368	Adj	0	0
VH1806	cfDNA	6,585	0
VH369	HCC	44,55	51
VH370	Adj	0,419	2,68
VH1810	cfDNA	7,064	4,59

VH369B	HCC	0	72,85
VH370B	Adj	0	0
VH1810D	cfDNA	0	0
VH371	HCC	76,014	69,26
VH372	Adj	0	0
VH1817	cfDNA	1,525	1,54
VH373	HCC	22,987	28,97
VH374	Adj	0,02	0
VH1818	cfDNA	2,757	2,24
VH375	HCC	0,0385	1,47
VH376	Adj	0,011	0
VH1822	cfDNA	3,403	3,47
VH377	HCC	1,823	3,29
VH378	Adj	0,271	2,36
VH1830	cfDNA	1,313	1,85
VH381	HCC	32,887	37,72
VH382	Adj	0,0208	0
VH1845	cfDNA	3,052	38,4
B1921	HCC	29,1	39,16
VH1921	cfDNA	35,594	43,37
B1932	HCC	3,265	1,08
VH1932	cfDNA	23,757	34,23
B1933	HCC	0	0

VH1933	cfDNA	29,754	33,61
VH383	HCC	0	0
VH384	Adj	0,0229	0
VH1847	cfDNA	4,954	3,85
VH391	HCC	0	0
VH392	Adj	0	0
VH1855	cfDNA	3,018	5,53
VH393	HCC	19,837	0
VH394	Adj	0	0
VH1862	cfDNA	1,329	0
VH401	HCC	22,376	17,2
VH402	Adj	0,269	0
VH1906	cfDNA	3,193	0
VH409	HCC	0,0129	0
VH410	Adj	0,0383	0
VH1935	cfDNA	0,0632	0
VH411	HCC	42,085	53
VH412	Adj	0,0529	1,33
VH1939	cfDNA	2,537	1,91
VH413	HCC	54,979	33,59
VH414	Adj	1,377	0
VH1946	cfDNA	0	0
VH417	HCC	26,707	27,91

VH418	Adj	8,686	3
VH1951	cfDNA	0,239	0,86
VH427	HCC	0	0
VH428	Adj	0,098	0
VH1952	cfDNA	1,456	2,85

10.2. Scientific article derived from this doctoral thesis

- Higuera M, **Vargas-Accarino E**, Torrens M, Gregori J, Salcedo MT, Martínez-Campreciós J, Torres G, Bermúdez-Ramos M, Bilbao I, Guerrero-Murillo M, Serres-Créixams X, Merino X, Rodríguez-Frías F, Quer J, Mínguez B. Ultra Deep Sequencing of Circulating Cell-Free DNA as a Potential Tool for Hepatocellular Carcinoma Management. Cancers (Basel). 2022;14(16):1-17.

cancers

Article

Ultra Deep Sequencing of Circulating Cell-Free DNA as a Potential Tool for Hepatocellular Carcinoma Management

Mónica Higuera [1], Elena Vargas-Accarino [1,2], María Torrens [1], Josep Gregori [3,4], María Teresa Salcedo [2,5,6], Joan Martínez-Campreciós [1,2], Gloria Torres [1], María Bermúdez-Ramos [1,2,4], Itxarone Bilbao [2,4,7], Mercedes Guerrero-Murillo [3], Xavier Serres-Créixams [8], Xavier Merino [8], Francisco Rodríguez-Frías [9,10], Josep Quer [3,4,10] and Beatriz Mínguez [1,2,4,11,*]

[1] Liver Cancer Research Group, Liver Diseases, Vall d'Hebron Institut de Recerca (VHIR), Vall d'Hebron Barcelona Hospital Campus, 08035 Barcelona, Spain

[2] Department of Medicine, Campus of the UAB, Universitat Autònoma de Barcelona (UAB), Bellaterra, 08193 Cerdanyola del Vallès, Spain

[3] Viral Hepatitis Research Group, Liver Diseases, Vall d'Hebron Institut de Recerca (VHIR), Vall d'Hebron Barcelona Hospital Campus, 08035 Barcelona, Spain

[4] Centro de Investigación Biomédica en Red de Enfermedades Hepáticas y Digestivas (CIBERehd), Instituto de Salud Carlos III, 28029 Madrid, Spain

[5] Pathology Department, Hospital Universitario Vall d'Hebron, Vall d'Hebron Barcelona Hospital Campus, 08035 Barcelona, Spain

[6] Spanish Biomedical Research Network Centre in Oncology (CIBERONC), Instituto de Salud Carlos III, 28029 Madrid, Spain

[7] Hepatobiliary Surgery and Transplant Department, Hospital Universitario Vall d'Hebron, Vall d'Hebron Barcelona Hospital Campus, 08035 Barcelona, Spain

[8] Radiology Department, Hospital Universitario Vall d'Hebron, Vall d'Hebron Barcelona Hospital Campus, 08035 Barcelona, Spain

[9] Biochemistry and Microbiology Department, Hospital Universitari Vall d'Hebron, Vall d'Hebron Barcelona Hospital Campus, 08035 Barcelona, Spain

[10] Biochemistry and Molecular Biology Department, Campus of the UAB, Universitat Autònoma de Barcelona (UAB), 08193 Bellaterra, Spain

[11] Liver Unit, Hospital Universitario Vall d'Hebron, Vall d'Hebron Barcelona Hospital Campus, 08035 Barcelona, Spain

* Correspondence: beatriz.minguez@vallhebron.cat; Tel.: +34-93-274-61-40 (ext. 6561)

check for updates

Simple Summary: In this unicentric prospective study, we analyzed the most prevalent mutations in HCC (TERT promoter, TP53, CTNNB1, AXIN1 and ARID1A) in plasma cfDNA by next-generation sequencing, aiming to elucidate their value as prognostic noninvasive biomarkers. Total cfDNA (cut-off value 2 ng/μL), number of mutated genes and number of detectable mutations on cfDNA were significantly related to mortality. Number of mutated genes and number of detected mutations in cfDNA and the ratio between number of mutations and total amount of cfDNA were also significantly associated with recurrence. Detection of more than four mutations in cfDNA correlated with a higher risk of death. Dynamic changes in cfDNA mutations were detected prior to radiological detection of HCC recurrence. We believe that these results support the proof of principle and launching of validation studies to confirm that total cfDNA and detection of prevalent HCC mutations could have prognostic implications in early-stage HCC patients.

Abstract: Background: Cell-free DNA (cfDNA) concentrations have been described to be inversely correlated with prognosis in cancer. Mutations in HCC-associated driver genes in cfDNA have been reported, but their relation with patient's outcome has not been described. Our aim was to elucidate whether mutations found in cfDNA could be representative from those present in HCC tissue, providing the rationale to use the cfDNA to monitor HCC. Methods: Tumoral tissue, paired nontumor adjacent tissue and blood samples were collected from 30 HCC patients undergoing curative therapies. Deep sequencing targeting HCC driver genes was performed. Results: Patients with more than 2 ng/μL of cfDNA at diagnosis had higher mortality (mean OS 24.6 vs. 31.87 months, $p = 0.01$) (AUC = 0.782). Subjects who died during follow-up, had a significantly higher number

---

187

of mutated genes ($p = 0.015$) and number of mutations ($p = 0.015$) on cfDNA. Number of mutated genes ($p = 0.001$), detected mutations ($p = 0.001$) in cfDNA and ratio (number of mutations/cfDNA) ($p = 0.003$) were significantly associated with recurrence. However, patients with a ratio (number of mutations/cfDNA) above 6 (long-rank $p = 0.0003$) presented a higher risk of recurrence than those with a ratio under 6. Detection of more than four mutations in cfDNA correlated with higher risk of death (long-rank $p = 0.042$). Conclusions: In summary, cfDNA and detection of prevalent HCC mutations could have prognostic implications in early-stage HCC patients

1. Introduction

Hepatocellular carcinoma (HCC) is ranked as the seventh most common neoplasm and the fourth leading cause of cancer death worldwide. HCC is the most frequent primary liver cancer and is the leading cause of death among patients with cirrhosis [1].

Tumor biopsy remains the standard diagnostic procedure for cancer diagnosis. However, in HCC, biopsy has a limited role in clinical practice because, in cirrhotic patients, noninvasive radiological criteria are well established and validated, leaving biopsy as an indication for patients without cirrhosis or for those patients with cirrhosis with tumors not showing the specific radiological features [2].

Most of the reported knowledge regarding molecular features, molecular classification and potential biomarkers of HCC has been developed using surgical samples from patients at initial stages of the disease. However, tumorigenesis is a dynamic process and new molecular features different from the ones present at initial-stage disease progress over time. Tumor resistance to therapy could occur during treatment, possibly due to newly acquired molecular features that were not present in the initial biopsy sample [3]. Nevertheless, in the era of molecular oncology, where many treatments for different neoplasms are guided by molecular alterations, in clinical practice, the most used tools to classify patients, allocate optimal treatments and estimate prognosis of HCC patients are exclusively clinical algorithms [4].

In this context, despite tumor biopsies still representing the standard procedure for diagnosis and molecular testing to guide precision therapies, liquid biopsy and, in particular, cell-free DNA (cfDNA) from plasma is rapidly emerging as an important and minimally invasive alternative to standard tumor biopsies [5]. Liquid biopsy is a valuable tool for cancer detection and monitoring during and after treatment, and it has been demonstrated to be useful for molecular characterization [6]. cfDNA could also be beneficial in overcoming the problem with tumor heterogeneity, usually under-represented in small or partial tumor samples [7]. Liquid biopsy has shown advantages over conventional tissue biopsy due to its minimally invasive nature, which reduces the risk of complications for patients [8]. Moreover, it is also easily repeatable during patient follow-up [9], allowing monitoring of potential changes at the molecular level. These factors underline the importance of developing liquid biopsy techniques for HCC, considering cancerous cells from this tumor adapt to pharmacological pressure and acquire new molecular alterations that may have been missed or not detected at initial diagnosis [10].

cfDNA concentrations in plasma of HCC patients are up to 20 times higher than in healthy people [11]. Furthermore, cfDNA concentration has been found to be associated with tumor size, portal vein invasion and inversely correlated with prognosis and shorter overall survival [11–13]. The potential applications of cfDNA analysis and its mutations also include the detection of potential molecular targets for acquired resistance, uncover potential targets not detected in small biopsy samples or the detection of minimal residual disease after surgical resection [14,15].

There are limited reports on cfDNA in HCC, but recent publications described the detection of HCC-associated driver genes, such as TP53, CTNNB1 and TERT in cfDNA [16–20]. Several

of these studies have investigated a small number of patients, reporting only the mutation landscape at the moment of resection with no derived information about the relationship between mutations found and risk of recurrence and patient outcomes.

The aims of this study were to (1) elucidate whether mutations found in plasma cfDNA could be confidently detected using next-generation sequencing, evaluating if they were representative of the most commonly described driver mutations present in HCC tissue, and (2) provide the proof of principle to further develop this technology to monitor the evolution of those mutations in HCC patients during their follow-up. To address these questions, we prospectively recruited 30 HCC patients at early stages undergoing curative therapies and synchronously collected tumor, surrounding liver tissue and whole blood samples, in which deep sequencing targeting HCC driver genes and mutation hotspots was performed.

2. Materials and Methods

2.1. Study Design and Participants

All patients were recruited at the Liver Unit, Hospital Universitari Vall d'Hebron and prospectively enrolled in the study. Samples from 30 patients with confirmed HCC, either with noninvasive radiological criteria or histological confirmation, were prospectively collected. Matched blood and tissue (HCC and surrounding nontumoral liver) samples were collected simultaneously from these 30 patients receiving curative treatments with surgical resection (n = 27) or local ablation (n = 3). Historical samples from 2 of these patients, obtained prior HCC diagnosis, were retrieved for this study. Serial blood samples were subsequently collected at multiple follow-up time points. Ten samples from healthy adults were obtained from blood donors from the Blood and Tissue Bank (Banc de sang I teixits, BST, Barcelona, Spain). Additionally, 21 blood samples from HCC patients at intermediate and advanced stages of the disease (BCLC B, n = 7; BCLC C, n = 8; and BCLC D, n = 6) were also prospectively collected.

The detailed study design is shown in Figure 1A. In total, 57 tissue (30 HCC tissues and 27 matched surrounding liver tissues) and 113 blood samples (83 plasma samples to extract cfDNA and 30 samples of peripheral blood mononuclear cells (PBMC) to extract germ line) were collected. The study was conducted in accordance with the Declaration of Helsinki. The institutional ethical review board approved the protocol (PR(AG)194/2015), and all patients gave written informed consent before inclusion.

2.2. Sample Collection

Peripheral venous blood was collected at least within the 24–48 h prior to surgery in a lithium heparin tube (BD Biosciences, Franklin Lakes, NJ, USA) and processed within 4 h of collection. Plasma was collected after a first centrifugation at $1600\times g$ for 15 min at 4 °C, and then was further centrifuged at $16,000\times g$ for 10 min at 4 °C and was immediately stored at −80 °C. Liver specimens were collected ad hoc for this study at the operation room and brought to the Pathology Department to be processed with the help of an expert pathologist for specific tissue sampling and immediately stored at −80 °C.

2.3. DNA Extraction and Quantification

Circulating DNA was isolated from 1 mL of plasma using the MagMAX™ Cell-Free DNA Isolation Kit (Thermo Fisher, Waltham, MA, USA). Blood and tissue DNA was isolated using the QIAamp DNA Mini Kit (Qiagen, Hilden, Germany) according to the manufacturer recommendations. Purified DNA concentration was measured by fluorometric quantitation using Qubit (Thermo Fisher, Waltham, MA, USA).
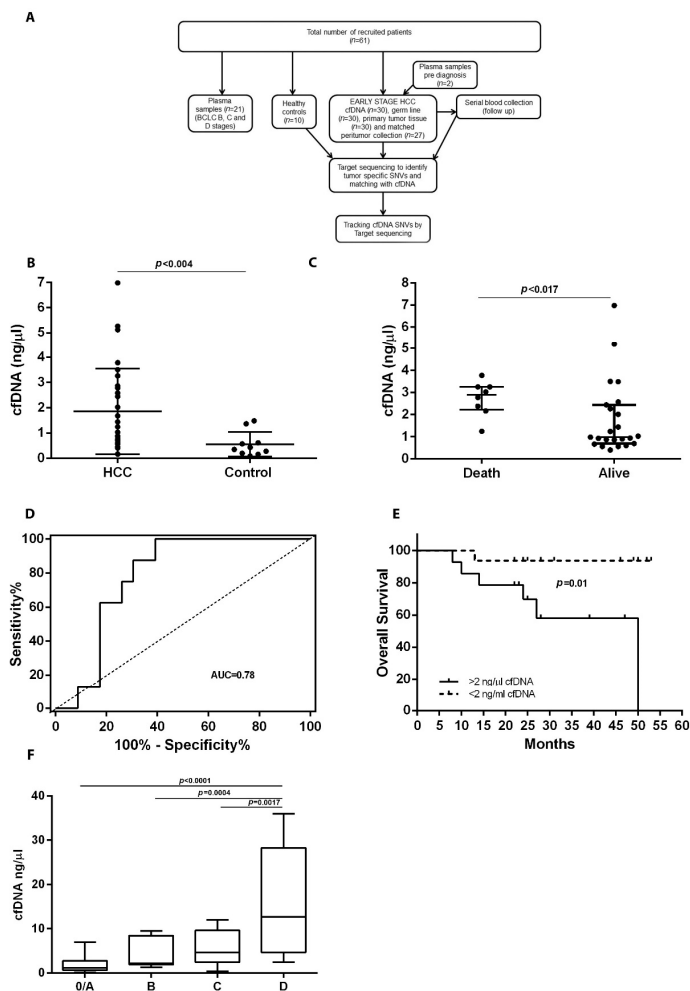
Figure 1. (**A**) Flow diagram of the study design. (**B**) cfDNA concentrations in patients with early-stage HCC and healthy controls. (**C**) cfDNA concentrations in patients with early-stage HCC who were dead or alive at the end of follow-up. (**D**) ROC curve distinguishing patients with more than 2 mutations. (**E**) Kaplan–Meier curve of overall survival for HCC patients stratified by baseline cfDNA level; *p*-value from the log-rank test. (**F**) cfDNA levels stratified by BCLC stage (0: Very early, A: Early, B: Intermediate, C: Advanced and D: End-stage), cfDNA: cell-free DNA.

2.4. Primer Design and PCR

Primers were designed to amplify different regions enriched with hotspot containing frequent mutations in TERT promoter, TP53, CTNNB1, AXIN1 and ARID1A (Supplementary Materials Table S1). PCR reactions and conditions were performed with the Start High Fidelity PCR system dNTPack (Roche Applied Science, Penzberg, Germany) following manufacturer recommendations, adding 5 µL of template DNA (Supplementary Materials Table S1). PCR products were then subjected to 15 cycles of a universal MID PCR using FastStart Taq DNA polymerase (Roche Applied Science, Penzberg, Germany) as previously published [21]. The final MID amplification yielded from 185 to 216 bp fragments (Supplementary Materials Table S1). The PCR products were analyzed by 2% agarose gel electrophoresis, purified with DNA clean-up (NZY tech, Lisbon, Portugal) and quantified by fluorometric quantitation using Qubit (Thermo Fisher, Waltham, MA, USA). Amplicon quality was analyzed using a BioAnalyzer DNA 1000 LabChip (Agilent, Santa Clara, CA, USA) prior to sequencing using Illumina MiSeq platform (Illumina, San Diego, CA, USA).

2.5. Library Preparation and Next-Generation Sequencing

For the sequencing using the MiSeq platform (Illumina, San Diego, CA, USA), amplification products were pooled and purified using Kapa pure beads (Roche Applied Science, Penzberg, Germany). Pools were quantified by Qubit (ThermoFisher, Waltham, MA, USA). The genomic libraries were processed following the manufacturer instructions for DNA library preparation kit Kapa Hyper Prep kit (Roche, Applied Science, Penzberg, Germany) and indexed using SeqCap Adapter Kit A/B (Roche, Applied Science, Penzberg, Germany). The final library was quantified by LightCycler 480 (Roche, Applied Science, Penzberg, Germany) and sequenced using MiSeq sequencing platform with MiSeq Reagent kit v2 (2 × 150 bp mode with the 300 cycle kit) (Illumina, San Diego, CA, USA).

2.6. Data Analysis

The raw fastq files acquired from MiSeq were first submitted to FLASH [22] to overlap the paired-end reads and reconstruct full amplicons. Sequencing data analysis was conducted as previously published [21]. An overlapping of paired ends (2 × 300) with a minimum of 20 overlapping bases, and a maximum of 10% differences were established. Full reads carrying 5% or more bases below a Q30 Phred score were discarded. The third step was a demultiplexing by specific amplicon primers with a maximum of three differences. Reads were then collapsed into haplotypes with corresponding frequencies. All haplotypes with abundances below 0.1%, and not common to both strands were discarded and, finally, we filtered all variants below an abundance of 1% [21,23,24].

Raw sequencing data from samples included in this article will be openly available upon publication via Sequence Read Archive of the NCBI (accession number PRJNA791805).

2.7. Statistical Analysis

Quantitative clinical variables were described using mean ± standard deviation or median (interquartile range (IQR)) as appropriate to distribution. For qualitative variables, frequency and percentage were calculated. Boxplots by main outcomes have been constructed. Associations between cfDNA levels and clinical outcomes were assessed by nonparametric Mann–Whitney U-test. An ROC analysis was performed to identify cfDNA concentration capacity to discriminate patients with more than two mutations. Kaplan–Meier survival curves were estimated for survival and recurrence by cfDNA level. Hazard ratios and their 95% confidence intervals were calculated from univariate Cox regression for clinical and mutation-related variables. Data analysis was performed in R version 4.1.0 and Stata 15.1. Statistical analysis has been carried out by Statistics and Bioinformatics Unit (UEB), Vall d'Hebron Research Institute (VHIR).

3. Results

3.1. Study Design and Patient Characteristics

We prospectively profiled blood and tissue samples from 30 patients with early HCC receiving curative therapy and 10 healthy controls. Matched blood and fresh frozen tissue samples were available for the 30 HCC patients. The median follow-up was 22.5 (1–50) months. At least one follow-up sample was analyzed for every patient (Figure 1A). The clinical and demographic parameters of these patients are summarized in Supplementary Materials Table S2. The median age of HCC patients was 61.5 years, 76.6% were male, and liver cirrhosis was present in 26.6% of patients; viral etiology was observed in 43.2% and 16.6% presented metabolic-associated fatty liver disease (MAFLD). The median diameter of the largest tumor was 3.75cm (range, 1–12 cm), while microvascular invasion (mVI) was present in 20% of the tissue samples. During study follow-up, tumor recurrence was observed in 12 patients (40%) and 7 patients died (23.3%).

3.2. Quantification of cfDNA in HCC Patients

Median level of plasma cfDNA was significantly higher in HCC patients compared to control subjects (1.73 ng/µL, IQR 0.87–3.08 and 0.38 ng/µL, IQR 0.18–0.79; $p = 0.004$) (Figure 1B). Median cfDNA levels at diagnosis were significantly higher in patients who died during follow-up ($n = 7$) than in patients remaining alive by the end of follow-up (2.90 ng/µL, IQR 2.23–3.26 and 0.98 ng/µL, IQR 0.70–2.44; $p = 0.0174$) (Figure 1C). To investigate the correlation between the concentration of preoperative cfDNA and survival, a cut-off value of 2 ng/µL of cfDNA was established by an ROC curve analysis with AUC = 0.782 (Figure 1D). Patients presenting with greater than 2 ng/µL of cfDNA had a higher mortality compared to patients with less than 2 ng/µL (mean survival time 24.6 months vs. 31.87 months, $p = 0.01$) based on Kaplan–Meier's survival analysis (Figure 1E). No correlation was observed between cfDNA concentration and tumor size, AFP levels or presence of vascular invasion.

Additionally, cfDNA was quantified in patients with intermediate and advanced HCC ($n = 7$ BCLC B, $n = 8$ BCLC C and $n = 6$ BCLC D) to compare cfDNA levels along BCLC stages. The clinical and demographic parameters of these patients are summarized in Supplementary Materials Table S3. As expected, those patients at more advanced stages (BCLC C and D) had a higher median cfDNA level (5.58 ng/µL, IQR 2.42–9.63 and 15.80 ng/µL, IQR 4.65–28.25, respectively) compared to patients at earlier stages (BCLC 0/A) (1.85 ng/µL, IQR 0.65–2) (Figure 1F).

3.3. Mutations Identified in Plasma cfDNA and Matched HCC Tissue DNA

After observing detectable plasma levels of cfDNA in patients with HCC, NGS analysis was initially performed in early HCC tumor samples, matched surrounding tissue, cfDNA and PBMCs (as a germ line) from the 30 HCC patients who underwent curative treatments (resection $n = 27$ or local ablation $n = 3$); samples were analyzed by NGS with a median read depth of 46,281×. In total, 202 nonsynonymous somatic single-nucleotide variants (SNVs) with at least 1% of frequency were identified in the four types of samples analyzed from each HCC patient ($n = 30$). Among all identified SNVs, 87% of them (174/202) were reported in COSMIC database [25], meaning that their occurrence had been previously observed, and 13% (28/223) were novel mutations (Supplementary Materials Table S4).

The majority of patients had at least one mutation in HCC tissue DNA and cfDNA (70.6%—24/30; 86.7%—26/30, respectively). An average of 1.9 (range 0–9) mutations per patient were detected in HCC tissue, 4 (0–30) in cfDNA, 1.1 (0–10) in paired-adjacent tissue and 0.4 (0–3) in PBMCs (Figure 2A).
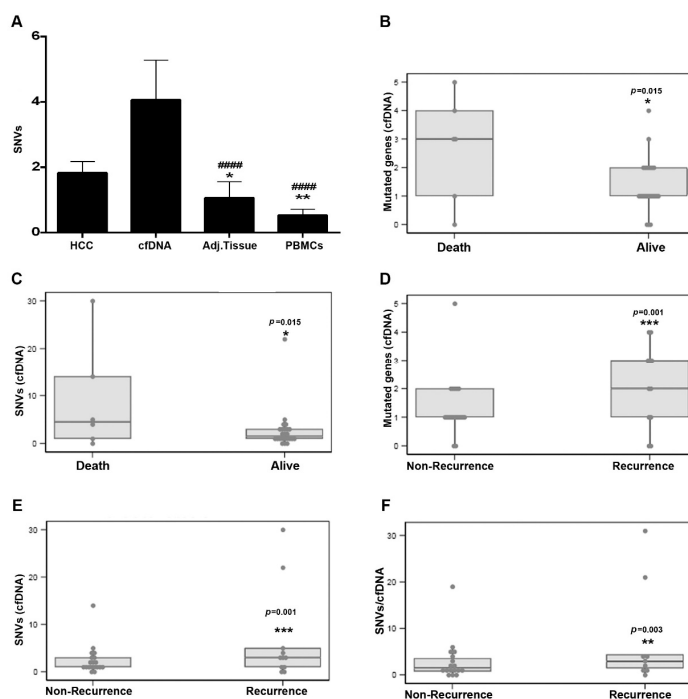
Figure 2. (**A**) Number of somatic mutations detected in HCC tissue, cfDNA, surrounding liver tissue and PBMCs of early-stage HCC patients, * $p < 0.05$, ** $p < 0.01$, *** $p<0.001$ vs. HCC tissue. #### $p < 0.0001$ vs. cfDNA. (**B**) Number of mutated genes detected in the cfDNA and (**C**) number of SNVs detected in the cfDNA of patients with early-stage HCC according to survival status (i.e., death vs. alive). Number of mutated genes (**D**), SNVs detected in the cfDNA (**E**) and ratio SNVs/cfDNA. (**F**) in early-stage HCC patients according to presence/absence of recurrence. cfDNA: cell-free DNA, SNV: single-nucleotide variant, PBMCs: peripheral blood mononuclear cell.

Concordance between genetic variants, both in HCC tissue DNA and cfDNA samples, was analyzed. A total of 55 mutations were found in HCC tissue DNA. Among them, 29 (52.7%) also had evidence of identical carcinogenic mutations in matched cfDNA. Importantly, additional mutations not present in HCC tissue DNA were found in cfDNA. From a total of 104 mutations detected in cfDNA, 75 were additional mutations over those described in HCC tissue DNA. Therefore, mutations identified in cfDNA could provide additional molecular information about the tumor.

We further evaluated whether the number of mutated genes or the number of mutations in cfDNA of patients with early HCC could be useful in predicting prognosis. Subjects who died during follow-up had a significantly higher median number of mutated genes on their cfDNA at baseline than those subjects who remained alive by the end of follow-up (3, 1–4 vs. 1, 1–2; $p = 0.015$) (Figure 2B and Table 1). Patients who died were also more likely to have detectable mutations in their cfDNA (4.5, 1–14 vs. 1.5, 1–3; $p = 0.015$) (Figure 2C and Table 1). The number of mutated genes (Figure 2D) ($p = 0.001$) and

Annex

detected mutations (Figure 2E) (*p* = 0.001) in cfDNA were also significantly associated with recurrence, as well as the ratio between number of mutations and total amount of cfDNA (number mutations/cfDNA), which was also significantly associated with recurrence of patients with early HCC (1.5, 0.8–3.6 vs. 2.9, 1.4–4.4; *p* = 0.003) (Figure 2F and Table 1).

Table 1. Univariate Cox analysis for mutation-related variables.

			Death			**Recurrence**	
Variable		HR	(95% CI)	*p*-Value	HR	(95% CI)	*p*-Value
Presence of mutations in HCC Tissue	No	1		0.939	1		0.802
	Yes	0.92	(0.11; 7.91)		0.82	(0.18; 3.82)	
Number of mutations in HCC Tissue		0.99	(0.82; 1.19)	0.886	1.03	(0.93; 1.14)	0.592
Number of mutated genes in HCC tissue		0.76	(0.36; 1.59)	0.465	1.11	(0.71; 1.73)	0.643
Presence of mutations in cfDNA	No	1		0.589	1		0.484
	Yes	0.55	(0.06; 4.91)		0.57	(0.12; 2.72)	
Number of mutations in cfDNA		**1.11**	**(1.02; 1.20)**	**0.015 ***	**1.16**	**(1.06; 1.27)**	**0.001 ***
Number of mutated genes in cfDNA		**2.37**	**(1.18; 4.74)**	**0.015 ***	**2.88**	**(1.52; 5.47)**	**0.001 ***
Number of Mutations/cfDNA[(1)]		1.07	(0.99; 1.16)	0.089	**1.2**	**(1.06; 1.35)**	**0.003 ***
Presence of mutations in Adj Tissue	No	1		0.158	1		0.9280
	Yes	0.21	(0.02; 1.85)		0.95	(0.30; 3.04)	
Number of mutations in Adj Tissue		0.97	(0.80; 1.17)	0.754	1.06	(0.98; 1.15)	0.1359
Number of mutated genes in HCC tissue		0.25	(0.03; 2.02)	0.193	1.17	(0.79; 1.72)	0.4285

Number of obs = 26; HCC: hepatocellular carcinoma, cfDNA: cell-free DNA. Data in bold mean the significant values. *: Statistically significant.

The multivariate analysis showed that detection of more than four mutations in cfDNA correlated with a higher risk of death (long-rank *p* = 0.042) (Figure 3A and Table 2). Those patients with a ratio (number of mutations/cfDNA) higher than six presented a higher risk of recurrence than those with a ratio under six mutations/cfDNA (long-rank *p* = 0.0003) (Figure 3B and Table 2). Patients who presented mutations in more than two genes showed a higher risk of death and recurrence (long-rank *p* = 0.028 and *p* = 0.009, respectively) (Figure 3C,D and Table 2).

Next, we sought to assess the relation between mutational status of cfDNA with well-known poor prognosis factors in clinical practice, observing that those patients with more than one HCC nodule had a higher ratio (number of mutations/cfDNA) (6, 1–31.3 vs. 1.7, 0.8–4.0; *p* = 0.04) (Figure 3E). Moreover, both the number of mutations detected in the cfDNA and the ratio (number of mutations/cfDNA) were observed to be significantly associated with the presence of microvascular invasion (*p* = 0.03 and *p* = 0.04, respectively) (Figure 3F,G). Among clinical and analytical parameters included in Supplementary Materials Table S5, only size of the main nodule was found to be an independent risk factor of tumor recurrence.

3.4. Variant Characteristics in Plasma and HCC Tissue

Further analysis of mutations showed that the most commonly mutated gene in the total HCC patient cohort was TERT. At least one mutation of TERT promoter was found in the 76.7% (23/30 patients) in both cfDNA and HCC tissue. The most common mutation detected in TERT promoter (C228T) was also validated by ddPCR, obtaining a detectable and similar mutation rate in all samples where C228T mutation was detected by sequencing (Supplementary Materials Table S6). At least one mutation in TP53 gene was detected in 50% (15/30) of cfDNA samples versus 33.3% (10/30) of HCC tissue, and CTNNB1 was mutated in 10% of cfDNA (3/30) and 33.3% (10/30) of HCC tissue of patients. Finally, 16.7% (5/30) and 10% (3/10) of patients presented mutations in AXIN1 on their cfDNA or HCC tissue, respectively, and mutations in ARID1A were found in 10% (3/30) and 6.7% (2/30) of patients in cfDNA and HCC tissue (Figure 4A).
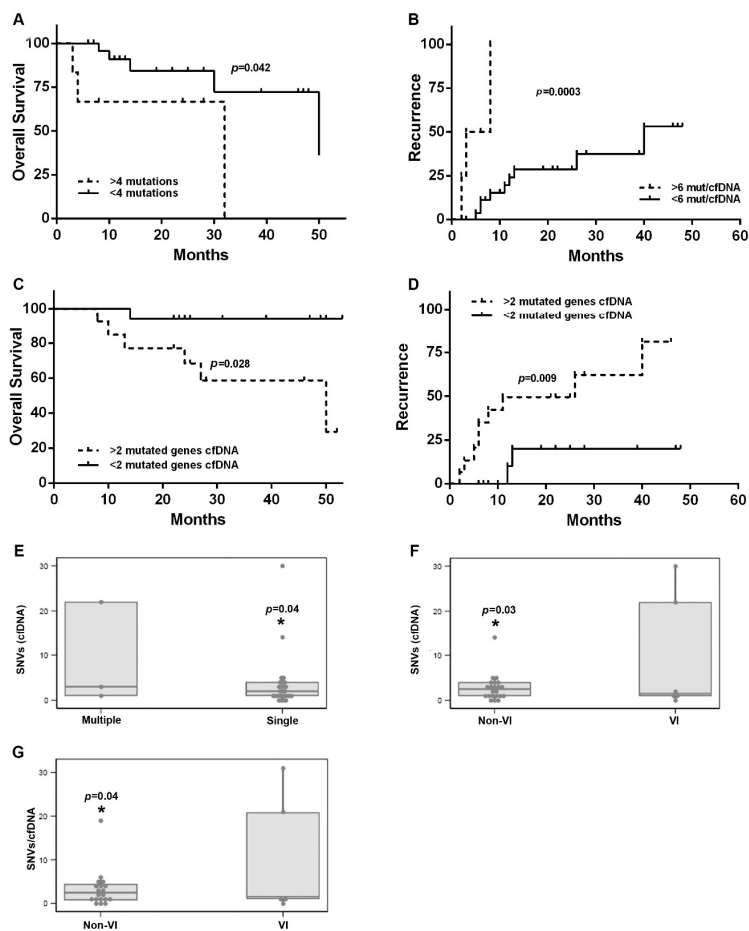
Figure 3. (**A**) Kaplan–Meier curve of overall survival for HCC patients stratified by number of mutations in the cfDNA. *p*-value from the log-rank test. (**B**) Kaplan–Meier curve of recurrence for HCC patients stratified by the ratio of number of mutations/cfDNA. *p*-value from the log-rank test. (**C**) Kaplan–Meier curve of overall survival for HCC patients stratified by number of mutated genes in cfDNA. *p*-value from the log-rank test. (**D**) Kaplan–Meier curve of recurrence for HCC patients stratified by number of mutated genes in cfDNA. *p*-value from the log-rank test. (**E**–**G**) Correlation between SNVs with poor prognosis status: number of SNVs detected in the cfDNA of early HCC patients with single or multiple foci of HCC (**E**), number of SNVs detected in the cfDNA of HCC patients with or without vascular invasion (**F**) and ratio of SNVs/cfDNA (**G**) detected in early HCC patients with or without vascular invasion. SNV: single-nucleotide variant, cfDNA: cell-free DNA, VI: vascular invasion. * *p* < 0.05.

Table 2. Multivariate Cox regression analysis for mutation-related variables.

		Death			Recurrence		
Cut-Off Values		**HR**	**(95% CI)**	***p*-Value**	**HR**	**(95% CI)**	***p*-Value**
Number of mutations in HCC Tissue	No (<6)	1		0.4796	1		0.346
	Yes (>6)	2.23	(0.24; 20.4)		2.09	(0.45; 9.74)	
Number of mutations in cfDNA	No (<4)	**1**		**0.0078 ***	1		0.06
	Yes (>4)	**11.66**	**(1.91; 71.2)**		3.54	(0.94;13.35)	
Number of mutated genes in cfDNA	No (<2)	**1**		**0.0287 ***	**1**		**0.009 ***
	Yes (>2)	**5.31**	**(1.19; 23.77)**		**9.61**	**(1.75; 52.7)**	
N Mutations/cfDNA	No (<6)	1		0.051	**1**		**0.007 ***
	Yes (>6)	7.07	(0.99; 50.5)		**7.44**	**(1.71; 32.3)**	

HCC: hepatocellular carcinoma, cfDNA: cell-free DNA. Data in bold mean the significant values. *: Statistically significant.
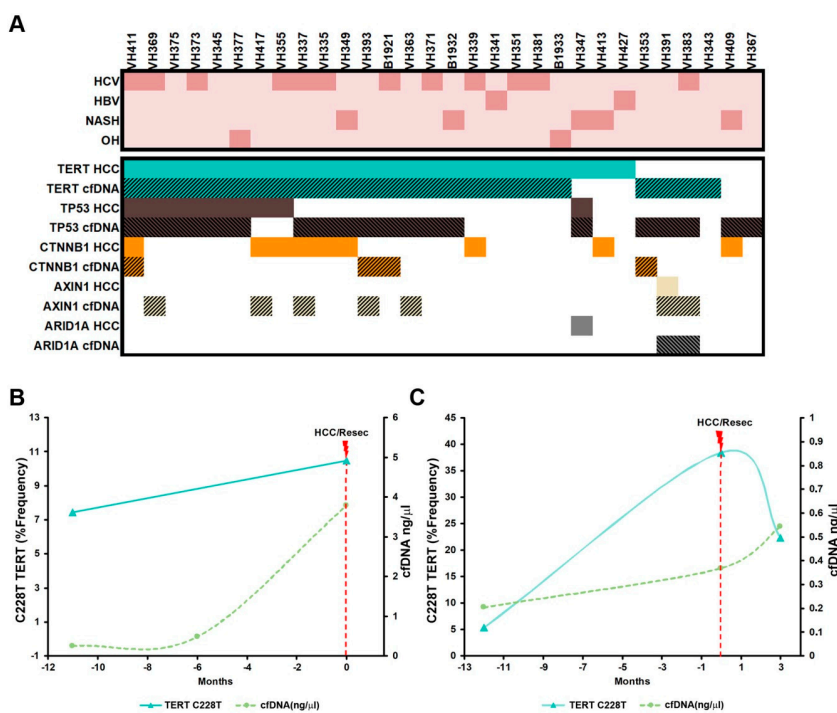
Figure 4. (**A**) Mutational landscape of patients with early-stage HCC using mutations found in cfDNA and HCC tissue in 30 patients. The heatmap illustrates the nonsynonymous mutations detected in plasma cfDNA and HCC tissue and the etiology information of the 30 HCC patients at the time of the curative intervention. (**B**,**C**) Early detection of C228T TERT mutation (−124) before HCC diagnosis in two patients. The activating TERT promoter mutation C228T was detected in the cfDNA 11 and 12 months before diagnosis in VH341 and VH381 patients, respectively. HCV: hepatitis C virus, HCB: hepatitis B virus, NASH: nonalcoholic steatohepatitis OH: alcohol, cfDNA: cell-free DNA.

3.5. Early Detection of Mutations in Driver Genes Prior to HCC Diagnosis

Very few studies have focused on the evaluation of cfDNA detection in early-stage cancers (BCLC 0/A) with even less data available on the detection of ctDNA in pre-HCC-diagnosis stored blood samples from HCC patients. We had the opportunity to analyze cfDNA from previously stored samples from two HCC patients. Samples were collected months before radiological diagnosis of HCC. Samples were analyzed in order to identify potential driver mutations detectable before the radiological diagnosis of HCC. One TERT mutation was found in the cfDNA of patients VH341 (HBV-related HCC) and VH381 (HCV-related HCC) 11 and 12 months before HCC diagnosis, respectively (Figure 4B,C).

Two mutations were detected in the cfDNA from plasma obtained 11 months before the radiological diagnosis of HCC in patient VH341. The activating TERT promoter mutation C228T was detected at a frequency of 8% 12 months before diagnosis and 10% at the time of diagnosis (Figure 4B). Tumor tissue frequency of C228T mutation was 1.95%. R249S mutation in TP53 was also detected at a frequency of 1.65% and 1.4% in cfDNA 11 months before diagnosis and at the time of diagnosis, respectively. The R249S variant was detected at a frequency of 0.4% in tumor tissue.

The activating TERT promoter mutation C228T was also detected 12 months before diagnosis in patient VH381 at a frequency of 5.34%, being 38.4% by the time of HCC diagnosis. Tumor tissue frequency of C228T mutation was 37.72% (Figure 4C).

3.6. Dynamics of cfDNA and Mutations during HCC Progression

Next, to further explore whether cfDNA and SNVs dynamically change along with clinical evolution of patients, we analyzed sequential plasma samples collected from our cohort during their clinical course.

As shown in Figure 5A, as an example, patient VH335 showed dynamical changes in SNV number and cfDNA levels correlating with HCC progression. Before receiving surgical treatment, low levels of cfDNA (1.03 ng/μL) were quantified and only the C228T in TERT promoter was detected in both cfDNA and HCC tissue (Figure 5B). After 31 months of follow-up with no visible tumor lesions by MRI, cfDNA levels increased to 1.99 ng/μL, and a total of 37 mutations were detected in the cfDNA distributed along the five genes tested: TERT (16), TP53 (9), AXIN1 (6), ARID1A (4) and CTNNB1 (2) (Figure 5B). Radiological progression was diagnosed 37 months after diagnosis and the patient was then treated with radiofrequency ablation. Both cfDNA levels (from 1.81 to 1.27 ng/μL) and observed tumor SNVs decreased after that therapeutic intervention, when four SNVs were detected in TERT promoter. Finally, after 45 months of follow-up, the patient progressed to an advanced HCC, increasing cfDNA levels to 4.25 ng/μL (Figure 5).

Dynamic changes in cfDNA and SNV frequency of another three HCC patients have been included as supplementary data (Figures S1 and S2). Patient VH343 presented fluctuation in cfDNA levels and TERT mutation C228T (−124) correlating with HCC progression and tyrosine kinase treatment (Figure S1a). Moreover, patient VH369 showed dynamical changes in cfDNA levels, which were increased before second HCC relapse (16 months) (Figure S1b). Patient VH371 presented an increase in cfDNA levels and in the number and frequency of mutations months before radiological detection of relapse, 11 months after surgery (Figure S2).
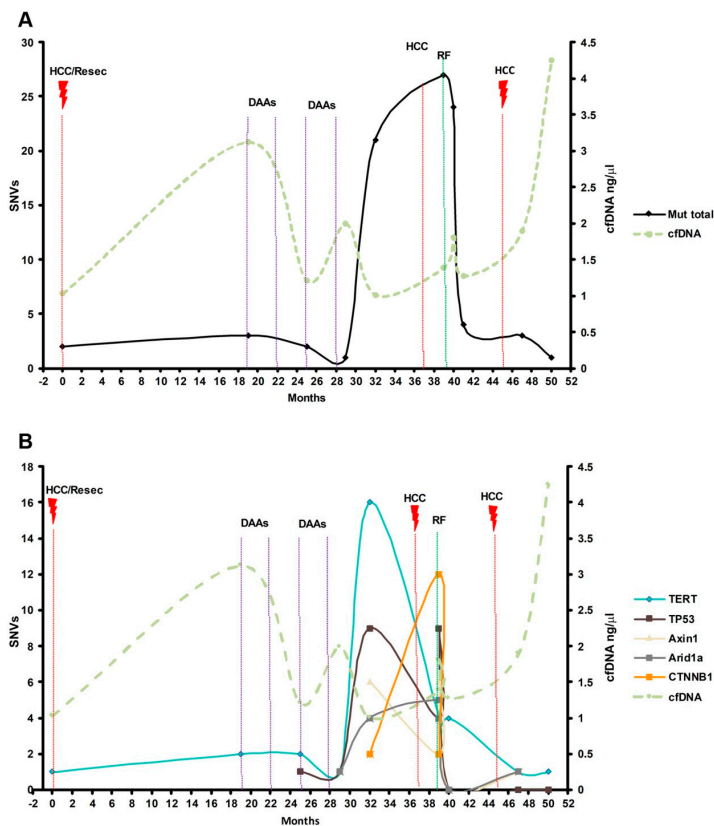
Figure 5. (**A**) Dynamical changes in cfDNA levels and absolute mutational load correlating with HCC progression (Patient VH335). (**B**) Dynamical fluctuations in cfDNA levels and number of mutations in the five driver genes tested along the 52 months of follow-up. HCC/Resec: detection and surgical resection of HCC, DAAs: HCV treatment with direct-acting antivirals, RF: radiofrequency ablation, cfDNA: cell-free DNA, SNVs: single-nucleotide variant.

4. Discussion

Real-time monitoring of cfDNA levels and mutational burden for patients with HCC has been proposed as a potential tool to improve early diagnosis of HCC and early detection of recurrence after treatment. Recently, the use of cfDNA levels and its molecular analysis has been reported to provide useful information about tumor burden and prognosis by genetic and epigenetic analysis [16,18,26,27].

In this exploratory and prospective study, we investigated the usefulness of cfDNA collected at the time of diagnosis and before curative intervention (resection or local ablation) for quantification and molecular profiling in early-stage HCC patients. Patients at early stages, mostly candidates to surgical resection were selected, aiming first to evaluate the concordance

between cfDNA and tumor tissue mutations and, second, to assess dynamic changes in cfDNA after potentially curative treatment to determine its potential value as a biomarker. The selection of patients at early stages defines a very homogeneous population to study cfDNA value, but, at the same time, it is less likely to capture events such as HCC recurrence or death during follow-up to estimate the prognostic value of cfDNA in a short unicentric cohort. We considered this design optimal to explore potential biomarkers to be thereafter validated in a larger cohort. Even with this small sample size, the data are very promising.

Early-stage HCC levels of cfDNA were significantly higher than cfDNA levels in healthy controls, and, as described in prior reports, the highest cfDNA levels were detected in patients with more advanced disease, as a likely consequence of greater tumor cell burden and cfDNA release [19,28]. More interestingly, we found a baseline cut-off value of 2 ng/μL (AUC = 0.782) able to discriminate patients with high and low mortality during follow-up, suggesting that just the quantitative amount of detectable cfDNA could have a prognostic value.

We specifically targeted the most significantly mutated genes and regions in HCC (TERT promoter, TP53, CTNNB1, AXIN1 and ARID1A), evidencing that high-depth sequencing analysis of plasma-derived cfDNA could be used to detect tumor-related gene mutations in plasma cfDNA. Analyzing paired samples of plasma cfDNA and HCC tissue DNA in this cohort, a consistency of types of genes mutated detected in both types of samples of 52.7% was demonstrated, similar to the concordance reported in other studies [7,17]. Our results suggest that most prevalent mutations in HCC identified in the cfDNA are representative of those present in the HCC tumor tissue.

We observed that a high number of variants in plasma could not be confirmed in tumor samples (104 mutations found in cfDNA vs. 55 mutations found in HCC tissues), suggesting that cfDNA could be more informative at a molecular level than small biopsy/surgical under-representative samples. As previously reported, RNAseq studies from different distant regions within the same tumor have evidenced differences in transcription factor signaling [3]. This could explain the fact that finding more mutations in cfDNA than in tumor tissue samples defines the complex molecular heterogeneity in HCC [29]. Subclones could be localized in a different topographic location in the primary tissue [30–32], and coexistence of different subclones with distinctive mutational profiles and different spatial location could have considerable practical implications when extracting molecular information from biopsies or partial surgical samples.

The most frequently mutated gene in plasma was TERT promoter, with a frequency of 76.7% (23/30 patients), followed by TP53 mutated in 50% (15/30) of cfDNA samples, consistent with it being described in the previous literature about the mutational profile of early-stage HCC [7,33,34].

Despite the small number of patients included in our study, we have found that the mutational load, defined as the total number of variants detected in cfDNA and the number of mutated genes were associated with overall survival and recurrence in a univariate analysis. In our cohort, interestingly, patients presenting four or more mutations in cfDNA at baseline had shorter survival. Accordingly, a higher number of mutations detected in cfDNA were also associated with well-described poor prognostic factors in the HCC setting, such as the presence of multiple foci of HCC or the presence of microvascular invasion at pathology exam. Interestingly, while those variables, cfDNA number of mutations and genes mutated, showed association with patient outcomes, prognostic clinic-pathological parameters commonly used in clinical practice, such as number of nodules, presence of microvascular invasion or alpha-fetoprotein levels, showed no association with recurrence or overall survival in our cohort. This is probably a consequence of the small number of patients evaluated, all of them at early stages of the disease, being less likely to develop events. These findings provide the proof of principle to test this approach in a larger multicentric cohort of plasma samples of patients at early stages to validate the potential value of our findings.

cfDNA alterations evidenced from our early HCC samples could also be tested in at-risk patients with liver cirrhosis under ultrasound screening programs, given the easy access to blood samples, without needing invasive procedures. In this study, we are reporting two cases in which analysis of cfDNA was performed in patients with liver disease and with no sign of malignancy during the prior HCC screening by abdominal ultrasound, detecting mutations almost 1 year before imaging detection. Recently, detection at low frequency of HCC driver mutations (TP53, CTNNB1 and TERT promoter) has been reported in cfDNA of cirrhotic patients [35]. With our approach, we found that C228T TERT promoter mutation was detected at a frequency of 8% and 5.34% 12 and 10 months before diagnosis in patients VH341 and VH381, respectively. Nevertheless, this is exploratory and preliminary evidence, and further support to confirm the potential role of cfDNA in improving early diagnosis of HCC in at-risk patients is required. A multicentric study analyzing the levels of driver mutations as TERT [36–38] in the cfDNA of cirrhotic patients would be an appealing future approach to further develop the potential usefulness of cfDNA as a diagnostic biomarker.

Even after curative treatment, relapse remains a significant threat for many cancer patients, and it is difficult to detect minimal residual disease by imaging or tissue biopsy. Previous studies showed that ctDNA could be used for monitoring disease load, providing clinically relevant lead times compared to imaging techniques in colorectal cancer [39]. It has also been observed that cfDNA-positive patients are more likely to experience a relapse than the cfDNA-negative ones, showing a shorter disease-free survival [34,40]. Furthermore, it has been reported that cfDNA can be used to monitor dynamic changes in tumor burden, analyzing both genetic and epigenetic status, using minimally invasive blood sampling [41,42]. In addition, genetic analysis of cfDNA during clinical follow-up of patients could be useful in identifying the appearance of resistant subclones [43,44]. Another study investigated cfDNA and protein biomarkers in a long-term follow-up of patients with HCC, concluding that both SNVs and copy number variations (CNVs) possessed the capability to dynamically reflect HCC tumor burden [9]. In this study, we have observed that the somatic mutations on known HCC-related driver genes, such as as TERT, TP53 and CTNNB1 in cfDNA, were consistently and dynamically correlated with tumor burden during patient follow-up.

Genetic information from cfDNA could provide a tumor-specific molecular profile of tumors. This information could guide targeted therapy, improving the choice of the appropriate treatment for each patient. The half-life of cfDNA in the circulation is between 16 min and 2.5 h [45]; for this reason, cfDNA can be considered a real-time snapshot reflecting the molecular evolution of tumors [43]. Noninvasive access to molecular information allows real-time monitoring of treatment effectiveness in some type of tumors. Unfortunately, the most prevalent mutations in HCC, explored in the present study, are not therapeutic targets. Our approach, selecting the regions enriched with hotspot containing frequent mutations in TERT promoter, TP53, CTNNB1, AXIN1 and ARID1A, avoids the cost of performing more expensive techniques, such as whole exome or genome sequencing, which is unaffordable for the economic health system.

Analysis of cfDNA requires the evaluation of nontumor variant background noise. To achieve this aim, we included a control group of healthy patients, as well as PBMCs from each patient. Nonetheless, there are still many unknown aspects about the origin of variants in plasma and its biological meaning.

The main limitation of our study is its small sample size, primarily due to the unicentric nature of the study. This also led to the possibility that specific mutations as potential biomarkers for prognosis could not be identified. However, the potential prognostic value of cfDNA levels and number of mutations in plasma observed in our series deserves further investigation and validation in larger cohorts of patients. It is plausible to predict that cfDNA might play a major role in the near future in early diagnosis, prognostic estimation and management of HCC.

5. Conclusions

In conclusion, total cfDNA levels and detection of the most prevalent HCC mutations have prognostic implications that could refine the standard surveillance after curative treatment of early-stage HCC patients.

Abbreviations

cfDNA: cell-free DNA; HCC: hepatocellular carcinoma; MAFLD: metabolic-associated fatty liver disease. AFP: alpha-fetoprotein, PBMC: peripheral blood mononuclear cells, SNV: single-nucleotide variants, CNV: copy number variations.

References

1. IARC. Fact Sheets by Population-Globocan-IARC. Available online: http://globocan.iarc.fr/pages/fact_sheets_population.aspx (accessed on 27 April 2022).
2. Galle, P.R.; Forner, A.; Llovet, J.M.; Mazzaferro, V.; Piscaglia, F.; Raoul, J.L.; Schirmacher, P.; Vilgrain, V. EASL Clinical Practice Guidelines: Management of hepatocellular carcinoma. *J. Hepatol.* **2018**, *69*, 182–236. [CrossRef] [PubMed]
3. Losic, B.; Craig, A.J.; Villacorta-Martin, C.; Martins-Filho, S.N.; Akers, N.; Chen, X.; Ahsen, M.E.; von Felden, J.; Labgaa, I.; D'Avola, D.; et al. Intratumoral heterogeneity and clonal evolution in liver cancer. *Nat. Commun.* **2020**, *11*, 291. [CrossRef] [PubMed]

4. Bruix, J.; Reig, M.; Sherman, M. Evidence-Based Diagnosis, Staging, and Treatment of Patients With Hepatocellular Carcinoma. *Gastroenterology* **2016**, *150*, 835–853. [CrossRef] [PubMed]

5. Crowley, E.; Di Nicolantonio, F.; Loupakis, F.; Bardelli, A. Liquid biopsy: Monitoring cancer-genetics in the blood. *Nat. Rev. Clin. Oncol.* **2013**, *10*, 472–484. [CrossRef] [PubMed]

6. Kaseb, A.O.; Sánchez, N.S.; Sen, S.; Kelley, R.K.; Tan, B.; Bocobo, A.G.; Lim, K.H.; Abdel-Wahab, R.; Uemura, M.; Pestana, R.C.; et al. Molecular Profiling of Hepatocellular Carcinoma Using Circulating Cell-Free DNA. *Clin. Cancer Res. Off. J. Am. Assoc. Cancer Res.* **2019**, *25*, 6107–6118. [CrossRef] [PubMed]

7. Labgaa, I.; Villacorta-Martin, C.; D'avola, D.; Craig, A.J.; Von Felden, J.; Martins-Filho, S.N.; Sia, D.; Stueck, A.; Ward, S.C.; Fiel, M.I.; et al. A pilot study of ultra-deep targeted sequencing of plasma DNA identifies driver mutations in hepatocellular carcinoma. *Oncogene* **2018**, *37*, 3740–3752. [CrossRef]

8. Phallen, J.; Sausen, M.; Adleff, V.; Leal, A.; Hruban, C.; White, J.; Anagnostou, V.; Fiksel, J.; Cristiano, S.; Papp, E.; et al. Direct detection of early-stage cancers using circulating tumor DNA. *Sci. Transl. Med.* **2017**, *9*, 403. [CrossRef]

9. Cai, Z.; Chen, G.; Zeng, Y.; Dong, X.; Li, Z.; Huang, Y.; Xin, F.; Qiu, L.; Xu, H.; Zhang, W.; et al. Comprehensive Liquid Profiling of Circulating Tumor DNA and Protein Biomarkers in Long-Term Follow-Up Patients with Hepatocellular Carcinoma. *Clin. Cancer Res. Off. J. Am. Assoc. Cancer Res.* **2019**, *25*, 5284–5294. [CrossRef] [PubMed]

10. Amirouchene-Angelozzi, N.; Swanton, C.; Bardelli, A. Tumor evolution as a therapeutic target. *Cancer Discov.* **2017**, *7*, 805–817. [CrossRef] [PubMed]

11. Huang, Z.; Hua, D.; Hu, Y.; Cheng, Z.; Zhou, X.; Xie, Q.; Wang, Q.; Wang, F.; Du, X.; Zeng, Y. Quantitation of plasma circulating DNA using quantitative PCR for the detection of hepatocellular carcinoma. *Pathol. Oncol. Res.* **2012**, *18*, 271–276. [CrossRef]

12. Ren, N.; Qin, L.X.; Tu, H.; Liu, Y.K.; Zhang, B.H.; Tang, Z.Y. The prognostic value of circulating plasma DNA level and its allelic imbalance on chromosome 8p in patients with hepatocellular carcinoma. *J. Cancer Res. Clin. Oncol.* **2006**, *132*, 399–407. [CrossRef] [PubMed]

13. Tokuhisa, Y.; Iizuka, N.; Sakaida, I.; Moribe, T.; Fujita, N.; Miura, T.; Tamatsukuri, S.; Ishitsuka, H.; Uchida, K.; Terai, S.; et al. Circulating cell-free DNA as a predictive marker for distant metastasis of hepatitis C virus-related hepatocellular carcinoma. *Br. J. Cancer* **2007**, *97*, 1399–1403. [CrossRef] [PubMed]

14. Parikh, A.R.; Leshchiner, I.; Elagina, L.; Goyal, L.; Levovitz, C.; Siravegna, G.; Livitz, D.; Rhrissorrakrai, K.; Martin, E.E.; Van Seventer, E.E.; et al. Liquid versus tissue biopsy for detecting acquired resistance and tumor heterogeneity in gastrointestinal cancers. *Nat. Med.* **2019**, *25*, 1415–1421. [CrossRef] [PubMed]

15. Leal, A.; van Grieken, N.C.T.; Palsgrove, D.N.; Phallen, J.; Medina, J.E.; Hruban, C.; Broeckaert, M.A.M.; Anagnostou, V.; Adleff, V.; Bruhm, D.C.; et al. White blood cell and cell-free DNA analyses for detection of residual disease in gastric cancer. *Nat. Commun.* **2020**, *11*, 525. [CrossRef]

16. Liao, W.; Yang, H.; Xu, H.; Wang, Y.; Ge, P.; Ren, J.; Xu, W.; Lu, X.; Sang, X.; Zhong, S.; et al. Noninvasive detection of tumor-associated mutations from circulating cell-free DNA in hepatocellular carcinoma patients by targeted deep sequencing. *Oncotarget* **2016**, *7*, 40481–40490. [CrossRef] [PubMed]

17. Huang, A.; Zhao, X.; Yang, X.-R.; Li, F.-Q.; Zhou, X.-L.; Wu, K.; Zhang, X.; Sun, Q.-M.; Cao, Y.; Zhu, H.-M.; et al. Circumventing intratumoral heterogeneity to identify potential therapeutic targets in hepatocellular carcinoma. *J. Hepatol.* **2017**, *67*, 293–301. [CrossRef] [PubMed]

18. Cai, Z.X.; Chen, G.; Zeng, Y.Y.; Dong, X.Q.; Lin, M.J.; Huang, X.H.; Zhang, D.; Liu, X.L.; Liu, J.F. Circulating tumor DNA profiling reveals clonal evolution and real-time disease progression in advanced hepatocellular carcinoma. *Int. J. Cancer* **2017**, *141*, 977–985. [CrossRef] [PubMed]

19. Howell, J.; Atkinson, S.R.; Pinato, D.J.; Knapp, S.; Ward, C.; Minisini, R.; Burlone, M.E.; Leutner, M.; Pirisi, M.; Büttner, R.; et al. Identification of mutations in circulating cell-free tumour DNA as a biomarker in hepatocellular carcinoma. *Eur. J. Cancer* **2019**, *116*, 56–66. [CrossRef] [PubMed]

20. Ng, C.K.Y.; Di Costanzo, G.G.; Tosti, N.; Paradiso, V.; Coto-Llerena, M.; Roscigno, G.; Perrina, V.; Quintavalle, C.; Boldanova, T.; Wieland, S.; et al. Genetic profiling using plasma-derived cell-free DNA in therapy-naive hepatocellular carcinoma patients: A pilot study. *Ann. Oncol.* **2018**, *29*, 1286–1291. [CrossRef] [PubMed]

21. Soria, M.E.; Gregori, J.; Chen, Q.; García-Cehic, D.; Llorens, M.; de Ávila, A.I.; Beach, N.M.; Domingo, E.; Rodríguez-Frías, F.; Buti, M.; et al. Pipeline for specific subtype amplification and drug resistance detection in hepatitis C virus. *BMC Infect. Dis.* **2018**, *18*, 446. [CrossRef]

22. Magoč, T.; Salzberg, S.L. FLASH: Fast length adjustment of short reads to improve genome assemblies. *Bioinformatics* **2011**, *27*, 2957–2963. [CrossRef] [PubMed]

23. Gregori, J.; Esteban, J.I.; Cubero, M.; Garcia-Cehic, D.; Perales, C.; Casillas, R.; Alvarez-Tejado, M.; Rodríguez-Frías, F.; Guardia, J.; Domingo, E.; et al. Ultra-deep pyrosequencing (UDPS) data treatment to study amplicon HCV minor variants. *PLoS ONE* **2013**, *8*, e83361. [CrossRef]

24. Ramírez, C.; Gregori, J.; Buti, M.; Tabernero, D.; Camós, S.; Casillas, R.; Quer, J.; Esteban, R.; Homs, M.; Rodriguez-Frías, F. A comparative study of ultra-deep pyrosequencing and cloning to quantitatively analyze the viral quasispecies using hepatitis B virus infection as a model. *Antivir. Res.* **2013**, *98*, 273–283. [CrossRef] [PubMed]

25. COSMIC Database. Available online: https://cancer.sanger.ac.uk/cosmic (accessed on 27 April 2022).

26. Ikeda, S.; Tsigelny, I.F.; Skjevik, Å.A.; Kono, Y.; Mendler, M.; Kuo, A.; Sicklick, J.K.; Heestand, G.; Banks, K.C.; Talasaz, A.; et al. Next-Generation Sequencing of Circulating Tumor DNA Reveals Frequent Alterations in Advanced Hepatocellular Carcinoma. *Oncologist* **2018**, *23*, 586–593. [CrossRef] [PubMed]

27. Lu, C.-Y.; Chen, S.-Y.; Peng, H.-L.; Kan, P.-Y.; Chang, W.-C.; Yen, C.-J. Cell-free methylation markers with diagnostic and prognostic potential in hepatocellular carcinoma. *Oncotarget* **2017**, *8*, 6406–6418. [CrossRef] [PubMed]

28. Schulze, K.; Imbeaud, S.; Letouzé, E.; Alexandrov, L.B.; Calderaro, J.; Rebouissou, S.; Couchy, G.; Meiller, C.; Shinde, J.; Soysouvanh, F.; et al. Exome sequencing of hepatocellular carcinomas identifies new mutational signatures and potential therapeutic targets. *Nat. Genet.* **2015**, *47*, 505–511. [CrossRef] [PubMed]

29. Temraz, S.; Nasr, R.; Mukherji, D.; Kreidieh, F.; Shamseddine, A. Liquid biopsy derived circulating tumor cells and circulating tumor DNA as novel biomarkers in hepatocellular carcinoma. *Expert Rev. Mol. Diagn.* **2022**, *22*, 507–518. [CrossRef] [PubMed]

30. Maley, C.C.; Galipeau, P.C.; Finley, J.C.; Wongsurawat, V.J.; Li, X.; Sanchez, C.A.; Paulson, T.G.; Blount, P.L.; Risques, R.A.; Rabinovitch, P.S.; et al. Genetic clonal diversity predicts progression to esophageal adenocarcinoma. *Nat. Genet.* **2006**, *38*, 468–473. [CrossRef]

31. Clark, J.; Attard, G.; Jhavar, S.; Flohr, P.; Reid, A.; De-Bono, J.; Eeles, R.; Scardino, P.; Cuzick, J.; Fisher, G.; et al. Complex patterns of ETS gene alteration arise during cancer development in the human prostate. *Oncogene* **2008**, *27*, 1993–2003. [CrossRef] [PubMed]

32. Navin, N.; Krasnitz, A.; Rodgers, L.; Cook, K.; Meth, J.; Kendall, J.; Riggs, M.; Eberling, Y.; Troge, J.; Grubor, V.; et al. Inferring tumor progression from genomic heterogeneity. *Genome Res.* **2010**, *20*, 68–80. [CrossRef]

33. Ikeda, S.; Lim, J.S.; Kurzrock, R. Analysis of Tissue and Circulating Tumor DNA by Next-Generation Sequencing of Hepatocellular Carcinoma: Implications for Targeted Therapeutics. *Mol. Cancer Ther.* **2018**, *17*, 1114–1122. [CrossRef] [PubMed]

34. Zhu, G.Q.; Liu, W.R.; Tang, Z.; Qu, W.F.; Fang, Y.; Jiang, X.F.; Song, S.S.; Wang, H.; Tao, C.Y.; Zhou, P.Y.; et al. Serial circulating tumor DNA to predict early recurrence in patients with hepatocellular carcinoma: A prospective study. *Mol. Oncol.* **2022**, *16*, 549–561. [CrossRef] [PubMed]

35. Alunni-Fabbroni, M.; Weber, S.; Öcal, O.; Seidensticker, M.; Mayerle, J.; Malfertheiner, P.; Ricke, J. Circulating Cell-Free DNA Combined to Magnetic Resonance Imaging for Early Detection of HCC in Patients with Liver Cirrhosis. *Cancers* **2021**, *13*, 521. [CrossRef] [PubMed]

36. Nault, J.C.; Mallet, M.; Pilati, C.; Calderaro, J.; Bioulac-Sage, P.; Laurent, C.; Laurent, A.; Cherqui, D.; Balabaud, C.; Zucman-Rossi, J.; et al. High frequency of telomerase reverse-transcriptase promoter somatic mutations in hepatocellular carcinoma and preneoplastic lesions. *Nat. Commun.* **2013**, *4*, 2218. [CrossRef] [PubMed]

37. Nault, J.C.; Calderaro, J.; Di Tommaso, L.; Balabaud, C.; Zafrani, E.S.; Bioulac-Sage, P.; Roncalli, M.; Zucman-Rossi, J. Telomerase reverse transcriptase promoter mutation is an early somatic genetic alteration in the transformation of premalignant nodules in hepatocellular carcinoma on cirrhosis. *Hepatology* **2014**, *60*, 1983–1992. [CrossRef] [PubMed]

38. Brunner, S.F.; Roberts, N.D.; Wylie, L.A.; Moore, L.; Aitken, S.J.; Davies, S.E.; Sanders, M.A.; Ellis, P.; Alder, C.; Hooks, Y.; et al. Somatic mutations and clonal dynamics in healthy and cirrhotic human liver. *Nature* **2019**, *574*, 538–542. [CrossRef] [PubMed]

39. Reinert, T.; Schøler, L.V.; Thomsen, R.; Tobiasen, H.; Vang, S.; Nordentoft, I.; Lamy, P.; Kannerup, A.-S.; Mortensen, F.V.; Stribolt, K.; et al. Analysis of circulating tumour DNA to monitor disease burden following colorectal cancer surgery. *Gut* **2016**, *65*, 625–634. [CrossRef]

40. Lecomte, T.; Berger, A.; Zinzindohoué, F.; Micard, S.; Landi, B.; Blons, H.; Beaune, P.; Cugnenc, P.-H.; Laurent-Puig, P. Detection of free-circulating tumor-associated DNA in plasma of colorectal cancer patients and its association with prognosis. *Int. J. Cancer* **2002**, *100*, 542–548. [CrossRef]

41. Tie, J.; Cohen, J.D.; Wang, Y.; Li, L.; Christie, M.; Simons, K.; Elsaleh, H.; Kosmider, S.; Wong, R.; Yip, D.; et al. Serial circulating tumour DNA analysis during multimodality treatment of locally advanced rectal cancer: A prospective biomarker study. *Gut* **2019**, *68*, 663–671. [CrossRef] [PubMed]

42. Tie, J.; Wang, Y.; Cohen, J.; Li, L.; Hong, W.; Christie, M.; Wong, H.L.; Kosmider, S.; Wong, R.; Thomson, B.; et al. Circulating tumor DNA dynamics and recurrence risk in patients undergoing curative intent resection of colorectal cancer liver metastases: A prospective cohort study. *PLoS Med.* **2021**, *18*, e1003620. [CrossRef]

43. Wan, J.C.M.; Massie, C.; Garcia-Corbacho, J.; Mouliere, F.; Brenton, J.D.; Caldas, C.; Pacey, S.; Baird, R.; Rosenfeld, N. Liquid biopsies come of age: Towards implementation of circulating tumour DNA. *Nat. Rev. Cancer* **2017**, *17*, 223–238. [CrossRef] [PubMed]

44. Goldberg, S.B.; Narayan, A.; Kole, A.J.; Decker, R.H.; Teysir, J.; Carriero, N.J.; Lee, A.; Nemati, R.; Nath, S.K.; Mane, S.M.; et al. Early Assessment of Lung Cancer Immunotherapy Response via Circulating Tumor DNA. *Clin. Cancer Res. Off. J. Am. Assoc. Cancer Res.* **2018**, *24*, 1872–1880. [CrossRef] [PubMed]

45. Diehl, F.; Schmidt, K.; Choti, M.A.; Romans, K.; Goodman, S.; Li, M.; Thornton, K.; Agrawal, N.; Sokoll, L.; Szabo, S.A.; et al. Circulating mutant DNA to assess tumor dynamics. *Nat. Med.* **2008**, *14*, 985–990. [CrossRef] [PubMed]

203